THE ROLE OF THE CYTOSKELETON IN THE POLARISATION OF *MARCHANTIA POLYMORPHA* SPORES

Sarah Thurza Attrill

St Hugh's College

Department of Biology

University of Oxford

Thesis submitted for the degree of Doctor of Philosophy

Michaelmas 2023

Abstract

All multicellular land plants start life as a single cell. By polarising – developing asymmetry – and dividing asymmetrically, this single cell can form two distinct cell lineages and establish the first plant body axis. How these cells establish polarity from a non-polar state is little known. A novel single-celled polarity system is the spore of the liverwort *Marchantia polymorpha*. This haploid cell polarises, by unknown mechanisms, and divides asymmetrically to form a proliferating stem cell and differentiated rhizoid cell. My project aimed to define the dynamics of the cytoskeleton - microtubules and actin filaments - in the establishment of spore polarity. By live timelapse imaging of spores expressing fluorescent reporters, I show that the nucleus migrates from the cell centre to the basal cortex to orient the first asymmetric division. Movement of the nucleus is led by a microtubule organising centre (MTOC) nucleating a dense astral array. An actin filament network also forms in the space between the migrating nucleus and the basal cortex. These data support the hypothesis that the cytoskeleton is required for nuclear migration during spore polarisation. Cytoskeleton organisation and dynamics requires tight regulation by proteins such as the microtubule severing enzyme, katanin. By mutating katanin, I discovered that katanin severing is required for MTOC formation and microtubule organisation in *M. polymorpha*. Collectively these findings propose that microtubules, MTOCs, actin filaments and possibly katanin are required for the establishment of spore polarity and to orient the first asymmetric division plane, thereby defining the first apical-basal body axis of *M. polymorpha*.

Table of Contents

Acknowledgements

My mind is bursting full of people to thank, and I hope that these written acknowledgements can express my immense gratitude to you all.

Firstly, to my supervisor Liam Dolan: for your endless enthusiasm, advice, time, and support which has developed me both as a scientist and person. You gave me an amazing project - full of plants and microscopy - and you let me direct the way. Thank you for all these years.

Secondly, to my funders. I am very grateful to *moa* for sponsoring this exciting research, and especially to my *moa* supervisors, Clément Champion and Maria Gravato-Nobre, for their enthusiasm, support, and great scientific advice. A further thank you to the Gregor Mendel Institute who generously provided extra funding during my time in Vienna.

My PhD journey started in the Oxford Plant Sciences Department, and here are the people I want to thank; Charlotte Kirchhelle for her great imaging advice, Laura Moody and Maddy Seale for their helpful assessment feedback, and Gem and Roni for their administrative help. Next to the Gregor Mendel Institute. Thank you to all the administrative and scientific staff for aiding with our lab move and organising fun retreats. To the GMI researchers who made this community such a scientifically full and welcoming one. Finally, to both Plant Sciences and GMI for providing the space and equipment necessary to undertake my research.

I'd like to acknowledge several other researchers and facilities who provided resources for my research. To Clément Champion, Hugh Mulvey and Henrik Buschmann for kindly providing fluorescent reporters. To the Vienna BioCenter Core Facilities for their excellent services. In particular, the BioOptics Facility for providing incredible microscopes and especially to Alberto and Pawel for their constant imaging assistance. The ProTech Facility, especially Jana, for their construction of plasmids. The Media Lab, Plant Growth Facility and Sequencing Facility for all their resources. Finally, a very special thanks to our technicians Magda and Kathi for transforming and genotyping a ridiculous number of my plant lines!

Now to the Dolan lab members past and present; your contribution to my PhD through your scientific ideas, experimental aid, and constructive criticism was insurmountable… but it was much more than that. Together we lived through a pandemic, moved countries, setup a new lab, explored Vienna, hiked in the mountains, and endlessly chatted about plants and life over coffee and cake. I have loved being part of this lab group. Thank you all.

Lastly my personal thanks. To Frazer, for always challenging me and proving that hard feats are achievable. To Kate, for your love, support, and unwavering belief that I would fly. Lastly to Mum and Dad, for guiding me through this with endless encouragement and compassion. I cannot express how grateful I am, the best I can do is to say “Thank you” with all my heart.

Each of you laid a stone in the pathway to my PhD. Through the years I have run, wandered, skipped, and stumbled down that path, but now I’ve finally made it to the end. It has been a long journey but I’m thankful for every step and for each of you. Cheers to that!

Abbreviations

ABP	Actin Binding Proteins
ACD	Asymmetric Cell Division
ARP	Actin-Related-Protein
ATP	Adenosine Triphosphate
BASL	BREAKING OF ASYMMETRY IN THE STOMATAL LINEAGE
bp	Base Pair
BRXf	BREVIS RADIX family
Cas9	CRISPR-associated endonuclease 9
CDZ	Cortical Division Zone
CRISPR	Clustered Regularly Interspaced Short Palindromic Repeats
DMSO	Dimethyl sulfoxide
DNA	Deoxyribonucleic Acid
EB1	END BINDING 1
gDNA	genomic DNA
GFP	Green Fluorescent Protein
GTP	Guanosine Triphosphate
KIN	KINESIN
KTN	KATANIN

LatB	Latrunculin B
Mp	*Marchantia polymorpha*
MAP	Microtubule Associated Protein
mRNA	microRNA
MTOC	Microtubule Organising Centre
MYO	MYOSIN
NaDCC	Sodium Dichloroisocyanurate
nm	Nanometre
PCR	Polymerase Chain Reaction
PO	Polar Organiser
PPB	Pre-Prophase Band
RNA	Ribonucleic Acid
RFP	Red Fluorescent Protein
ROP	Rho in Plants
sgRNA	single guide RNA
Tak-1	Takaragaike-1
Tak-2	Takaragaike-2
TUB	TUBULIN
VSP	Vesicular Sorting Protein
WDL	WAVE DAMPENED LIKE

Chapter 1: General Introduction

1.1 Polarity and asymmetric cell division in organism development

1.1.1 An introduction to cell polarity and asymmetric cell divisions

Cell polarity, broadly defined as the asymmetric distribution of components and activities across a cell, is a universal feature of organism development. During polarisation, an internal or external cue triggers a cascade of subcellular events which irreversibly defines one cell pole as different from the other (Campanale *et al.*, 2017) (**Figure 1.1**). At the cellular level, polarity directs cell growth, orient division planes and confers specialised cell functions. At a larger scale, polarity can define tissue architecture and apical-basal body axes. Polarity can be distinguished at two levels: ‘unicellular polarity’ formed across a single isolated cell and ‘multicellular polarity’ formed across multiple neighbouring cells to generate a tissue or body axis (Bloch, 1943; Roeder *et al.*, 2022). The latter is well understood, whilst relatively little is known about the former. Overall, polarity is utilised at numerous stages of organism development.

Cell polarity provides an axis along which an asymmetric cell division (ACD) can occur. ACD is whereby cell components, such as proteins or organelles, are asymmetrically portioned into the two daughter cells to confer two distinct cell fates (De Smet & Beeckman, 2011) (**Figure 1.1**). Unequal sizes and shapes of the two daughter cells can make ACD easily recognisable, although in some cases only intrinsic factors distinguish the two daughter cells. In summary, ACD can generate new cell types during organism development.

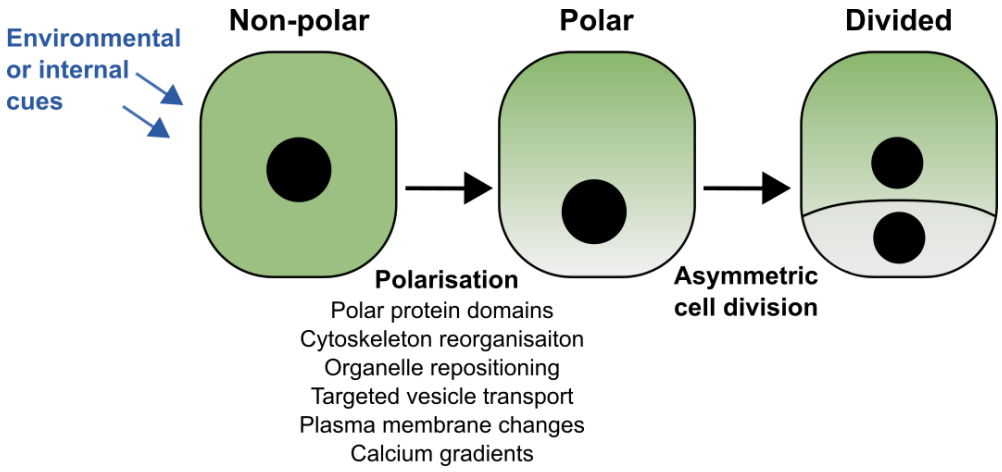

Figure 1.1: Polarisation and asymmetric division of a single isolated cell in response to external or internal cues. Starting from a non-polar state, a series of subcellular changes generates asymmetry within the cell. This is followed by asymmetric division forming two cells with distinct fates.

1.1.2 Polarity and asymmetric cell division can establish the first body axis

All multicellular organisms start life as a single cell. From this one cell, a diversity of cell types must be generated to build and pattern the organism. To achieve this, polarity and ACD are employed in this first cell to establish two different cell lineages and thus form the first body axis (an apical-basal or posterior-anterior axis) (De Smet & Beeckman, 2011; Campanale *et al.*, 2017). From this first axis, patterning of the rest of the body can follow.

Most multicellular organisms, such as animals, develop from a zygote. Zygotes are single diploid cells, formed through the fertilisation of a haploid egg cell. By contrast, multicellular land plants can develop from a zygote or from a spore dependent on their lifecycle. Spores are single haploid cells formed through meiosis of a diploid megaspore (Brown & Lemmon, 2011b). For most land plants, like angiosperms, their multicellular phase is a diploid sporophyte which develops from a zygote (a sporophyte-dominant lifecycle). Whilst for others, like bryophytes, their multicellular phase is a haploid gametophyte which develops from a spore (a gametophyte-dominant lifecycle). Despite the fundamental differences between spores and zygotes, both cells polarise and divide asymmetrically to generate two cell lineages and establish the first apical-basal body axis. For example, on division of an angiosperm zygote the small apical cell forms the pro-embryo and the large basal cell forms

the suspensor (Lau *et al.*, 2012). Whilst, on division of a fern spore the large apical cell forms the prothallus, and the small basal cell differentiates into the first rhizoid (Suo *et al.*, 2015). Overall, polarisation and ACD of these single cells is the first step to generating the diversity of multicellular body plans seen across land plants.

1.1.3 Internal and environment cues can orient the cell polarity axis

Correctly defining the orientation of asymmetry within a cell - the polarity axis - is critical in organism development, as this defines the first division plane and thus the body axis. There are three main mechanisms to orient cell polarity: inheritance of polarity from the parental cell, intrinsic signals triggering polarity or guidance by external or environmental cues.

The cues guiding polarity at the single-cell stage of organism development varies between species. Zygotes can inherit cell polarity from the egg cell, as exemplified by angiosperm zygotes (Wang *et al.*, 2019). In these zygotes, polarity can be built upon but is not established from a non-polar state. Alternatively, the sperm entry site can act as the polarity cue. In *C. elegans*, the egg cell is non-polar and the zygote requires sperm-derived centrosomes to initiate polarity (Cowan & Hyman, 2004). Overall, inheritance and sperm entry are the main cues orienting zygote polarity.

Environmental cues can orient polarity in cells which are directly exposed to environmental gradients, such as plant spores and alga zygotes. By using unilateral light and/or gravity to orient their polarity axis, these cells can orient the first division plane to form a rooting cell towards the earth and a photosynthetic cell towards the sun. Examples include the spores of the fern, *Ceratopteris richardii*, which are polarised primarily by gravity and secondly by light (Edwards & Roux, 1998). Whilst spores of the liverwort, *Marchantia polymorpha*, depend solely on light to orient their first division (Rötzer *et al*., unpublished). In the absence of external cues, one hypothesis is that spores rely on polarity inherited from the parental megaspore, although evidence suggests that spores start from a non-polar state (Bloch, 1943). Brown alga zygotes also polarise to light cues but use sperm entry site as a backup

mechanism. The sperm entry site initially defines the polarity axis but unilateral light can overrule and reorient the axis at 10 - 14 hours after fertilisation (Goodner & Quatrano, 1993; Hable & Kropf, 2000). In summary, plant spores and algal zygotes polarise to environmental cues to orient the first division and to promote successful organism development.

1.1.4 A cascade of subcellular events establishes cell polarity

Symmetry breaking or *de novo* polarisation is whereby a cell, starting from a non-polar state, endures a rapid series of subcellular events ending with the establishment of asymmetry across a polarity axis (Munro & Bowerman, 2009; Slaughter *et al.*, 2009). Polarity cues provide the initial trigger for this subcellular cascade and as one event triggers another and another, polarity is transduced across the cell (St Johnston & Ahringer, 2010). Eventually a state is reached where cell polarity cannot be reversed, known as 'polar axis fixation' (Fowler & Quatrano, 1995). Although the exact sequence of events is unique to each cell type, there are many common mechanisms driving cell polarisation. These include formation of calcium and pH gradients, repositioning of organelles, plasma membrane changes, and targeted vesicle trafficking (Shaw & Quatrano, 1996; Love *et al.*, 1997; Hable & Kropf, 1998; Hadley *et al.*, 2006). At the epicentre of most polarity systems are two mechanisms: polar localisation of proteins and cytoskeleton reorganisation (Raman *et al.*, 2018). In this review, I will briefly touch upon polar proteins before exploring the cytoskeleton in detail.

1.1.5 The formation of polarity domains by polar protein complexes

Proteins that polarise at specific plasma membrane domains – 'polar proteins' – are required to generate asymmetry within a cell. By formation of one or two opposing domains, polar proteins can define a cell pole and/or cell axis to orient division planes, direct cell growth, target vesicle transport and position organelles (Wallner, 2020; Hartman & Muroyama, 2023). Polar proteins are highly diverse with a multitude of functions. Common types include scaffolds or adaptors for protein recruitment, and enzymes such as GTPases and kinases

for modulation of protein activity (Wallner, 2020). Animals and yeast often employ highly conserved proteins families, such as PARs and Rho GTPases (St Johnston & Ahringer, 2010). Whilst plants employ a diversity of novel plant-specific proteins (Hartman & Muroyama, 2023). Through the precise localisation of certain proteins in a spatiotemporal manner, polar protein complexes are formed to drive specific activities at distinct cell poles.

Formation of proteins domains at two opposing cell poles can develop an internal axis along which ACD can be oriented and components segregated (Hartman & Muroyama, 2023). For example, a protein complex composed of BREAKING OF ASYMMETRY IN THE STOMATAL LINEAGE (BASL) and BREVIS RADIX family (BRXf) polarises to the corner of stomata precursor cells and 'repels' the nucleus away from this zone (Dong *et al.*, 2009; Muroyama *et al.*, 2020). This orients the ACD at the distal cell end. Meanwhile, OCTOPUS-LIKE (OPL) proteins define a distinct polarity domain at the opposing cell pole (Wallner *et al.*, 2023). On cell division, BASL/BRXf and OPL are differentially segregated into the two daughter cells and OPL determines the 'stem-ness' of the smaller cell (Wallner *et al.*, 2023). Overall, polar proteins can orient the ACD plane, and their differential inheritance can specify the daughter cell fates.

Other polar proteins, such as Rho GTPases, can specify a single domain for cell outgrowth by controlling cytoskeleton dynamics and vesicle targeting. In budding yeast, Cdc42 (Rho) localises to the future bud site to break cell symmetry and to initiate the formation of actin cables which traffic vesicles to the outgrowth site (Adams *et al.*, 1990; Slaughter *et al.*, 2009). Functioning in a similar capacity, Rho in Plants (ROP) - a subfamily of Rho-family GTPases - localises to the tips of *Arabidopsis* root hairs and *Marchantia* rhizoids to direct tip-growth (Molendijk *et al.*, 2001; Mulvey & Dolan, 2023). In summary, polar protein domains define regions of subcellular activities which can alter cell morphology.

At a tissue scale, co-ordinated localisation of polar proteins across multiple cells can orient tissue development and body axis formation (Ramalho *et al.*, 2022). One example is

SOSEKI which localises to cell corners in *Arabidopsis*, *Physcomitrium* and *Marchantia* and acts as a scaffold to recruit additional proteins (Yoshida *et al.*, 2019; Dop *et al.*, 2020). By generating domains across multiple cells within a tissue, SOSEKI forms a 'planar polarity field' thought to co-ordinate cell divisions on a global scale. Overall, polar proteins can align the polarity axis of cells relative to the organ axes, thereby defining tissue morphogenesis.

In summary, proteins located within discrete plasma membrane domains can define distinct activities at each cell pole to generate cell asymmetry. Polar proteins often achieve this through interaction with the cytoskeleton. This review will now focus on the cytoskeleton and its role in cell polarity and asymmetric cell division in plant cells.

1.2 The role of the cytoskeleton in cell growth, polarity, and division

1.2.1 Introduction to the cytoskeleton: structure, nucleation, and dynamics

The cytoskeleton is comprised of two elements: microtubules and actin filaments. Both polymers are dynamic, structurally polar, and well-suited to their functions in organelle migration, vesicle trafficking and structural rigidity for cell growth, division, and polarisation (reviewed in Alberts *et al.*, 2007; Sahi & Baluška, 2018).

Microtubules are composed of α and β- tubulin monomers which bind GTP and dimerise (Alberts *et al.*, 2007; Sahi & Baluška, 2018) (**Figure 1.2.A**). End-to-end joining of αβ- tubulin heterodimers forms a protofilament, thirteen of which bond together to form the characteristic hollow 'pipe' structure. Multiple overlapping parallel filaments can then generate bundles. Microtubules are innately polar structures with stable minus ends and dynamic plus ends. At the minus end, filaments are nucleated by γ-tubulin ring complexes (Farache *et al.*, 2018). Opposingly at the plus end, αβ-tubulin heterodimers bind and hydrolyse GTP for rapid microtubule growth. Subsequent loss of this 'GTP-cap' causes dissociation and microtubule shrinkage. Microtubules are therefore highly polarised and dynamically unstable structures.

Actin filaments (F-actin) are thin, flexible, 'rope-like' structures composed of two interweaving protofilaments made of globular actin (G-actin) monomers (Alberts *et al.*, 2007; Sahi & Baluška, 2018) (**Figure 1.2.B**). Like microtubules, actin filaments have a stable minus end and growing plus end. Nucleation at the minus end requires Actin-Related-Protein (ARP) complexes or formins typically located at the plasma membrane or filament sides. From these sites, filaments rapidly polymerise towards the cell centre by addition of ATP-bound G-actin monomers to the plus ends. Actin filaments can form a range of structures, from stable bundles to dynamic webs, dependent on their nucleation, polymerisation, and cross-linking.

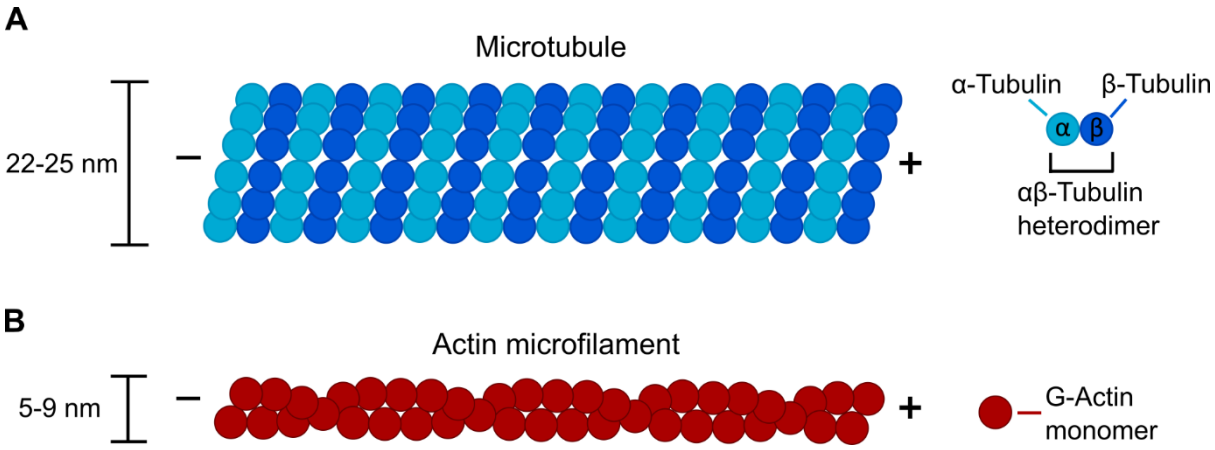

Figure 1.2: Microtubules and actin filaments are dynamic polymers with a stable minus end and a polymerising plus end.
(A) A microtubule is a hollow tubular polymer made up of 13 protofilaments, composed of αβ-tubulin heterodimers made of α-tubulin and β-tubulin monomers. **(B)** An actin filament is a rope-like filamentous polymer made up of two strands of globular (G-) actin monomers.

1.2.2 Organisation of the interphase cytoskeleton

The interphase cytoskeleton has distinct organisations across species. Centrosomes are the central point of microtubule organisation in animal and algal cells (Bettencourt-Dias & Glover, 2007). Composed of centrioles filled with y-tubulin and embedded in a matrix, centrosomes nucleate microtubules arrays which polymerise throughout the cytoplasm from this central location. By contrast, land plants lack centrosomes and instead utilise stochastic undefined nucleation sites located on the nucleus, plasma membrane and other microtubules (Chan *et al.*, 2003; Lee & Liu, 2019). From these sites, dispersed microtubule

arrays polymerise throughout the cytoplasm and across the cell cortex. Microtubules at the cell cortex - ‘cortical arrays’ - guide the deposition of cellulose and direct cell expansion (Burk & Ye, 2002). Parallel arrays lead to anisotropic cell growth whilst random arrays lead to isotopic cell growth (Hamada, 2014). Overall, animals and plants organise their interphase microtubules in fundamentally different ways, with centrosomes and cortical arrays being characteristic features of animal and land plant cells respectively.

The interphase actin cytoskeleton nucleates from points on the plasma membrane, forming a network in the cortex below - ‘the actin cortex’ - in both plant and animal cells (Henty-Ridilla *et al.*, 2013; Chugh & Paluch, 2018). Generated from an abundance of nucleation and cross-linking proteins alongside motor proteins, the actin cortex generates cortical tension and acts to strengthen and shape the cell (Salbreux *et al.*, 2012). Actin filaments further weave around the nucleus and extend through the cytoplasm, driving organelle movement and cytoplasmic streaming in plant cells (Shimmen & Yokota, 2004). Overall, the actin cortex is an almost universal feature used to maintain and define cell shape.

In summary, within an interphase cell, microtubules and actin filaments have separate, distinct organisations and therefore distinct roles in generating cell asymmetry.

1.2.3 The interphase cytoskeleton: generating internal cell asymmetry

Generating internal cell asymmetry through directional movement of subcellular components, such as vesicles, proteins, mRNA, and organelles, is one of the principal functions of the interphase cytoskeleton in cell polarity. By delivery of components to specific membrane sites, the cytoskeleton can form polar domains and alter membrane properties. One mechanism of this is by vesicle trafficking. As actin filaments nucleate from complexes at the cell cortex and polymerise inwards, vesicles can be efficiently trafficked to specific membrane regions along these filaments (Li & Gundersen, 2008). For example, cortical adhesives are delivered via actin cables to the base of brown alga zygotes for secretion

(Hable & Kropf, 1998). To further aid this directional endocytosis, microtubules reposition the endoplasmic reticulum towards the basal pole (Peters & Kropf, 2010). Microtubules have the opposite directionality to actin filaments, nucleating from MTOCs or foci in the cell centre and polymerising outwards to the cell cortex. Stabilisation of microtubules can form 'highways' for directional protein transport by direct deposition, cargo transport or vesicle trafficking (Li & Gundersen, 2008). One infamous example is the tea1p and tea4p proteins in fission yeast which are deposited at the distal cell ends via stabilised microtubules plus ends (Behrens & Nurse, 2002; Martin *et al.*, 2005). Taken together, the cytoskeleton uses a variety of mechanisms to target protein and cargo to specific domains.

Cytoskeleton dynamics can also mediate asymmetry on a larger scale by driving organelle reorganisation and cytoplasmic flow. Microtubules can drive organelle transport, specifically nuclear movement, via two main mechanisms. The first method requires attachment of microtubules to the nucleus often via an MTOC embedded in nuclear envelope. Subsequent depolymerisation of microtubules at the cortex, or sliding relative to the cortex, can then pull the nucleus towards the cortex (Tanenbaum *et al.*, 2011). A second method is the direct transport of the nucleus along microtubules arrays via motor proteins. Actin filaments can also move the nucleus by interaction with the nucleus via transmembrane linker proteins (Davidson & Cadot, 2021). Alternatively, actin filaments can induce cytoplasmic flow - the bulk flow of cytoplasmic components - which can rapidly generate asymmetry of organelles, proteins, and mRNA across the whole cell. This is driven by two main mechanisms. First by asymmetric contraction of the actin cortex. For example, in *C. elegans* embryos the cortical actin mesh becomes restricted to the anterior end and contracts asymmetrically, generating a flow of cytoplasm to the anterior pole (Munro *et al.*, 2004). The second mechanism uses cytoplasmic actin filaments to rapidly transport organelles through the cytoplasm (Shimmen & Yokota, 2004). Overall, the cytoskeleton can directionally move large organelles and stream cytoplasm to rapidly polarise the cell.

To summarise, the cytoskeleton drives the directional movement of vesicles, proteins, cytoplasmic components, and organelles to generate internal asymmetry.

1.2.4 The interphase cytoskeleton: generating polarised cell growth

Alongside the generation of internal asymmetry, the cytoskeleton can drive morphological asymmetry by specifying a direction of cell growth. In plants, there are two main types of polarised cell growth. During diffuse anisotropic growth, cortical arrays align perpendicular to the growth direction to restrict cell expansion to one direction (Hamada, 2014). During tip growth, cortical arrays align parallel to the growth direction to provide structural rigidity and actin filaments form a dynamic cortical domain to localise exocytosis to the cell tip (Hepler *et al.*, 2001). Polarised growth is characteristic of specialised cell types such as root hairs and pollen tubes (Sieberer *et al.*, 2005). Polarised growth can also proceed ACD. In such cases cell polarity has a dual function; to specify a growth direction and to orient ACD. In summary, morphological asymmetry is an expression of polarity mediated by the cytoskeleton.

1.2.5 Organisation of microtubules during prophase

Cell division is a fundamental process and relies on a series of cytoskeleton-based structures which can differ between species. In land plants, cell division begins in prophase with the formation of a pre-prophase band (PPB); a ring of longitudinal cortical microtubules encompassing the cell and foreshadows the future division plane (Rasmussen *et al.*, 2013) (**Figure 1.3.A**). The PPB forms by the alignment and narrowing of the cortical arrays during prophase. Once formed, the PPB deposits proteins at a ‘cortical division zone’ (CDZ), which remains throughout mitosis to guide cytokinesis. PPB formation is not necessary to define the CDZ, as some cells do not form a PPB, but does improve the reliability of correctly orienting the division plane (Schaefer *et al.*, 2017). In the absence of a PPB, non-PPB cortical microtubules may also deposit cortical proteins to guide cytokinesis (Buschmann &

Müller, 2019). In summary, land plants pre-determine the division plane prior to mitosis by establishing cortical marks during prophase which guide the cytokinesis machinery.

The mitotic spindle (reviewed in next section) is the centrepiece to mitosis, but determination of spindle organisation begins earlier in the cell cycle. In animal cells, the centrosomes persist throughout each cell cycle stage, eventually nucleating the mitotic spindle and being inherited by the daughter cells (Bettencourt-Dias & Glover, 2007). As land plants lack centrosomes, they employ variety of novel transient structures to nucleate the mitotic spindle. During late prophase, angiosperms form an ordered bipolar microtubule array or 'polar cap' around the nucleus (Chan *et al.*, 2005). Whilst bryophytes form a diversity of acentrosomal microtubule organising centres (MTOCs) during early prophase (Brown & Lemmon, 2011a). These MTOCs are analogous to centrosomes but they lack centrioles and instead contain an abundance of γ-tubulin to nucleate an early prophase spindle. Thus they act as an evolutionary 'half-way' point between the centrosomes in algae and the polar caps in angiosperms (Buschmann & Zachgo, 2016). Hornworts have a moon-shaped MTOC known as the plastid-associated axial microtubule system (Brown & Lemmon, 2011a). Moss gametophores have a single dispersed MTOC called the gametosome (Kosetsu *et al.*, 2017). Lastly, liverworts have two 'polar organisers' located on either side of the nucleus (Brown & Lemmon, 1990). Polar organisers form *de novo* in each cell, generated through bipolar aggregation of microtubule foci around the nucleus during early prophase (Buschmann *et al.*, 2016). The two polar organisers form prior to the PPB and nucleate peri-nuclear arrays which engulf the nucleus and astral arrays which polymerise towards the cell cortex (**Figure 1.3.A**). In late prophase, the polar organisers breakdown and γ-tubulin disperses into diffuse mini-poles cupping either side of the nucleus (Brown *et al.*, 2004). These poles nucleate the mitotic spindle, and thus polar organisers are not inherited by the daughter cells. Overall, land plants have invented a diversity of transient prophase structures which are later used to organise the mitotic spindle.

1.2.6 Organisation of the cytoskeleton during mitosis and cytokinesis

Cell division consists of two main stages: separation of chromosomes towards opposing cell poles (mitosis) and physical separation of the two daughter cells (cytokinesis). Mitosis is undertaken by a mitotic spindle; a dynamic bipolar array of microtubules which attaches to the chromosomes (Goshima & Scholey, 2010) (**Figure 1.3.B**). This is a universal structure across organisms. By contrast, cytokinesis is undertaken by a variety of structures. Animal cells form a contractile actin ring which constricts and cleaves the dividing cell in two (Miller, 2011). Whilst plant cells form a phragmoplast; a radially expanding ring of short microtubules and actin filaments between the separated nuclei (Smertenko *et al.*, 2017) (**Figure 1.3.C**). Membrane-filled vesicles shuttle along the phragmoplast arrays towards the midzone to form a new cell plate in the cell centre. To correctly orient the division, the phragmoplast expands towards the cortex and contracts the CDZ where the cell plate fuses (Smertenko *et al.*, 2018). In summary, across the cell cycle a variety of cytoskeleton-based structures are utilised. Several of these structures are divergent between species, which impacts the mechanisms utilised to orient the cell division plane.

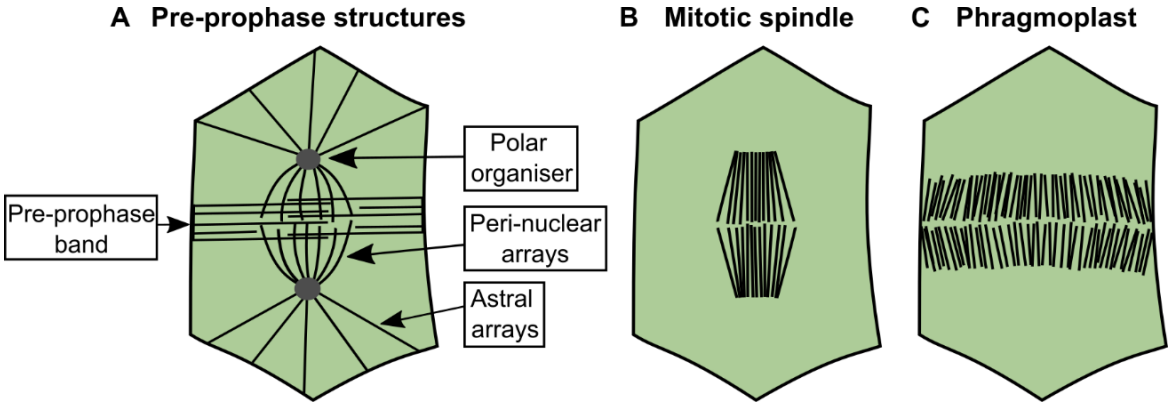

Figure 1.3: Microtubule structures at different stages of a plant cell cycle
Diagram of the different microtubule structures (black lines) in *Marchantia polymorpha* cells. **(A)** Structures which form during prophase including two polar organisers (grey circles) which nucleate astral arrays and peri-nuclear arrays, and the pre-prophase band at the cell cortex. **(B)** The mitotic spindle which forms during mitosis. **(C)** The phragmoplast which forms during cytokinesis.

1.2.7 The cytoskeleton's role in positioning asymmetric cell division planes

To divide a cell symmetrically into two equal parts, the division plane is set relative to the cell's morphological axis. By contrast, for ACD the division plane must be set in relation to the cell's polarity axis. In animal cells, the cleavage plane is determined by the position of the anaphase spindle, which is orientated by astral arrays anchoring to points on the cell cortex (Bringmann & Hyman, 2005). For ACD, astral arrays can preferentially interact with polar cortical domains to orient the anaphase spindle relative to the cell's polarity axis (Siller & Doe, 2009). Alignment can also rely on the centrosome positioning, as seen in brown algal zygotes. First a partial alignment occurs in prophase by rotation of the centrosomes led by astral arrays anchoring to basal cortical adhesion sites (Bisgrove & Kropf, 2001). Later, the anaphase spindle elongates and rotates into perfect alignment to divide the cell asymmetrically. Overall, ACD planes can be specified late in mitosis.

A fundamentally different mechanism is used in land plants where the division plane is defined prior to mitosis. In symmetrically dividing cells, the PPB spans the shortest geometric cell width, depositing cortical proteins to guide the phragmoplast (Smertenko *et al.*, 2017). For ACD, these cortical cues are overridden by polarity cues. Numerous polar proteins have been implicated in orienting ACD, and must in some capacity position the nucleus, PPB, or mitotic spindle. However the exact mechanism linking polar proteins to division plane alignment is still murky (Hartman & Muroyama, 2023). One mechanism has been characterised in stomatal development. The BASL/BRXf polarity domain locally destabilising cortical arrays, preventing local PPB formation and forcing the PPB to form at the distal cell end (Muroyama *et al.*, 2023). Further, the BASL/BRXf domain drives nuclear movement to this distal end (Muroyama *et al.*, 2020). Together this orients the ACD. Nuclear migration is a common prerequisite for ACD and although the polarity signals are often unclear, a polarised cytoskeleton is required. In *A. thaliana* zygotes, actin cables distribute vacuoles to the basal zone and the nucleus to the apex for ACD (Kimata *et al.*, 2016, 2019). On actin inhibition the nucleus does not migrate, and the zygote divides symmetrically.

Similarly in the spores of the fern, *Onoclea sensibilis*, prevention of nuclear migration by disruption of nuclear-associated microtubules resulted in symmetric cell divisions (Vogelmann *et al.*, 1981). Overall, the cytoskeleton appears to integrate signals from polar membrane domains and cell shape to position the pre-mitotic nucleus and orient ACDs in plant cells. Nevertheless, the full mechanistic picture is far from resolved.

1.3 Regulation of cytoskeleton organisation and dynamics

1.3.1 Microtubule associated proteins and actin binding proteins control cytoskeleton organisation during cell polarisation

The organisation and dynamics of the cytoskeleton is strictly controlled during cell polarisation and ACD. A diversity of accessory proteins and associated enzymes regulate the cytoskeleton. Microtubule-associated proteins (MAPs) bind to tubulin or polymerised microtubules, whilst actin binding proteins (ABPs) bind to G-actin monomers or filamentous actin (Alberts *et al.,* 2007). There are multiple classes of plant MAPs and ABPs, including plant-specific families, which undertake numerous functions like filament nucleation, cross-linking, stabilisation, and destabilisation (McCurdy *et al.*, 2001; Krtková *et al.*, 2016).

How do MAPs and ABPs regulate the cytoskeleton during cell polarisation? First, nucleating proteins can determine the location and directionality of cytoskeleton arrays with respect to the cell polarity axis (Li & Gundersen, 2008). For example, formins nucleate actin cables, therefore their position can determine the direction of vesicle transport (Liu *et al.*, 2018). Second, stabilising and destabilising proteins can influence the longevity and density of the polymer subpopulations. For example, stabilisation of microtubule plus-ends at a specific cortical site can generate locally stable arrays to deliver proteins to a specific membrane domain (Meiring *et al.*, 2020). Third, cross-linking and bundling proteins can determine the cytoskeleton's 3D structure and thus function in polarity (Higaki *et al.*, 2010). Overall, by

regulating the position, dynamics and network architecture of the cytoskeleton, accessory proteins enable the generation of cell asymmetry.

Alongside MAPs and ABPs, there are enzymes that sever cytoskeleton polymers and motor proteins that generate mechanical cytoskeletal force. Next in this review, I will explore the role of severing enzymes and motor proteins in plant development and cell polarisation.

1.3.2 Microtubule severing enzymes: cut, reorient, repeat

Microtubule severing enzymes can remodel microtubule networks and alter microtubule dynamics. As their name suggests, these AAA ATPases cut microtubules to form shorter filaments using energy from ATP hydrolysis. Katanin, fidgetin and spastin are the three known severing enzymes in animals, however in plants only katanin has shown a severing function (McNally & Roll-Mecak, 2018).

Katanin, 'the cutting sword', is a highly conserved heterodimer consisting of a catalytic p60 subunit and regulatory p80 subunit for targeted microtubule severing (McNally & Vale, 1993; Hartman *et al.*, 1998). Through multiple independent mutant screens in *A. thaliana,* katanin's function in plant morphogenesis and cell growth was discovered. At*bot1*, At*fra2*, At*erh3*, At*lue2* and At*ktn1-2* plant lines all bear mutations within At*KATANIN*. Collectively these mutants exhibit shorter stature, wider rounder cells and disorganised cortical arrays compared to wild type (Bichet *et al.*, 2001; Burk *et al.*, 2001; Webb *et al.*, 2002; Bouquin *et al.*, 2003; Nakamura *et al.*, 2010). From these observations, katanin was hypothesised to generate parallel cortical arrays which orient cellulose deposition and restrict cell growth to a single direction (Burk & Ye, 2002). Katanin can also trigger the reorientation of cortical arrays in response to external cues. In response to blue light, katanin was shown to reorient cortical arrays from transverse to longitudinal to induce hypocotyl bending (Lindeboom *et al.*, 2013). Overall, katanin regulates cortical array architecture to orient cell growth, which in turn impacts development at a tissue, organ, and whole plant level.

To generate unidirectional cortical arrays, katanin cuts microtubules at points of branching or cross-over (Nakamura *et al.*, 2010; Zhang *et al.*, 2013). This can induce depolymerisation of the shorter end, removing the non-parallel 'discordant' filaments and leaving behind the parallel arrays which are prone to bundling. Alternatively to reorientate arrays, katanin cuts discordant filaments which then regrow and amplify, generating a new array in the new orientation (Lindeboom *et al.*, 2013). In summary, katanin severs selected filaments to maintain or reorientate microtubule arrays and to control the overall array architecture.

Alongside cell growth, katanin also functions in plant cell division. Division of plant cells utilises multiple highly dynamic microtubule arrays. Katanin was shown to localise across the PPB, at the mitotic spindle poles and at the distal phragmoplast arrays indicating a potential role for katanin in maintaining these structures (Sasaki *et al.*, 2019). In agreement with this, these arrays are abnormal in At*ktn* mutants. Tubulin immunostaining of At*ktn* cells identified peri-nuclear arrays with supernumerary poles and misaligned PPBs compared to wild type (Panteris *et al.*, 2011; Panteris & Adamakis, 2012). Further, live cell imaging of At*ktn* noted broader and abnormal PPBs and increased rotation of the mitotic spindles compared to wild type (Komis *et al.*, 2017). In both studies, the phragmoplasts were 'arrowhead' shaped in the At*ktn* mutants unlike the short parallel arrays in wild type. Altogether, katanin regulates PPB formation, mitotic spindle stability and phragmoplast structure. Katanin severing was also implicated in PPB narrowing, mitotic progression and phragmoplast expansion, as the kinetics of these processes were delayed in At*ktn* mutants (Komis *et al.*, 2017). Ultimately by controlling microtubule organisation and dynamics during mitosis, katanin orients cell divisions. This evidenced by the misalignment of cell division planes in multiple A*tktn* mutants (Bichet *et al.*, 2001; Webb *et al.*, 2002). However which one of katanin's multiple functions is most critical for correct division orientation is still unclear.

In summary, katanin regulates microtubule dynamics and organisation throughout the cell cycle to control plant cell growth and division. Katanin localisation and activity is therefore highly regulated by proteins such as ROP6, SPIRAL2 and CHORDs (Lin *et al.*, 2013;

Wightman *et al.*, 2013; Sasaki *et al.*, 2019). Given katanin's functions, katanin's sensitivity to environmental cues, and katanin's interaction with polar proteins such as ROP, it is likely that katanin has roles in cell polarisation and ACD which have yet to be characterised.

1.3.3 Motor proteins: generating dynamic movement within cells

To develop asymmetry across a cell requires the generation of mechanical force across the cytoskeleton. This is achieved by motor proteins. By yielding energy from ATP hydrolysis, these multi-subunit ATPase enzymes can bind and walk along cytoskeletal filaments (Alberts *et al.*, 2007). Simultaneously, they can bind cargo, organelles, or other filaments to facilitate vesicle movement, organelle migration and the sliding of filaments relative the cortex or each other. Ultimately, motor proteins generate the mechanical force to drive cell asymmetry.

Myosins are the motor proteins of actin filaments. 79 myosin classes have now been identified in eukaryotes, with many myosins functioning in cell motility and muscle contraction (Hartman & Spudich, 2012; Kollmar & Mühlhausen, 2017). By contrast, there are only two classes in land plants, myosin XI and VIII, functioning in organelle transport and endocytosis respectively (Reddy & Day, 2001). In angiosperms there are five myosin-XI subclasses each with specialised functions including tip growth, organ straightening and defining nuclear shape (Peremyslov *et al.*, 2011). By comparison, bryophytes tend to have one subclass of each myosin to function in fundamental processes. In moss protonema, myosin-XI is required for tip growth, myosin-VIII for branch patterning and both are involved in cell division (Vidali *et al.*, 2010; Wu *et al.*, 2011; Wu & Bezanilla, 2014; Sun *et al.*, 2018). In summary, a small set of myosin take on essential and novel functions in land plants.

Dyneins and kinesins are motor proteins which move towards the microtubule minus and plus ends respectively. Cytoplasmic dyneins move organelles in animal cells but have been lost in land plants (Wickstead & Gull, 2007). In their place kinesin families have greatly expanded (Richardson *et al.*, 2006; Shen *et al.*, 2012). In particular, the kinesin -7, -12 and -14 families have diversified to replace the roles of dynein and to undertake plant-specific

functions (Gicking *et al.*, 2018; Nebenführ & Dixit, 2018). These includes PPB formation, spindle stabilisation, phragmoplast functions and tip growth. In summary, kinesins are the only functional microtubule motor proteins in plants and play diverse and novel roles.

1.3.4 Moving the nucleus for cell polarisation requires force and direction

One of the most distinct roles for motor proteins in cell polarity is in nuclear migration. I briefly described the mechanisms used to move the nucleus in section 1.2.3. Each of these mechanisms requires mechanical force generated by motor proteins. Dynein plays this role in budding yeast, fungi, and animal cells (Gundersen & Worman, 2013). In the absence of dyneins, plants utilise kinesins. Many members of the expanded plant kinesin-14 family have minus-end directed microtubule motility, like dynein, and are implicated in organelle movement (Gicking *et al.*, 2018). Specifically, kinesin with calponin-homology domain (KCH) was shown to position the nucleus in the centre of growing moss protonema (Yamada & Goshima, 2018). Myosins can also move plant nuclei. In *A. thaliana*, myosin-XI-I mediates nuclear migration after cell division in stomata development (Muroyama *et al.*, 2020). Overall microtubules and kinesins, actin and myosins, can power nuclear movement in plant cells.

1.3.5 Summary of the cytoskeletal mechanisms known in plant cell polarity

The cytoskeleton, accessory proteins, severing enzymes and motor proteins work together to generate cell asymmetry and ACD. In plants we have extensive knowledge on how the cytoskeleton is organised, regulated and functions within cells (Hamada, 2014). Despite this, our current understanding of their role in *de novo* polarisation and ACD is often limited, particularly at the one-cell stage of plant development. This in part due to the limited range of land plants studied. Until now, most research has focused on the zygote of angiosperms, but few have explored the polarisation of spores. My research uses a novel plant model – the spore of the liverwort *Marchantia polymorpha* – to investigate how polarity is generated from a non-polar state in a single cell to give rise to a multicellular haploid plant.

1.4 *Marchantia polymorpha* spores are a novel system to study the establishment of cell polarity

1.4.1 Introduction to the lifecycle and development of *Marchantia polymorpha*

The bryophyte *Marchantia polymorpha* is a thalloid liverwort which spends the majority of its lifecycle as a haploid gametophyte (Shimamura, 2016; Kohchi *et al.*, 2021; Bowman *et al.*, 2022). The gametophyte thallus is composed of air chambers regions covered by epidermal cells and with central air pores for gas exchange (**Figure 1.4**). Gemma cups form on the dorsal surface and hold gemmae; the asexual propagules of *M. polymorpha* which grow into clonal plants. The ventral thallus surface is covered in scales and protruding single-celled rhizoids for nutrient uptake. Liverworts are typically dioicous and to trigger reproductive development in *M. polymorpha* requires far-red light. Male plants grow flat antheridia which contain sperm and female plants grow umbrella-like archegonia which contain eggs (**Figure 1.4**). When crossed together, the fertilised diploid zygote develops into a mature sporophyte containing many diploid sporocytes. Sporocytes undergo meiosis to produce a tetrad of haploid spores, with a single sporangium holding thousands.

1.4.2 *Marchantia polymorpha* spores undergo *de novo* polarisation

M. polymorpha spores are single haploid cells encased in a sporopollenin coat. Once released from the sporangium the spores germinate under light; absorbing water, developing chloroplasts and growing isotopically in the first 24 hours (Nakazato *et al.*, 1999). The spore then divides asymmetrically giving rise to a large apical cell and small basal cell which defines the first body axis. The basal cell differentiates into the first rhizoid cell and undergoes tip growth. The apical cell continues to divide and forms vegetative cells and more rhizoids. Multicellular sporelings will develop into a pro-thallus with a meristem and eventually into the full gametophyte thallus structure (O'Hanlon, 1926) (**Figure 1.4**).

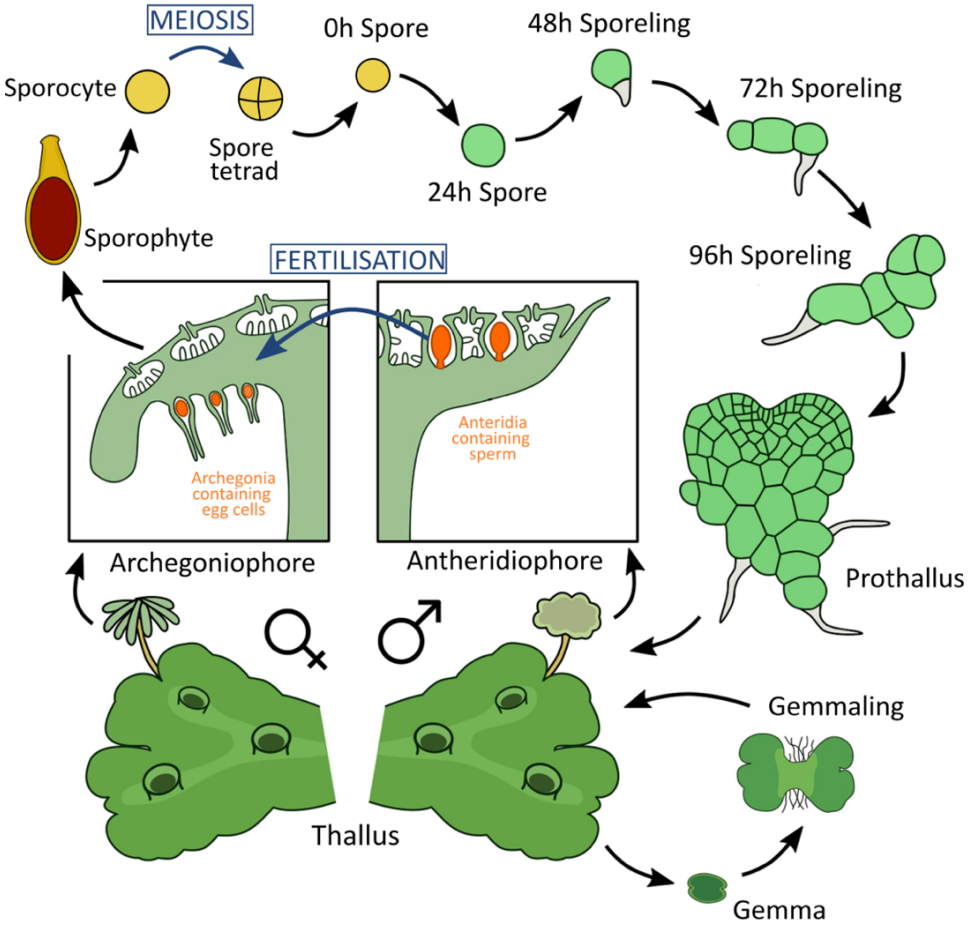

Figure 1.4: The lifecycle of *Marchantia polymorpha,* adapted from Flores-Sandoval *et al.*, 2018
Diagram of the lifecycle of *M. polymorpha.* A single-celled haploid spore divides to form a sporeling, then a prothallus with a meristem and finally a mature thallus. Mature plants reproduce asexually by gemma produced within gemma cups on the thallus surface. Sexual reproduction begins by the formation of archegoniophores on female plants, and antheridiophores on male plants. Egg cells from the archegonia are fertilised by sperm from the anteridia to form a diploid zygote. The zygote develops into a sporophyte containing many sporocytes. Sporocytes undergo meiosis to form haploid spores which begin the gametophyte lifecycle. The images are not scaled relative to each other.

Spores undergo an asymmetric cell division which indicates that spores are polarised prior to division. By comparison of spores to two other single cell polarity systems - the *Fucus* and *A. thaliana* zygotes - we can note a few key traits which distinguish spores as an exceptional system to study polarity (**Table 1.1**). Firstly, spores appear to establish polarity *de novo*. Spores are formed from a meiosis event and are freely released into the environment (Shimamura, 2016). There is no current evidence that spores inherit polarity, and spores receive no physical signals such as sperm entry and have no neighbouring cells to receive signals from. Instead, the polarity axis of spores, measured by the orientation of the first

division plane, is directed by unilateral blue light (Rötzer *et al*., unpublished). Polarity is therefore established or re-established after spores are released into the environment. The second key trait is that spores remain spherical leading up to and during the first division, this suggests that only internal polarity is generated without morphological asymmetry. Overall *M. polymorpha* spores provide a unique system to study polarity starting from a non-polar state, with no interference from surrounding cells and detached from mechanisms of polarised cell growth.

1.4.3 Advantages of using *Marchantia polymorpha* spores to study cell polarity

Marchantia polymorpha has become a model plant for genetic and developmental studies (Bowman *et al*., 2022). There are many characteristics which make *M. polymorpha* an excellent system in which to identify mechanisms controlling polarity and development. From a developmental viewpoint, *M. polymorpha's* simple morphology, short lifecycle and asexual propagules allows for fundamental processes to be investigated with relative ease (Kohchi *et al.*, 2021). From a genetic standpoint, research benefits from *M. polymorpha's* predominantly haploid lifecycle and sequenced genome with low genetic redundancy (Bowman *et al.*, 2017). From a technical perspective, an ever-expanding set of genetic techniques including transformation, CRISPR/Cas9 mutagenesis and fluorescent reporters are being developed and refined (Ishizaki *et al*., 2008, 2016; Sugano *et al.*, 2014, 2018). Studying the development of the spores of *M. polymorpha* exploits all these advantages.

Spores have many characteristics which benefit polarity research. Spores are freely accessible allowing for live-cell imaging and easy manipulation. Spores are generated in the thousands enabling statistical quantification and large-scale forward genetic screens. Other model plant systems are more technically limited by comparison (**Table 1.1**). Although the spore system also has drawbacks. Firstly, spore populations develop asynchronously and secondly there are very few well-established techniques for growing and imaging spores.

Nevertheless, once established, the *M. polymorpha* spore could become an unparalleled system to investigate the cellular and genetic mechanisms underpinning single cell polarity.

1.4.4 Current knowledge on the subcellular events during spore polarisation

How is asymmetry generated inside a spherical spore cell with light as the polarising cue? Very little research has addressed this question. To begin answering this, we first need to characterise the organisation of subcellular structures during spore development. One study revealed that the microtubule 'pro-spindle' - the polar organisers and peri-nuclear arrays surrounding the prophase nucleus - migrates to the basal cell pole prior to the first division (Sakai *et al.*, 2022) (**Table 1.1**). This is currently the earliest known sign of spore polarity and suggests microtubule involvement. However, the exact function of microtubules in spore polarity, and their interaction with other subcellular structures such as actin filaments, is still unclear. With such little known about spore development, studying spores provides a unique opportunity to unearth truly novel mechanisms establishing polarity in single plant cells.

	***Fucales* zygote**	***M. polymorpha* spore**	***A. thaliana* zygote**
Lineage	Brown algae	Bryophyte	Angiosperm
Formation	Fertilisation of egg cell	Meiosis of sporocyte	Fertilisation of egg cell
Ploidy	Diploid	Haploid	Diploid
Surroundings	Free-dwelling	Free-dwelling	Surrounded by tissue
Initial state	Egg cell unpolarised, but sperm entry acts as default polarity axis for zygote	No apparent polarity, uptakes water and grows isotopically	Egg cell is polarised and zygote further polarises on sperm entry
Polarity cue	Unilateral white light	Unilateral white light	Unknown
Cellular polarisation events	Local secretion, calcium gradient, F-actin patch, targeted vesicles, endomembrane polarisation and microtubule reorganisation to basal pole	Migration of microtubule prospindle to basal pole, accumulation of chloroplasts in apical hemisphere	Actin cap and microtubule ring forms at apical pole, nucleus moves to apical region, vacuoles accumulate at basal region
Morphological changes	Rhizoid pole outgrowth by local vesicles depositing new cell wall materials	Remains spherical, no visible shape change	Apical elongation by diffuse growth involving a transverse microtubule ring
Positioning of asymmetric division plane	Rotation of pre-mitotic nucleus followed by anaphase spindle alignmen and postioning of the telophase nuclei	Microtubule prospindle migrates to basal pole where the mitotic spindle forms	Nucleus migrates to cell apex where the pre-prophase band and mitotic spindle forms
Timing of division	18-24 hours after fertilisation	28-40 hours after release	28-32 hours after pollination
Apical cell	Larger cell, chloroplast rich	Larger cell, chloroplast rich	Smaller cell, cytoplasm rich
Apical cell fate	Proliferates to form the embryo proper	Proliferates to form the thallus	Proliferates to form the embryo proper
Basal cell	Smaller cell, Golgi and mitochondria rich	Smaller cell, chloroplast deficient	Larger cell, vacuole rich
Basal cell fate	Becomes a rhizoid cell and divides to form the holdfast	Remains unicellular, outgrows and becomes a rhizoid	Divides to form the embryo suspensor
Available techniques	Immuno-localisation and drug treatments	Fluorescent reporters, CRISPR/Cas9 mutagenesis, drug treatments, live imaging	Fluorescent reporters, CRISPR/Cas9 mutagenesis, drug treatments, live imaging
Benefits of system	Easily imaged and manipulated, light-controlled polarisation, population highly synchronous	*de novo* polarity, large numbers produced, many genetic resources, easily imaged and manipulated	Many genetic resources and estbalished imaging techniques
Drawbacks of system	Few genetic resources and techniques available, evolutionary distant from land plants	Populations develop highly asynchronously, imaging methods need refinement	Prior polarity in the egg cell, challenging to image and manipulate, low sample sizes

Table 1.1: Comparison of the first cell which polarises and divides asymmetrically to form the first apical-basal axis in three organisms: *Fucales* (brown algae), *Marchantia polymorpha* (bryophyte) *and Arabidopsis thaliana* (angiosperm).
Main information sources for the *Fucales* zygote: Goodner & Quatrano, 1993; Hable & Kropf, 2000; Bisgrove & Kropf, 2001; Corellou *et al.*, 2005; Hadley *et al.*, 2006.
Main information sources for the *M. polymorpha* spore: Shimamura, 2016, Sakai *et al.*, 2022.
Main information sources for the *A. thaliana* zygote: Kimata *et al.*, 2016, 2019; Wang *et al.*, 2019.

1.5 Summary and Research Rationale

Cell polarity and asymmetric division are fundamental to multicellular organism development and are universally driven by the cytoskeleton. Regulation of cytoskeleton organisation, dynamics and function relies on variety of associated proteins, in particular severing enzymes and motor proteins. Although our knowledge of the plant cytoskeleton and their regulators is expansive, their role in polarity and asymmetric division is relatively limited. This is particularly true at the one-cell stage of plant development. My research utilises a novel single-cell polarity system, the spore of *Marchantia polymorpha,* with the hopes of gaining unprecedented insights into how polarity is established from a non-polar state in plant cells.

My research specifically aimed to define the cytoskeletal mechanisms underpinning spore polarisation. First, I characterised the organisation and dynamics of the cytoskeleton during spore development. By live timelapse imaging of spores expressing fluorescent reporters, I discovered that the nucleus, microtubules, microtubule organising centres (MTOCs) and actin filaments all become asymmetrically organised in spores prior to the first asymmetric division. Next, I aimed to define the role of the microtubule-severing enzyme katanin in the regulation of microtubules, cell division and ultimately cell polarity in *M. polymorpha*. By taking a reverse genetics approach, I discovered that katanin regulates microtubule dynamics, MTOC formation and orients division in *M. polymorpha*. Overall, my research deepens our understanding of spore development and broadens our mechanistic knowledge of the role of the cytoskeleton in plant cell polarity and asymmetric division.

Chapter 2: Microtubule organisation during the polarisation of *Marchantia polymorpha* spores.

2.1 Abstract

Single cells can give rise to complex multicellular organisms through polarisation and asymmetric cell division. Microtubules are commonly required for these processes, yet microtubules dynamics have rarely been characterised in the single cells which develop into multicellular land plants; spores for the multicellular haploid phase and zygotes for the multicellular diploid phase. In this chapter, I establish a novel single-cell plant system – the spore of *Marchantia polymorpha* – to discover the role of microtubules in the establishment of cell polarity. By timelapse imaging of spores expressing nuclear and microtubule reporters, I show that two microtubule organising centres (MTOCs) form either side of a central nucleus. The nucleus subsequently migrates from the cell centre to the basal cortex to orient the first asymmetric division. This migration is led by one MTOC nucleating a dense astral array which polymerises towards the basal cortex. In parallel, I show that cortical microtubules deplete from the apical hemisphere. On inhibition of microtubule polymerisation, spores swell but do not divide. Altogether, microtubules, MTOCs and the nucleus reorganise during spore polarisation forming a clear apical-basal asymmetry and leading to the first asymmetric cell division. This ultimately establishes the first apical-basal body axis of *M. polymorpha*.

2.2 Introduction

The development of asymmetry within a cell – polarisation – can orient asymmetric cell divisions to segregate different molecular components into each daughter cell and determine their identities. In this way, polarity can generate new cell types and is fundamental to organism development. A variety of mechanisms can generate cell polarity including nuclear

migration, formation of polar protein domains, repositioning of organelles and reorganisation of the cytoskeleton, among others. In this chapter, I will focus on the role of the microtubule cytoskeleton in the development of cell polarity from a non-polar state.

All multicellular organisms start life as a single cell which can polarise and divide asymmetrically to generate the first body axis. In animal zygotes, microtubule dynamics have been well-described and highlight a diversity of microtubule-based polarity mechanisms (Raman *et al.*, 2018). By contrast, the microtubule dynamics in the single cells which give rise to multicellular land plants - zygotes and spores - are relatively undescribed. Currently, microtubules are best characterised in the angiosperm zygote and the fern spore. The zygote of *A. thaliana* is derived from a polarised egg cell (Wang *et al.*, 2019). A ring of microtubules forms around the zygote apex to elongate the cell before the first asymmetric division (Kimata *et al.*, 2016). By contrast, the polar axis of the fern spore is directed by light and gravity (Edwards & Roux, 1998). The spore nucleus migrates to the cell edge to orient an asymmetric division and this is prevented by the microtubule inhibitor, colchicine (Vogelmann *et al.*, 1981). These examples implicate microtubules in directional cell growth and nuclear migration in polarising plant cells. However, both systems are limited: the former by the existence of polarity in the egg cell and the latter by the lack of fluorescent reporters.

An alternative single isolated cell which develops into a multicellular organism, and uses microtubules to generate polarity, is the brown alga zygote. During polarisation, microtubules form asymmetric arrays around the nucleus that reorganise the endoplasmic reticulum and direct exocytosis towards the rhizoid pole (Peters & Kropf, 2010). Parallel cortical arrays also form at the rhizoid pole for tip outgrowth (Corellou *et al.*, 2005). This system has abundant technical advantages, however brown algae is evolutionary distant from land plants – algae are not plants (Archaeplastida) but evolved similar body plans by convergent evolution – therefore these mechanisms may not be conserved in land plants. In summary, the current research does not cover the full spectrum of plant lineages and misses the diversity of

polarity mechanisms used in single isolated plant cells. To address this, spores and zygotes from a greater range of land plants should be studied.

The model thalloid liverwort, *Marchantia polymorpha,* provides an excellent system to study polarity establishment. The lifecycle of *M. polymorpha* begins with a single-celled haploid spore generated through meiosis. Spores divide asymmetrically in an orientation specified by blue light to produce a large apical cell and small basal cell (Rötzer *et al*., unpublished). To divide asymmetrically the spore must be polarised, however the cellular mechanisms behind this polarisation are unknown. One recent study showed that a microtubule 'pro-spindle' migrates towards the cell cortex in developing spores (Sakai *et al.*, 2022). Given these observations and the importance of the cytoskeleton in other polarity systems, I hypothesis that microtubule reorganisation is required for *M. polymorpha* spore polarisation.

Microtubule organisation is partly dependent on the site of nucleation. Microtubules are often nucleated from microtubule organising centres (MTOCs) such as the centrosomes. By repositioning MTOCs cells can polarise their microtubule network, as seen in *C. elegans* and brown alga zygotes (Bisgrove & Kropf, 2001; Raman *et al.*, 2018). Land plants do not have MTOCs, with the exception of bryophytes which exhibit a variety of acentrosomal MTOCs; moss have a diffuse cytoplasmic MTOC termed the gametosome, whilst liverworts have two compact MTOCs called the polar organisers (Brown & Lemmon, 2011a; Kosetsu *et al.*, 2017). In *M. polymorpha*, polar organisers form *de novo* and nucleate peri-nuclear arrays which encage the nucleus and astral arrays which radiate out to the cortex (Buschmann *et al.*, 2016). Could polar organisers be utilised to polarise spore cells, like the centrosomes in animal and algal zygotes? Defining the position and dynamics of polar organisers in *M. polymorpha* spores could uncover analogous yet novel mechanisms in plant cell polarity.

To determine the organisation of microtubules during the polarisation of *M. polymorpha* spores, I conducted live timelapse imaging of spore expressing microtubule and nuclear reporters. I show that the nucleus migrates from the cell centre to the cell cortex, led by a

polar organiser nucleating a dense astral array which polymerises towards the basal cortex. The final location of the nucleus at the basal pole determines the first asymmetric division plane. Depolymerisation of microtubule using oryzalin prevented cell division and promoted cell swelling. My findings are consistent with the hypothesis that microtubules and MTOCs function to polarise *M. polymorpha* spores by directing nuclear migration.

2.3 Materials and Methods

2.3.1 Plant lines and growth conditions

The wild type *Marchantia polymorpha* accessions used were Takaragaike-1 (Tak-1) male and Takaragaike-2 (Tak-2) female. Transgenes were introduced into the progeny derived from crossing Tak-1 and Tak-2.

Plants were grown on ½-strength B5 Gamborg's medium containing 1.5 g/L B5 Gamborg, 0.5 g/L MES hydrate, 1% sucrose, pH adjusted to 5.5, set with 1% agar. Plants were grown at 23 °C in continuous white light at 50 - 60 µmol m^2s^1.

To induce reproductive development, 2 to 3-week-old plants were potted on soil, containing a 1:3 ratio of fine vermiculite and Neuhaus N3 compost, within SacO2 Microbox containers. Plants were watered and grown at 20°C in long day conditions of 16 hours light, 8 hours dark. White light was set at 50 - 60 µmol m^2s^1 and enhanced with far-red light at 30 - 40 µmol m^2s^1. Reproductive structures typically formed after 3 - 4 weeks in these conditions.

2.3.2 Crossing of *Marchantia* and sterilisation of sporangium

Male and female plants were crossed to generate spores. Male antheridiphores were submerged in water to release the sperm and a droplet used to fertilise female archegoniophores. Around 5 weeks after crossing, sporangia were produced, collected, and stored in water at 4°C. Sporangia were typically used within 2 weeks of storage.

Prior to use, sporangia were sterilised in 1 % sodium dichloroisocyanurate (NaDCC) for three minutes before washing twice with 1 mL water. Each sporangium was burst in 0.2 - 1 mL water to release the sterilised spores into the solution.

2.3.3 Reporter constructs

The *p*Mp*EF1α:GFP*-Mp*TUB1* (GFP-MpTUB1) and *p*Mp*EF1α:GFP*-At*ENDBINDING1a* (GFP-AtEB1) fluorescent reporters, labelling microtubules and microtubule plus ends respectively, were generated and kindly given by Henrik Buschmann (Buschmann *et al.*, 2016).

The *p*Mp*ROP:mScarletI–N7 (*mScarletI-N7*)* and *p*Mp*UBE2:mScarletI*-At*LTI6b* (mScarletI-AtLTI6b) fluorescent reporters, labelling the nucleus and plasma membrane respectively, were cloned into a double construct and kindly given Hugh Mulvey. Cloning of these plasmids used components from the OpenPlant toolkit (Sauret-Güeto *et al.*, 2020).

2.3.4 Amplification of plasmids and transformation into *Agrobacterium*

Plasmids were transformed into One Shot OmniMAX 2-T1R chemically competent *E. coli* cells (ThermoFisher Scientific) for amplification. 1 - 5 µL of plasmid was added to thawed *E. coli* cells and placed on ice for 30 minutes. Cells were heat-shocked at 42 °C for 30 seconds and returned to ice for 2 minutes. After adding 250 µL of warmed S.O.C medium, the mixture was incubated at 37 °C for 1 hour shaking at 225 rpm. The mixture was diluted into LB medium (1:50), spread onto solid LB media plates containing 100 µg/mL spectinomycin and incubated overnight at 37 °C. Single colonies were selected and grown at 37 °C overnight in liquid LB media containing 100 µg/mL spectinomycin. Plasmids were isolated from the transformed *E. coli* cells using the GeneJet Plasmid MiniPrep kit (ThermoFisher Scientific).

Amplified plasmids were transformed into the *Agrobacterium tumefaciens* GV3101 strain by electric shock. 1 µL plasmid and 50 µL thawed *Agrobacterium* were micro-pulsed before adding 1 mL of warm S.O.C media. The transformed *Agrobacterium* was streaked onto LB

media plates containing 50 µg/mL gentamycin and 50 µg/mL rifampicin, to select for the *Agrobacterium* strain, and 50 µg/mL spectinomycin, to select for plasmid expression. The culture was grown for 2 days at 28 °C and single transgenic colonies transferred into liquid LB antibiotic media.

2.3.5 Transformation of *Marchantia polymorpha*

Plasmids were transformed into *M. polymorpha* sporelings using transgenic *Agrobacterium* following the method developed in Ishizaki *et al.*, 2008 and improved upon in Honkanen *et al.*, 2016.

Wild type spores, derived from crossing Tak-1 and Tak-2, were grown in 25 mL M51C media in flasks for five days under 1500 - 200 lux at 23 °C. Transgenic *Agrobacterium* were grown in 5 mL liquid LB antibiotic media for 2 days before the culture supernatant was removed and 10 mL M51C media containing 100 µM acetosyringone was added. *Agrobacterium* was shaken for 6 hours at 28 °C. 1 mL of induced *Agrobacterium* and acetosyringone, to a final concentration of 100 µM, was added to the six-day-old sporelings. Sporelings and *Agrobacterium* were co-cultivated for two days on a 120 rpm shaker in light.

The *Agrobacterium* - sporeling solution was sieved through 40 µm cell strainers and washed with 150 mL sterile water to remove excess bacteria. Sporelings were spread on Gamborg media supplemented with 100 µg/mL cefotaxime, to kill the remaining *Agrobacterium*, and 10 µg/mL hygromycin or 0.5 µM chlorsulfuron, to select for transformants. After 1 to 2 weeks growth, sporeling were transferred onto new selective media to confirm their antibiotic resistance. Gemmae of surviving plants were screened for reporter fluorescence.

2.3.6 Stereomicroscope imaging of plants

Spores grown on media plates were imaged with a Keyence VHX-7000 digital microscope equipped with a VHX-7020 camera and VH-ZST lens.

2.3.7 Preparation of the spore imaging chamber

Spores for fluorescence imaging were setup within chambers, altered from Kirchhelle & Moore, 2017. A breathable gum boarder (Carolina Observation gel) was filled with Gamborg media and layered with cellophane soaked in liquid Gamborg media (½-strength B5 Gamborg's medium without agar). One sterile sporangium was burst into 200 µL water and 40 µL spore solution pipetted into each chamber. No perfluorodecalin was added. Spores were grown within the chamber for 29 to 50 hours in the conditions set in Chapter 2.3.1

Spores were derived from crosses between: plants expressing *p*Mp*EF1α:GFP*-Mp*TUB1* and Tak-1; plants expressing *p*Mp*ROP:mScarletI-N7* - *p*Mp*UBE2:mScarletI*-At*LTI6b* and plants expressing *p*Mp*EF1α:GFP*-Mp*TUB1*; plants expressing *p*Mp*EF1α:GFP*-At*EB1a* and Tak-2.

2.3.8 Spinning disk imaging of subcellular structures in spores

Spores were imaged using an Olympus IX3 Series (IX83) inverted microscope equipped with a Yokogawa W1 spinning disk, Hamamatsu ORCA-Fusion CMOS camera and a 100x/1.45 NA oil objective. For GFP, samples were excited at 488 nm and emission captured at 525 nm. For mScarlet, samples were excited at 561 nm and emission captured at 617 nm. For chlorophyll autofluorescence, samples were excited at 640 nm and emission captured at 685 nm. Z-stacks of 20 to 22 µm with 0.26 µm slices were captured unless otherwise stated. Lazer power and exposure time were tested and adjusted to prevent bleaching overtime. A Z-Drift compensation autofocus system stabilised imaging overtime. As spore populations developed asynchronously and were heterogeneous for the reporter expression, specific spores within each population were selected for imaging.

A few alterations to this method were required to capture microtubule plus ends (GFP-AtEB1). A Piezo Z stage and Hamamatsu ORCA-Flash 4.0 camera were used to rapidly capture Z-stacks of 0.99 µm with 0.33 µm slices at 1.3 second intervals.

2.3.9 Image deconvolution and image analysis

Deconvolution of selected images was done using Huygens software (Scientific Volume Imaging). Z-projections and central slices were converted for presentation using ImageJ Fiji (Schindelin *et al.*, 2012). For temporal projections, each image slice was deconvolved in Huygens then maximum projections for each timepoint were generated in ImageJ Fiji before temporal projection in ImageJ Fiji.

Analysis of cortical microtubule density used the ImageJ LPX package published in Higaki *et al.*, 2010 following the method in Chapter 4.3.14. Graphs were created in Microsoft Excel.

2.3.10 Oryzalin drug treatments on spores

Gamborg media plates containing oryzalin, dissolved in DMSO, were made to the final oryzalin concentrations: 0.01 μM, 0.03 μM, 0.1 μM, 0.33 μM, 1 μM, 3.3 μM and 10 μM. 1% DMSO was used as a control. Wild type spores, derived from crossing Tak-1 and Tak-2, were sterilised, and spread on the media containing oryzalin. Sporeling were grown in the conditions set in Chapter 2.3.1 and imaged at 2, 3 and 4 days using the Keyence microscope as stated in Chapter 2.3.6.

2.4 Results

2.4.1 *Marchantia polymorpha* spores typically divide between 32 and 48 hours after germination

To identify the key timepoints in the development of *Marchantia polymorpha* spores, wild type spores, derived from crossing Tak-1 to Tak-2, were grown on Gamborg media and imaged at 24, 32, 48 and 72 hours (**Figure 2.1.A, B**). At 24 hours, the spores were single-celled and had chloroplasts. At 32 hours, some spores had divided to form a small basal cell and large apical cell. At 48 hours, most spores had divided at least once. The basal cell had outgrown and occasionally a second division was observed in the apical cell. By 72 hours, the basal cell had elongated further but not divided, and the apical cell had undergone multiple rounds of cell division. This shows that the apical cell acts like a 'stem-cell' whilst the basal cell differentiates into a rhizoid. Overall, these data indicate that spore populations develop asynchronously, and the first division is between 32 and 48 hours after germination.

Spore development is known to vary across different growth conditions. In order to image subcellular events during spore development, spores had to be grown within an imaging chamber (Kirchhelle & Moore, 2017). To ensure these chambers enabled normal spore development, the growth of wild type spores in the chamber and on media plates was compared at 24, 32, 48 and 72 hours (**Figure 2.1.B, C**). At 24, 32 and 48 hours, spores developed similarly in both conditions and most spores had undergone the first asymmetric cell division by 48 hours. However, more ungerminated spores were observed in the chamber. At 72 hours, the apical cell of the chamber-grown spores had elongated whereas the apical cell in the plate-grown spores had undergone further cell divisions. Overall, the chamber enables normal development of *M. polymorpha* spores up to the first cell division (< 48 hours) but is unsuitable for observing spores beyond the two-celled stage (> 72 hours).

2.4.2 The nucleus repositions to the cell cortex in spores

The first asymmetric division of a spore produces a large apical cell and small basal cell. To divide asymmetrically, the pre-mitotic nucleus must be positioned asymmetrically within the cell. To investigate the position of the nucleus in single-celled spores, I used the nuclear - plasma membrane double reporter, *p*Mp*ROP:mScarletI-N7* - *p*Mp*UBE2:mScarletI*-At*LTI6b* made by Hugh Mulvey (Sauret-Güeto *et al.*, 2020). The first reporter (mScarlet-N7) is composed of an *N7* sequence, a nuclear targeting peptide, fused to mScarletI expressed under the *p*Mp*ROP* promotor. The second reporter (mScarlet-AtLTI6b) is composed the *A. thaliana LTI6b* sequence, which labels the plasma membrane, fused to mScarletI expressed under the constitutive *p*Mp*UBE2* promotor. Plants expressing the reporters were crossed to wild type to produce spore populations in which half expressed the reporters.

The nucleus was located is a variety of positions in a population of spores expressing mScarlet-N7 and mScarlet-AtLTI6b at 30 hours after germination. In single-celled spores, the nucleus was often located near the geometric centre of the spore - the centroid - and occasionally near the cell cortex (**Figure 2.1.D, E**). Central nuclei were typically circular whilst nuclei near the cortex were elongated in shape. In both cases the spores were spherical. In newly divided two-celled spores, the division plane was positioned asymmetrically between the two daughter cell nuclei (**Figure 2.1.F**). Together the two daughter cells form a sphere, indicating that no morphological asymmetry was generated in the parental cell prior to division. In larger two-celled spores, the apical cell nucleus had repositioned to the centroid and the basal cell had slightly protruded, indicating that morphological changes occur after the first division (**Figure 2.1.G**). Overall, these data are consistent with the hypothesis that the pre-mitotic nucleus repositions to the cell cortex during spore development to orient the ACD plane. Later in this chapter, I confirm this nuclear migration through timelapse imaging.

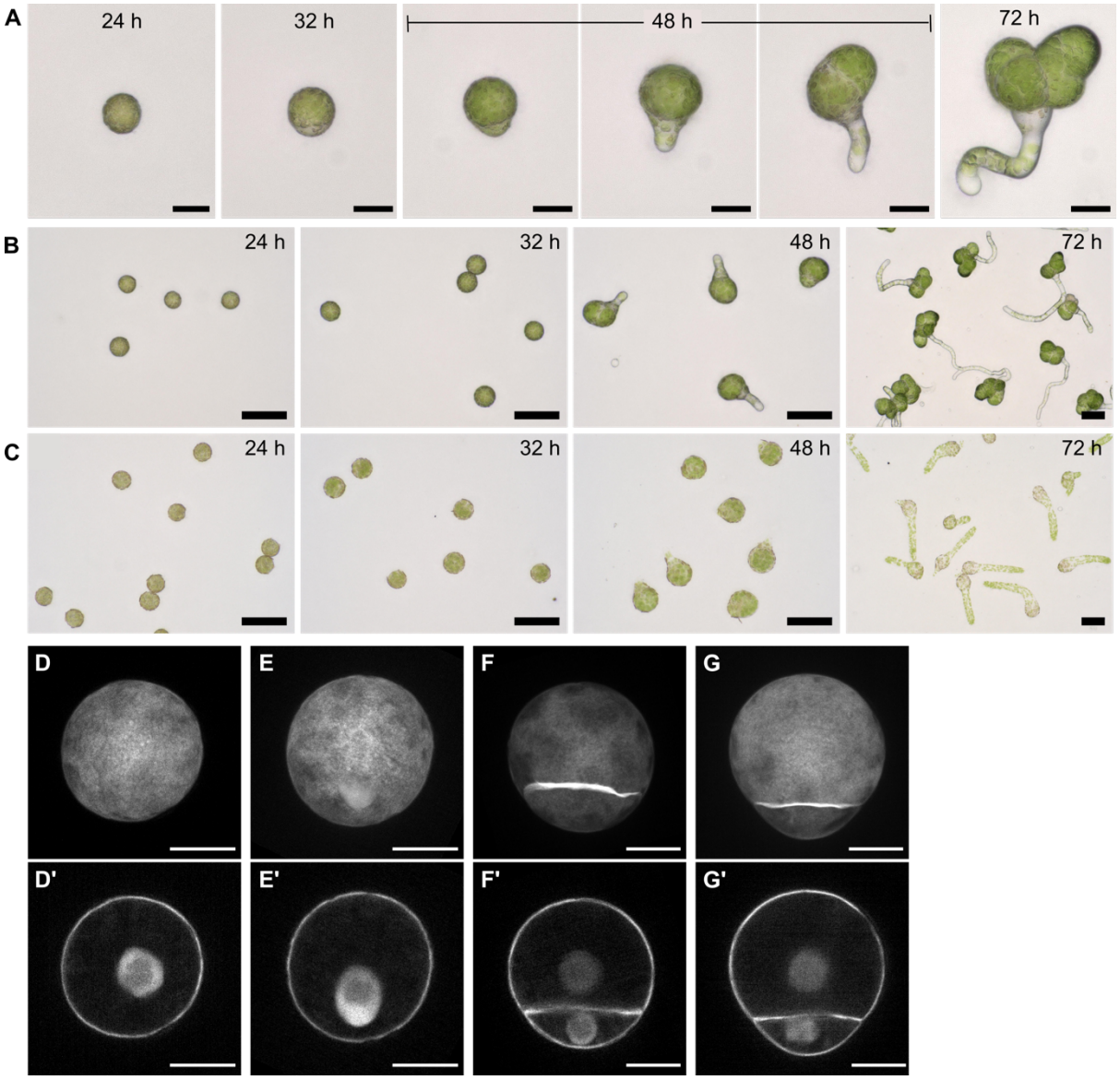

Figure 2.1: Spores divide asymmetrically between 32 and 48 hours after germination to define the first apical-basal body axis of *Marchantia polymorpha*

(A) Development of wild type spores across 72 hours. Imaged at 24, 32 and 48 hours after germination. Each spore is a different individual from the same population. Scale bars, 20 µm.

(B - C) Development of wild type spore populations grown on media plates **(B)** and within an imaging chamber **(C)**. Imaged at 24, 32, 48 and 72 hours after germination. Presented are different spores from the same population. Scale bars, 50 µm.

(D - G) Position of the nucleus and division plane in spores expressing *p*Mp*ROP:mScarletI-N7* - *p*Mp*UBE2:mScarletI*-At*LTI6b* at 30 hours after germination. Presented are Z-projections (D - G) and central planes in XY (D' - G') of four different spores. Single-celled spores had a central nucleus **(D)** or a basal nucleus **(E)**. Two-celled spores had divided asymmetrically **(F, G)**. Scale bars, 10 µm

2.4.3 Reorganisation of the interphase microtubule array occurs between 28 and 32 hours after spore germination

To investigate the organisation and dynamics of microtubules in developing spores, I labelled live microtubules using the *p*Mp*EF1α:GFP*-Mp*TUB1* reporter (GFP-MpTUB1), published in Buschmann *et al.*, 2016. This reporter is composed of the constitutive *p*Mp*EF1α* promotor expressing the *M. polymorpha β-TUBULIN 1* (Mp*TUB1)* gene fused to GFP. Plants expressing GFP-MpTUB1 were crossed to wild type to generate spore populations in which half expressed the reporter.

To gain initial insights into the microtubule organisation in spores, I compared the microtubule arrays formed in spores to those formed in epidermal cells. Multiple distinct arrays have been characterised in *M. polymorpha* epidermal cells (Buschmann *et al.*, 2016). There are interphase cortical arrays located below the cell membrane (**Figure 2.2.A1**). There are microtubule foci which form on the nuclear surface and aggregate into two polar organisers to nucleate peri-nuclear and astral arrays (**Figure 2.2.A2, A3**). There is the preprophase band (PPB) which forms in cells with polar organisers (**Figure 2.2.A3**). Lastly, there is the mitotic spindle which forms during mitosis and the phragmoplast which forms during cytokinesis (**Figure 2.2.A4, A5**). Each of these microtubule arrays were also observed in populations of unsynchronised spores at 29 hours after germination (**Figure 2.2.B**). However, the mitotic spindle, phragmoplast, and occasionally the polar organisers, were positioned asymmetrically in spores e.g., closer to one pole of the cell (**Figure 2.2.B4, B5**). This contrasts epidermal cells in which these structures are positioned centrally (**Figure 2.2.A4, A5**). Further, a PPB was never observed in spores which had polar organisers or microtubule foci, indicating that the PPB does not form in spores unlike most epidermal cells. Overall similar microtubule arrays form in *M. polymorpha* spores and epidermal cells, but some of these arrays are asymmetrically positioned in spores, and no PPB forms.

To determine the timing of microtubule re-organisations in these unsynchronised spore populations, spores were imaged at 24, 28 and 32 hours after germination (**Figure 2.2.C1-C3**). At each timepoint I quantified the number of spores which had microtubule foci, polar organisers, a mitotic spindle, a phragmoplast, a cell plate (divided) or only had interphase cortical arrays (**Figure 2.2.D**). At 24 hours, 86% of spores had only cortical arrays and 14% of spores had microtubule foci or polar organisers. At 28 hours, 60.9% of spores had microtubule foci or polar organisers and 10.5% of spores were in mitosis, cytokinesis or had divided. At 32 hours, 16.3% of spores were in mitosis or cytokinesis and 40.4% had divided. The number of spores with only cortical arrays stayed roughly the same at 28 and 32 hours (28.6% and 29.8% respectively) and these spores were predicted to not develop further. Overall, this indicated that the microtubule organisation progressively changes – from interphase cortical arrays to prophase arrays, spindle arrays and finally phragmoplast arrays – in asynchronous spore populations between 24 and 32 hours after germination. I selected 29 hours as the timepoint for imaging polarising spores, as 28 to 32 hours was the time window between polar organiser formation and the first asymmetric division.

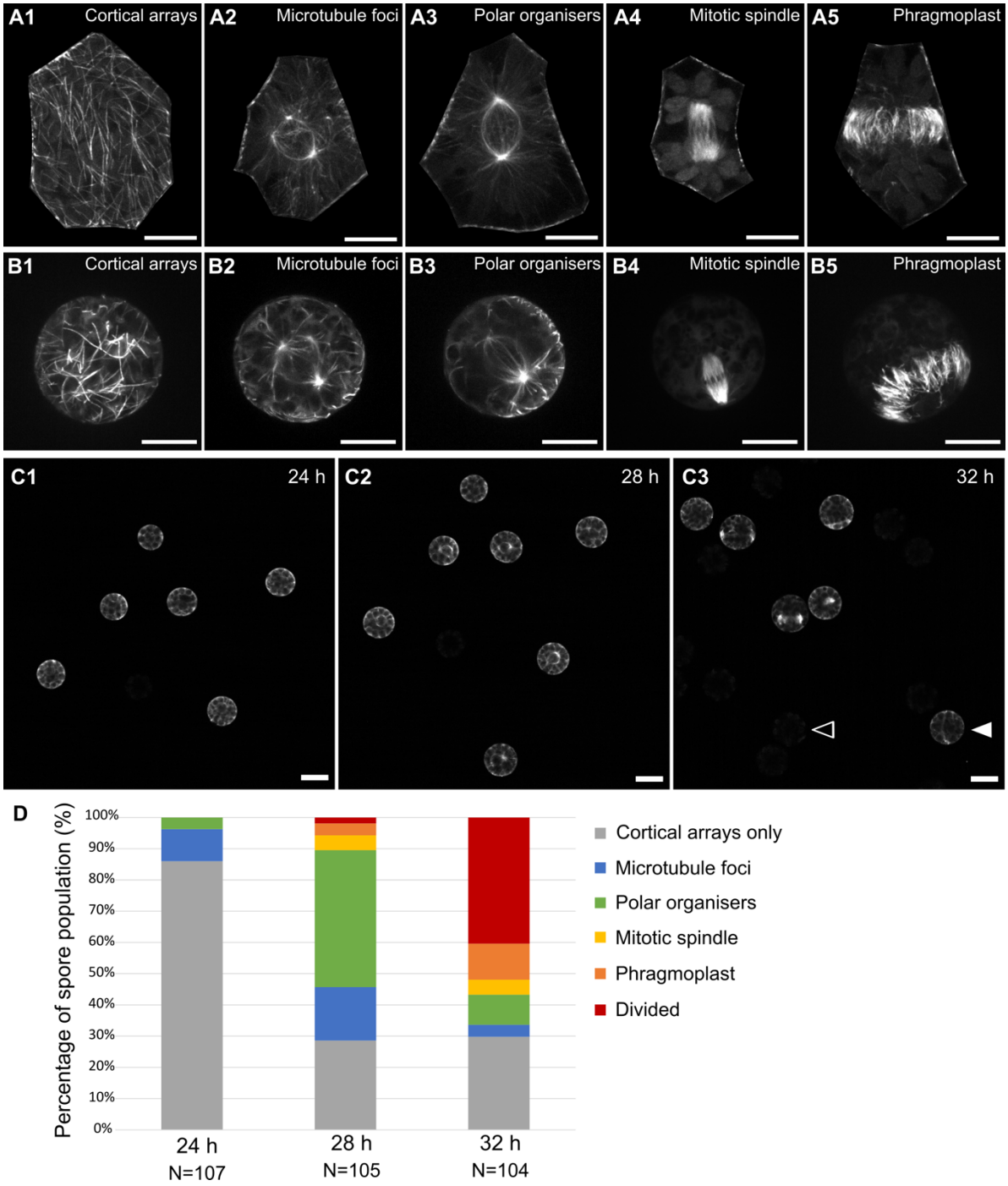

Figure 2.2: Microtubule organisation changes in spores between 28 and 32 hours
(A) The microtubule organisations in wild type epidermal cells of 2-day-old gemmae expressing *p*Mp*EF1α:GFP*-Mp*TUB1.* Presented are Z-projections of different individual cells. Scale bars, 10 µm.
(B) The microtubules organisations in wild type spores expressing *p*Mp*EF1α:GFP*-Mp*TUB1* between 29 and 32 hours after germination. Presented are full Z-projections (B1, B4, B5) or Z-projections of the central planes (B2, B3). Each spore is a different individual. Scale bars, 10 µm.
(C) Population of spores expressing *p*Mp*EF1α:GFP*-Mp*TUB1* imaged at 24, 28 and 32 hours after germination. The population is mixed; half express the reporter (filled arrow) and half do not (empty arrow). Presented are central slices in XY. Scale bars, 20 µm.
(D) Percentage of the spore population at 24, 28 and 32 hours after germination with each type of microtubule array. N is the number of spores analysed within the population at each timepoint.

2.4.4 Polar organisers form *de novo* in *M. polymorpha* spores

Microtubule foci and polar organisers were the first microtubule structures to form in spores, being present in a small percentage of the spore population at 24 hours after germination. By 28 hours, polar organisers were present in almost half the population (**Figure 2.2.D**). Polar organisers are therefore not inherited from the mother cell but instead form *de novo* after spore germination. Timelapse imaging of spores at 29 hours showed multiple low intensity microtubule foci near the centroid coalesce to form the two brighter foci of the polar organiser (**Figure 2.3.A**). This is consistent with polar organisers forming through aggregation of smaller microtubule foci around the nucleus, as observed in epidermal cells of *M. polymorpha* tissue (Buschmann *et al.*, 2016).

2.4.5 Polar organisers migrate from the cell centroid to the basal cortex

To capture microtubule reorganisation after the formation of polar organisers, 29-hour-old spores were imaged at 15-minute intervals for over 2.5 hours. The major events are presented in **Figure 2.3.B**. At the first timepoint, the 'microtubule basket' - the polar organisers and peri-nuclear arrays - was positioned near the cell centroid. At 60 minutes, the basket was positioned near the 'basal' cell cortex, oriented with one polar organiser very close to the cortex. By 90 minutes, the mitotic spindle had appeared at the same position as the microtubule basket had previously been. The cell then divided asymmetrically between 105 and 165 minutes via phragmoplast expansion. In summary, the microtubule basket becomes polar localised in spores and the spore divides asymmetrically at this plane.

2.4.6 The nucleus and polar organisers are tightly associated and migrate together from the cell centroid to the basal cortex

In *M. polymorpha* epidermal cells, the two polar organisers are located on each side of the prophase nucleus and the peri-nuclear arrays encompass the nucleus (Buschmann *et al.*, 2016). I therefore hypothesised that the nucleus would migrate together with the polar

organisers from the cell centroid to the basal cortex in spores. To identify the position of the nucleus during polar organiser migration, the nuclear - plasma membrane double reporter, *p*Mp*UBE2:mScarletI-N7* - *p*Mp*UBE2:mScarletI*-At*LTI6b,* was used in combination with the microtubule reporter, *p*Mp*EF1α:GFP*-Mp*TUB1*. Timelapses of spores expressing both reporters were captured at 29 hours after germination. In two representative timelapses, the nucleus was initially located between the two polar organisers near the cell centroid (**Figure 2.3.C1, C2**). As the polar organisers migrated from the cell centroid towards the basal cortex (0 - 30 minutes), the nucleus also migrated. On appearance of the mitotic spindle at the basal pole, the nuclear localised signal disappeared (60 or 45 minutes). Two daughter nuclei appeared in the apical and basal hemispheres during cytokinesis, separated by the expanding phragmoplast (**Supplementary Figure 2.1.A, B**). In summary, the nucleus and polar organisers migrate together from the cell centroid towards the basal cortex to become polar localised. The basal location of the nucleus positions the first division plane in spores.

2.4.7 Nuclear migration is led by one polar organiser and a dense astral array

To investigate the dynamics of the two polar organisers and the astral arrays during nuclear migration, further timelapses of spores were captured at 29 hours after germination. In the representative timelapse, the microtubule basket moved from near the cell centroid to the basal cortex led by one of the polar organisers (**Figure 2.3.D1**). Between 0 and 20 minutes, there was a dense array of microtubules between this leading ‘basal’ polar organiser and the basal cortex (**Figure 2.3.D2**). Later in this chapter I confirm that the array is nucleated from the polar organiser and polymerises outwards towards the cortex. At the opposing pole, there were few microtubules widely spread between the ‘apical’ polar organiser and the apical cortex (**Figure 2.3.D1**). This apical-basal microtubule asymmetry was consistent across polarising spores. Overall, the formation of a dense astral microtubule array correlates with the migration of the microtubule basket, and therefore nucleus, towards the basal cortex.

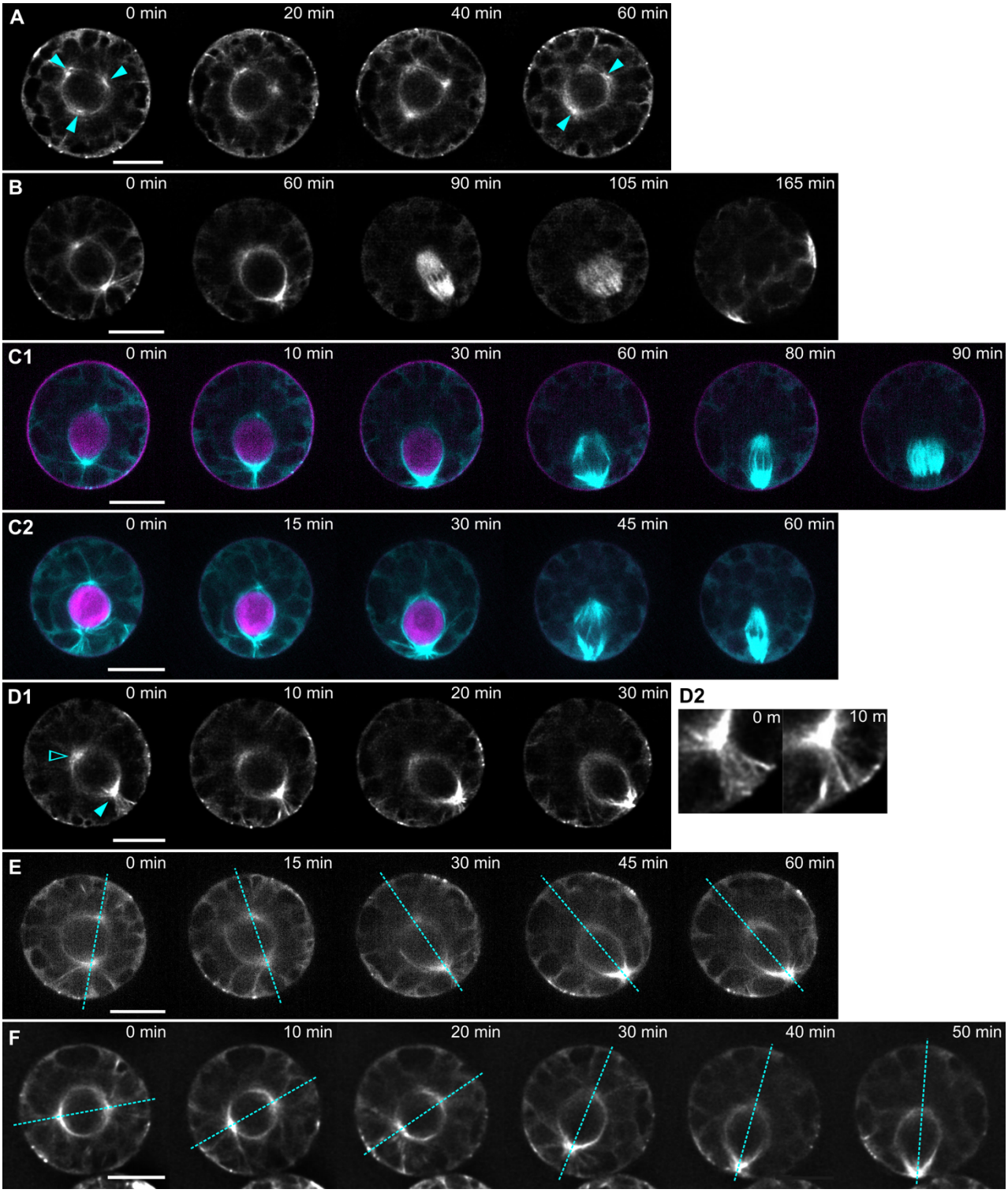

Figure 2.3: Migration of the nucleus and polar organisers from the cell centroid to the basal cortex is led by one polar organiser and a dense astral array

Timelapses of microtubule reorganisation in spores expressing *p*Mp*EF1α:GFP*-Mp*TUB1* starting at 29 hours after germination. Nucleus position was also captured in spores (C1, C2) by expressing *p*Mp*ROP:mScarletI-N7* - *p*Mp*UBE2:mScarletI*-At*LTI6b*. Presented are central slices in XY. Images (A, B, D, F) were deconvolved. Scale bars, 10 µm.

(A) Formation of two polar organisers (arrows at 60 min) from multiple smaller foci (arrows at 0 min).

(B) Major microtubule reorganisation events during spore development: polar organiser migration (0-60 min), mitosis (90 min) and cytokinesis (105-165 min).

(C) Co-migration of the nucleus (magenta) and microtubules (cyan) from the cell centroid to the cell cortex then mitosis at the basal pole in two separate spores **(C1, C2)**.
(D) The leading basal polar organiser (filled arrow) is led by a dense array of astral microtubules spanning from the polar organiser to the basal cortex **(D1)**, which is magnified in **(D2).** The opposing apical polar organiser (empty arrow) reduces in intensity **(D1)**.
(E) Subtle rotation of the polar organiser axis (dotted line) before migration to the cell cortex.
(F) Large, 90-degree rotation of the polar organiser axis (dotted line) before migration to the cortex.

2.4.8 Polar organisers can rotate before migration to the basal cortex

The trajectory of polar organiser migration, and its variability, was determined by further timelapse imaging of spores at 29 hours after germination. I observed that polar organisers near the cell centroid frequently rotated before their movement to the cell cortex. The degree of rotation varied between spores; often the shift was subtle (**Figure 2.3.E**) but occasionally larger rotations of up to 90 degrees from the starting orientation were observed (**Figure 2.3.F**). Some polar organisers rotated in three dimensions (**Supplementary Figure 2.2.A**). The axis formed by the two polar organisers can be defined as the 'polar organiser axis' and the axis between the future apical and basal daughter cell as the 'apical-basal axis'. Rotation of the polar organisers aligns their axis with the apical-basal axis prior to migration. This data is consistent with the hypothesis that polar organisers migrate towards a specific, pre-determined region at the cell cortex to correctly align the future division plane.

2.4.9 Spores have a random cortical microtubule network prior to polarisation

Alongside the nucleus-associated microtubule arrays, spores have a second microtubule population present at the cortex; the cortical arrays. To determine if the cortical network reorganises during spore development, I imaged cortical microtubules in spores at different developmental timepoints. At 24 hours after germination, before polar organiser formation, a sparse network of randomly organised microtubules covered the entire spore cortex (**Figure 2.4.A**). Most cortical arrays were short and highly dynamic, treadmilling across the spore surface (data not shown). In spores with microtubule foci or two central polar organisers at 29 hours after germination, the cortical arrays were randomly organised and variable in density (**Figure 2.4.B, C**). By contrast, in spores with polar organisers positioned at the

basal pole, the cortical arrays were consistently dense around the basal pole but absent at the apical pole (**Figure 2.4.D1-5**). These data show that microtubules are randomly distributed in the cortex before and during polar organiser formation, but then are basally distributed when the microtubule basket relocates to the basal pole.

2.4.10 Cortical microtubules deplete from the apical hemisphere during polar organiser migration

To investigate how cortical microtubule asymmetry develops in spores, timelapses of the cortical arrays in spores with migrating polar organisers were captured at 29 hours after germination. In the representative timelapse, the cortical microtubule network decreased in density as the polar organisers moved to, and remained near, the basal cortex (**Figure 2.4.E**). This depletion started at the apical pole and proceeded towards the basal pole as the polar organisers moved (0 - 60 minutes). Eventually only a few short, scattered microtubules remained near the basal pole (75 - 90 minutes). Quantification of microtubule density in this spore showed a steady reduction during polar organiser migration (0 - 105 minutes), then a sudden drop on mitosis (120 minutes) (**Figure 2.4.F**). By contrast, the bundling of microtubules increased over time, peaking and plateauing when the microtubules were basally distributed (60 to 105 minutes) (**Figure 2.4.G**). Occasionally a more organised ring of microtubules formed near the basal pole, perpendicular to the polar organiser axis (**Supplementary Figure 2.2.C**). In summary, there is a change from a random distribution to an asymmetric distribution of cortical microtubules as the polar organisers migrate.

2.4.11 Astral arrays rapidly polymerise from the basal polar organiser and potentially feed into the cortical microtubule population

I hypothesised that the cortical microtubule asymmetry could result from: a) microtubule depolymerisation in the apical hemisphere and/or b) feeding of microtubules nucleated from the basal polar organiser into the cortex at the basal hemisphere.

To investigate if microtubules nucleated from polar organisers can be fed into the cortex, I tracked microtubule polymerisation. The END BINDING 1 (EB1) protein binds microtubule plus ends in plant cells and can mark the sites of rapid microtubule polymerization (Chan *et al.*, 2003; Buschmann *et al.*, 2016). My work used the *p*Mp*EF1α:GFP*-At*EB1a* (GFP-AtEB1) reporter which labels microtubule plus ends in *M. polymorpha* (Buschmann *et al.*, 2016). The reporter is composed of the *A. thaliana EB1a* gene sequence fused to a GFP fluorophore expressed under the *M. polymorpha EF1α* promotor. Plants expressing *p*Mp*EF1α:GFP*-At*EB1a* were crossed to wild type to produce spore populations in which half expressed the reporter. In timelapses of spores expressing GFP-AtEB1 with 1.2 second intervals, EB1 comets moved in distinct tracks across the spore cortex (**Figure 2.4.H1, H2**). This confirmed that GFP-AtEB1 labels polymerising microtubules in *M. polymorpha* spores.

To test if microtubules nucleated from the basal polar organiser contribute to the basal cortical population, I tracked the direction and length of polymerising microtubules from the basal polar organiser. To achieve this, timelapses of EB1 using 1.2 second intervals were captured in spores at 29 hours after germination. Many EB1 proteins rapidly moved away from the basal polar organiser towards the cortex over the 2.4-minute timelapses (**Figure 2.4.I1, I2**). This confirmed that microtubules nucleated at the basal polar organiser polymerise towards cortex at a high rate. Generation of temporal projections showed that many of the EB1 tracks were short, suggesting that many arrays stop polymerising upon reaching the cortex (**Figure 2.4.I1, I2**). Other EB1 tracks were longer and extended into the cortex, suggesting that some microtubules polymerise into the cortex. This is consistent with the hypothesis that the microtubule population in the basal cortex is maintained by the activity of the basal polar organiser during migration to the basal pole.

To investigate the different contributions of the apical and basal polar organisers to the cortical microtubule population, I attempted to track EB1 at the apical pole. Movement of EB1 was difficult to observe from the apical polar organiser. In one cross-section view, EB1 proteins moved away from the apical polar organiser towards the opposing polar organiser

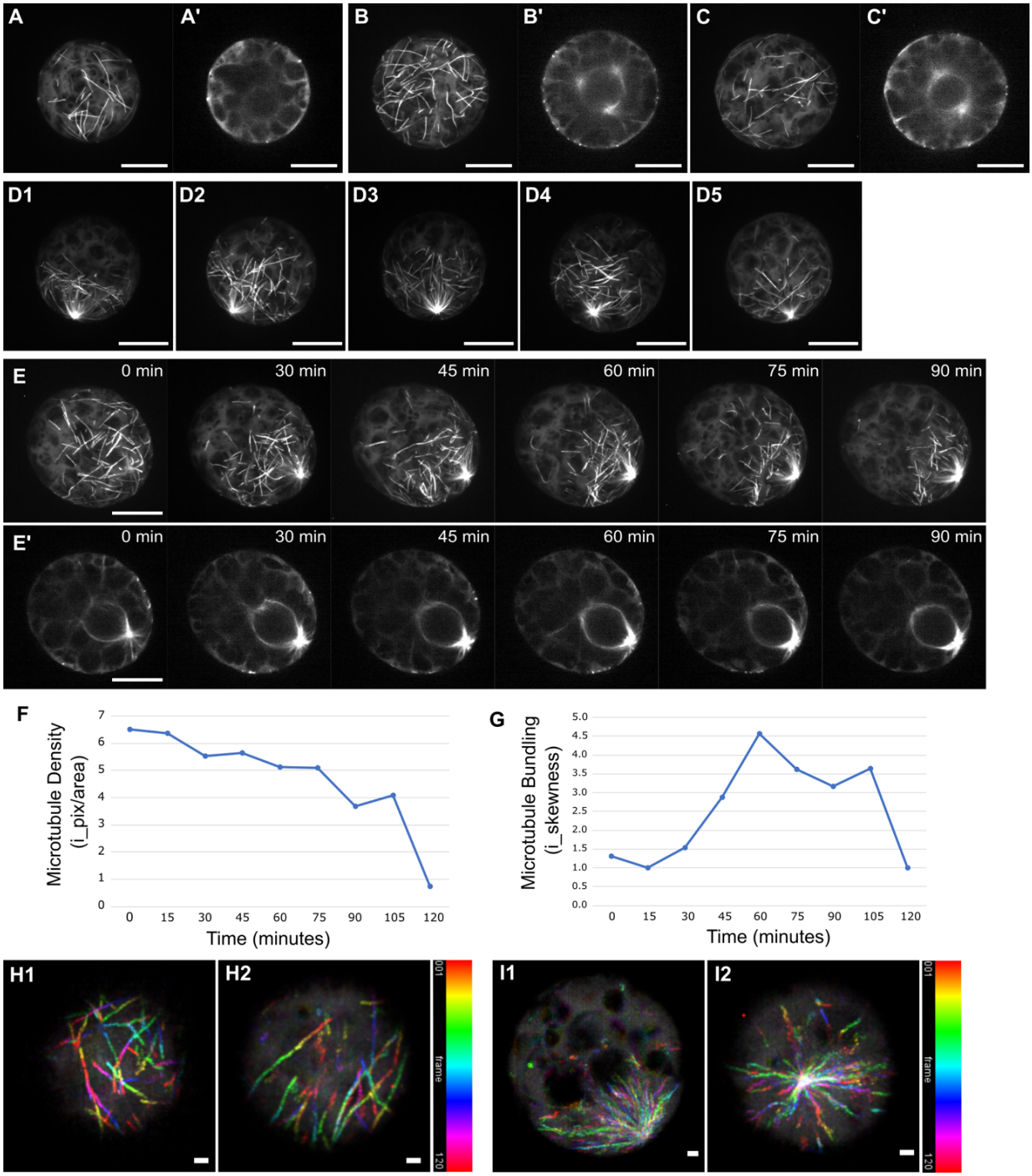

Figure 2.4: Cortical microtubules deplete from the apical pole during polar organiser migration
(A - D) Cortical microtubule organisation in spores expressing *p*Mp*EF1α:GFP*-Mp*TUB1* at 24 h **(A)** or 29 h **(B - D)** after germination. Presented are Z-projections (A, B, C, D1-5) and central planes in XY (A', B', C'). Cortical arrays were randomly organised in spores with no cytosolic microtubule arrays **(A)**, with microtubule foci **(B)** and with polar organisers near the cell centroid **(C).** Cortical arrays were basally localised in spores with polar organisers at the basal pole **(D1-5)**. Scale bars, 10 µm.
(E) Timelapse of a spore expressing *p*Mp*EF1α:GFP*-Mp*TUB1* starting at 29 hours after germination. The Z-projections (E) show the depletion of cortical microtubules from the apical cortex as the polar organiser, seen in the central XY planes (E'), migrates to the basal pole. Scale bars, 10 µm.
(F) Plot of the cortical microtubule density in spore (E) over 120 minutes.
(G) Plot of the cortical microtubule bundling in spore (E) over 120 minutes.

(H - I) Temporal projections of EB1 movement in spores expressing *p*Mp*EF1α:GFP*-At*EB1a*. Timelapses with 1.2s intervals (120 frames) were captured at 29 hours after germination. Images were first deconvolved and Z-projected before temporal projection. Presented are the colour-coded temporal projections of the EB1 movement across the cortex **(H1, H2)** and away from the basal polar organiser **(I1, I2)** in two spores each. Scale bars, 1 µm.

(e.g., peri-nuclear arrays) but very few EB1 proteins moved towards to the cortex (e.g., astral arrays) (**Figure 2.4.I1**). Although limited, this data is consistent with the hypothesis that the apical and basal polar organisers have different activity levels, e.g., rates of array nucleation, which contribute to the sparse apical arrays and dense basal arrays in polarising spores. To verify this, further timelapses of EB1 at the apical polar organiser are needed.

2.4.12 The mitotic spindle forms near the basal cortex of spores

I hypothesised that once the nucleus and microtubule basket had migrated to the basal pole, spore polarity was fixed. After migration, no rotation or significant movement of a microtubule basket away from the basal pole was ever observed. In a representative timelapse, the microtubule basket remained at the basal pole for 45 minutes and became shorter and rounder in shape (**Figure 2.5.A**). The polar organisers changed from single points of fluorescence (0 - 30 minutes) to broad flat areas (45 minutes) cupping the peri-nuclear arrays. This is consistent with polar organiser breakdown and dispersal of γ- tubulin into mini-poles to nucleate the mitotic spindle (Brown *et al.*, 2004). In summary, once docked at the edge, the microtubule basket does not move again before mitosis. This is consistent with the hypothesis that polarity is fixed at this timepoint.

I expected that the location of the microtubule basket would be retained by the mitotic spindle. To capture mitosis, spores were imaged using 5-minute intervals at 29 hours after germination. In the representative timelapse, the mitotic spindle formed rapidly after polar organiser breakdown (0 - 5 minutes) (**Figure 2.5.B**). The spore then passed through metaphase, anaphase, and telophase in the next 20 to 25 minutes. Importantly, the mitotic spindle retained the orientation and position of the microtubule basket throughout mitosis.

2.4.13 The phragmoplast expands to divide the spore in an asymmetric plane

To determine if the phragmoplast expands in a plane set by the mitotic spindle, timelapses of spores undergoing cytokinesis were captured at 29 hours after germination. In the representative timelapse, the phragmoplast formed at the mitotic spindle position and expanded centrifugally until it touched the cell cortex (0 - 40 minutes) (**Figure 2.5.C**). The orientation of expansion was perpendicular to the mitotic spindle axis – the axis between the spindle poles – and divided the spore into a small basal cell and large apical cell. Similar was observed in previous timelapses (**Figure 2.3.B, C1**). On reaching the cell cortex, the phragmoplast dismantled and cortical arrays repolymerised from dispersed cortical points (40 - 80 minutes). Overall, the phragmoplast retained the position and orientation of the mitotic spindle and thus the microtubule basket. Therefore, the final position of the microtubule basket, and nucleus, after migration determines the future cell division plane.

2.4.14 Distinct microtubule arrays are established in the two daughter cells

The first asymmetric cell division forms two cells with different fates: a large, proliferating apical cell and a small basal rhizoid cell. To investigate the microtubule organisation in these cells, spores were imaged at 50 hours after germination. In two-celled sporelings, a random cortical network covered each cell (**Figure 2.5.D**). Polar organisers occasionally formed near the centroid of the apical cell. In three-celled sporelings, the apical cell had divided and the two daughter cells both had random cortical arrays (**Figure 2.5.E**). By contrast, the basal cell had not divided but instead elongated with microtubules arranged parallel to the growth axis. These longitudinal arrays likely function in tip growth. Overall, the data indicates that microtubules are re-established after the first division to form different arrays in the apical and basal cells, reflecting their distinct cell fates in proliferation and tip growth respectively.

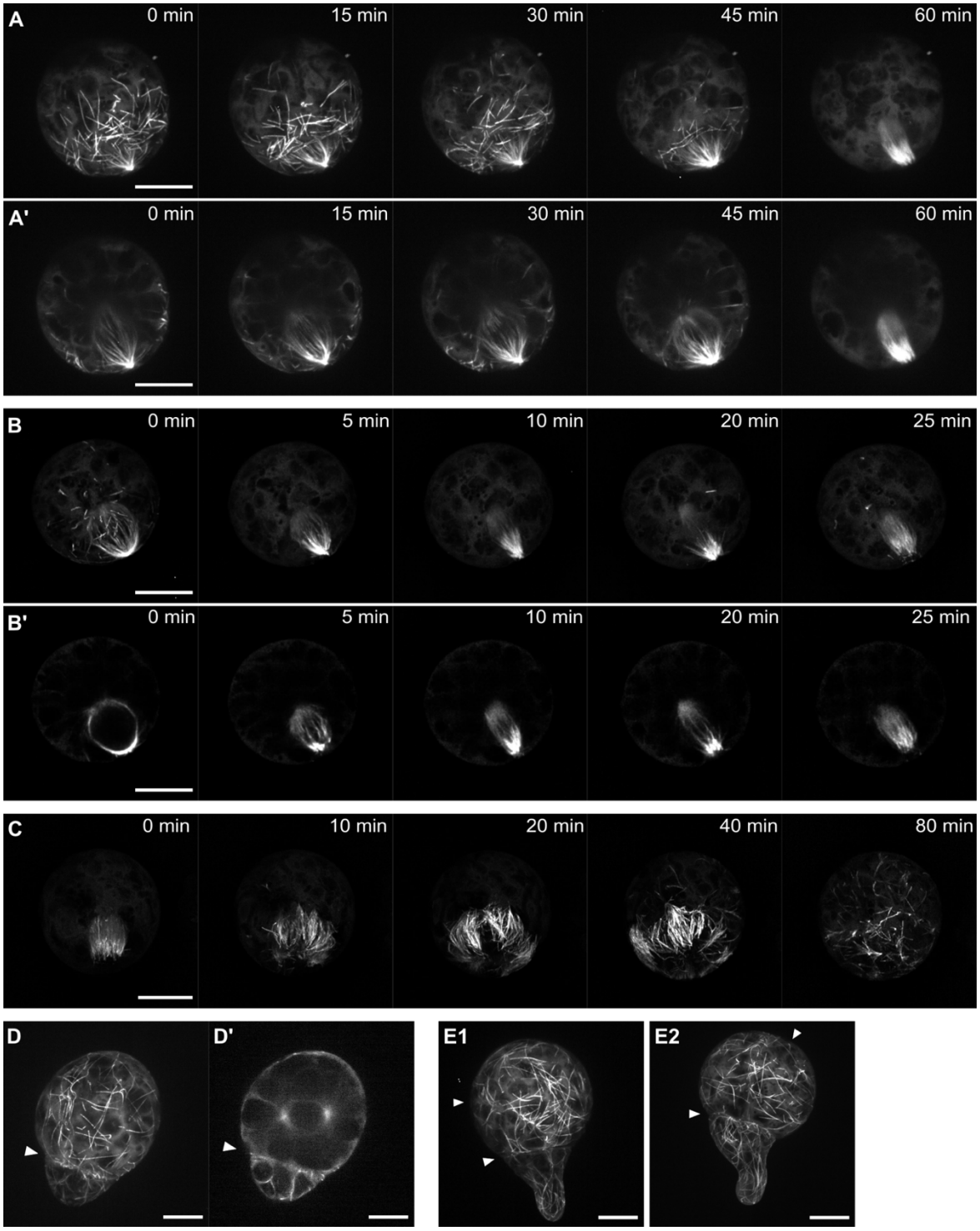

Figure 2.5: Basal position of the microtubule basket defines the first asymmetric division plane
(A - C) Timelapses of microtubule reorganisation prior to/during division of spores expressing *p*Mp*EF1α:GFP*-Mp*TUB1*, starting at 29 h after germination. Presented are Z-projections (A, B, C) and central planes in XY (A', B'). **(A)** Persistence of the microtubule basket at the basal pole and polar organiser breakdown. **(B)** Mitosis at the basal pole. **(C)** Phragmoplast expansion. Scale bars, 10 µm. **(D - E)** Microtubule organisation in multi-celled sporelings expressing *p*Mp*EF1α:GFP*-Mp*TUB1* at 50 h after germination. Presented are Z-projections (D, E1, E2) and central plane in XY (D'). **(D)** 2-celled sporeling with random cortical arrays and polar organiser in apical cell. **(E1, E2)** Three-celled sporelings with distinct cortical arrays in apical and basal cells. Arrows indicate the division planes. Scale bars, 10 µm.

2.4.15 Chloroplasts distribute asymmetrically in polarised spores

As the nucleus migrates towards the basal cortex, I hypothesised that chloroplasts would be repositioned leading to their unequal segregation into the two daughter cells. To test this, chloroplast organisation was characterised in spores at different stages of polarisation by capturing chlorophyll autofluorescence and GFP in spore expressing GFP-MpTUB1 at 29 hours after germination. In spores with only interphase cortical arrays, chloroplasts were evenly distributed throughout the cell (**Figure 2.6.A**). In spores with a central microtubule basket, chloroplasts were evenly distributed throughout the spore, apart from their absence in the cell centroid (**Figure 2.6.B**). In spores with a microtubule basket or mitotic spindle at the basal pole, chloroplasts filled the apical hemisphere but were depleted in the basal pole (**Figure 2.6.C, D**). There was one layer of chloroplasts surrounding the basket, but the cell edge was clear of chloroplasts. This was also reported in Sakai *et al.*, 2022 who suggested chloroplasts were attracted to the astral arrays, pulling them away from the cell edge. In dividing spores, the region apical of the phragmoplast had many chloroplasts whilst the region basal of the phragmoplast had only a few chloroplasts (**Figure 2.6.E**). Although the chloroplasts appeared equally spaced in each region. After division the basal cell inherited very few chloroplasts compared to the apical cell (**Figure 2.6.F**). In summary, chloroplast distribution changes from uniform to asymmetric during migration of the microtubule basket, and nucleus, to the basal pole. This results in the differential inheritance of chloroplasts by the apical and basal cells. However, it is still unclear if this chloroplast rearrangement proceeds the nuclear migration (e.g., the chloroplasts move independently away from the basal pole) or is a result of it (e.g., the chloroplasts are physically pushed out of the way by the nucleus, or the chloroplasts are moved via attachment to astral arrays).

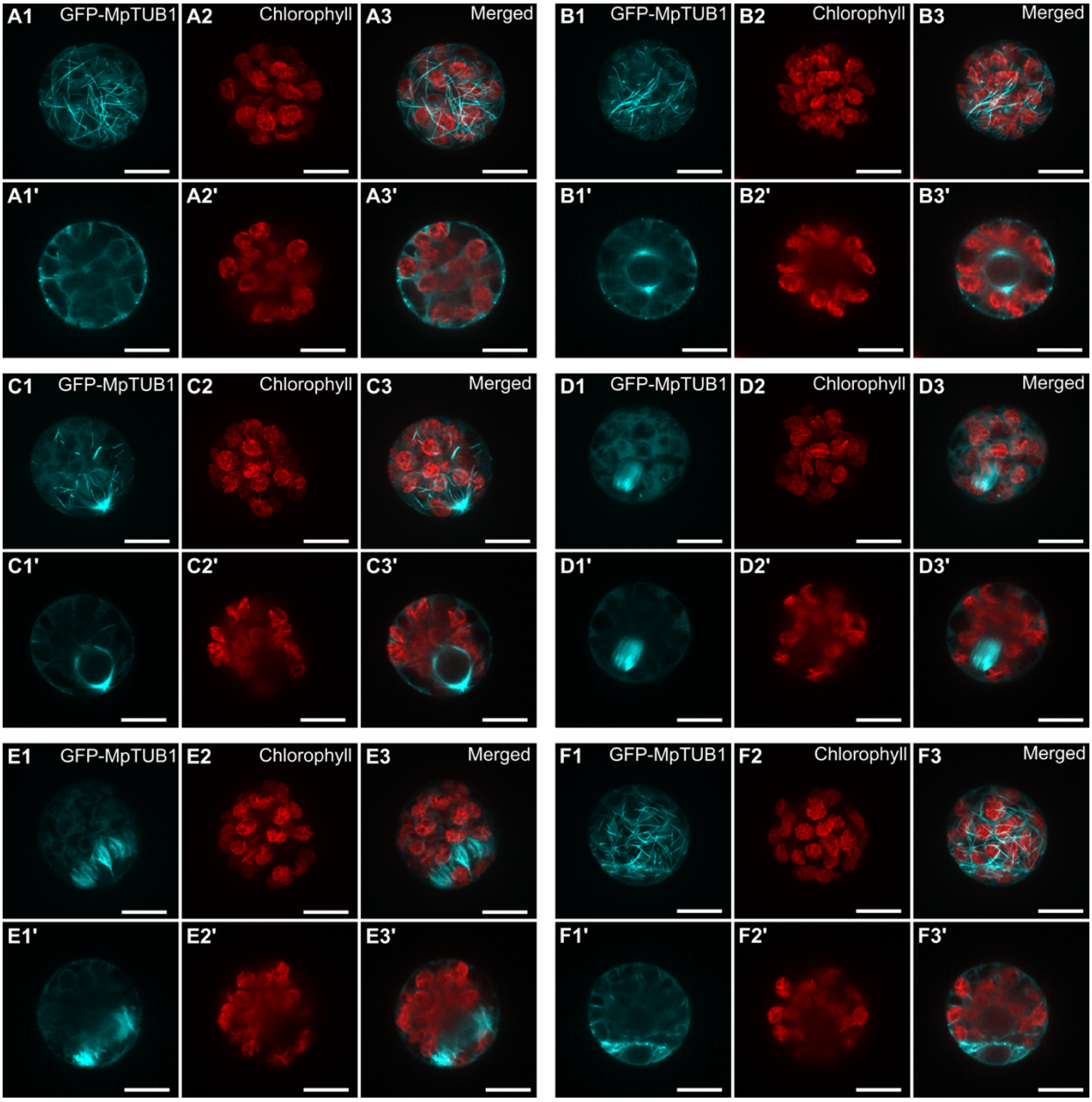

Figure 2.6: Chloroplasts distribute asymmetrically in polarised spores
Organisation of microtubules and chloroplasts in spores expressing *p*Mp*EF1α:GFP*-Mp*TUB1* at 29 hours after germination. Shown are GFP-MpTUB1 fluorescence (cyan, A1-F1), chlorophyll autofluorescence (red, A2-F2) and merged images (A3-F3) of each spore. Presented are the Z-projections (A-F) and central planes in XY (A'-F') of each channel. **(A)** Spores with no polar organisers are packed with chloroplasts. **(B)** Spores with two central polar organisers have a central clear zone. **(C)** Spores with a basal microtubule basket and **(D)** spores with a late mitotic spindle/early phragmoplast have a basal zone clear of chloroplasts. **(E)** Spores undergoing cytokinesis and **(F)** divided spores have an apical zone/cell with many chloroplasts and basal zone/cell with few chloroplasts. Scale bars, 10 μm.

2.4.16 Inhibition of microtubules prevents spore division and induces swelling

I have shown that the nucleus, polar organisers, and microtubules reorganise during spore polarisation and leads to an asymmetric division. This led me to hypothesise that microtubules are required for spore polarisation and that on inhibition of microtubules, spores would not polarise and therefore divide symmetrically. To test this hypothesis, spores were treated an inhibitor of microtubule polymerisation, oryzalin.

To first identify an oryzalin dose that inhibits microtubules but still enables the first division, wild type spores were grown on increasing concentrations of oryzalin for 2 days and the percentage of divided spores quantified. Overall, division rates decreased as the oryzalin concentration increased (**Figure 2.7.A, C**). When grown on the DMSO control, 44% of spores had clearly divided at least once. On 0.1 µM to 1 µM oryzalin, 29% to 31% of spores had divided. On 3.3 µM oryzalin only 8% of spore divided and on 10 µM oryzalin no spores divided. The position of the division planes was difficult to quantify in this setup, but clear asymmetric divisions were observed in many spores on DMSO and 0.1 to 1 µM oryzalin. In conclusion, high doses of oryzalin (> 3.3 µM) inhibit the first cell division in spores. However, there is currently no evidence that the division plane position is altered at lower doses.

The first asymmetrical division of spores forms a small basal cell which differentiates into a rhizoid. To determine if microtubule inhibition affects formation of the rhizoid cell, sporeling morphology was characterised after 3 to 4 days growth on oryzalin. When grown on DMSO and 0.01 µM to 0.1 µM oryzalin, spores had divided multiple times and produced elongated rhizoids (**Figure 2.7.A, B**). On 0.3 µM to 1 µM oryzalin, spores had divided multiple times and produced a few rhizoids which were short or branched (**Figure 2.7.A, B**). Some apical cells also appeared swollen by day 4. More dramatically, on 3.3 µM and 10 µM oryzalin spores remained undivided but swollen (**Figure 2.7.A, B**). The swelling had increased by day 4, and by day 8 many spores had burst and collapsed (data not shown). In conclusion, high doses of oryzalin prevent division and induce spore swelling, whilst lower doses enable rhizoid cell formation but disrupt rhizoid outgrowth.

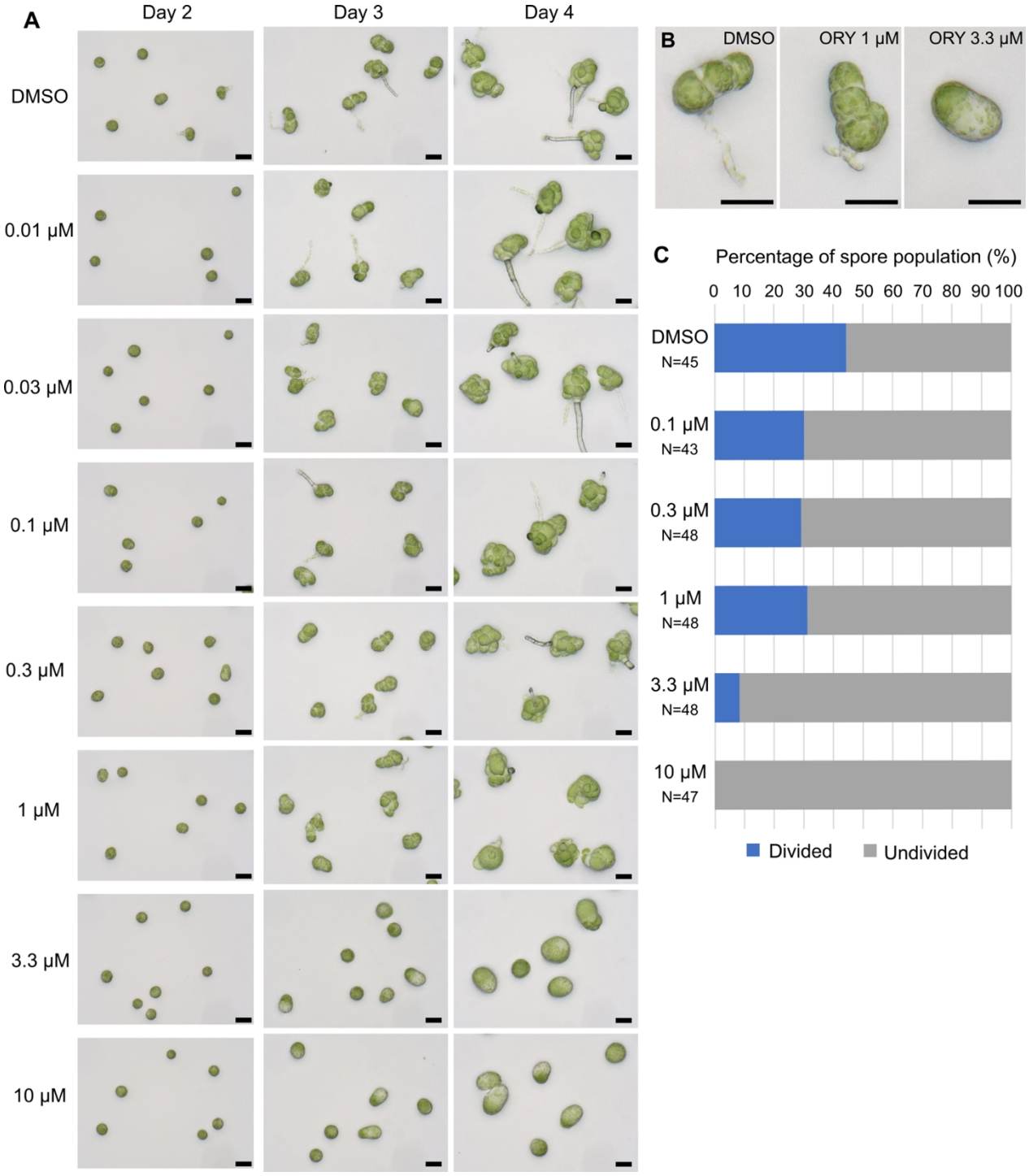

Figure 2.7: Oryzalin inhibits spores division and promotes swelling
(A) Development of wild type spores grown on Gamborg media containing increasing doses of oryzalin (0.01 µM to 10 µM) and a DMSO control. Presented are representative spores after 2-, 3- and 4-days growth. Scale bars, 50 µm.
(B) Enlarged images of representative spores after 3 days growth on DMSO, 0.1 µM and 3.3 µM oryzalin. Scale bars, 50 µm.
(C) Percentage of divided (blue) and undivided (grey) spores in a population grown for 2 days on 0.1 µM, 3.3 µM and 10 µM oryzalin and DMSO. N is the number of spores quantified for each dose.

This data identifies a range of oryzalin doses at which spore development is greatly altered (>3.3 μM) and subtly altered (<1 μM). There is no evidence of oryzalin disrupting the first asymmetric division, although testing of concentrations between this range may identify a dose at which spores divide symmetrically. To then accurately test if microtubules are required for spore polarisation, spores expressing a nuclear - plasma membrane reporter should be treated with oryzalin, and the position of the nucleus and division plane quantified.

2.5 Discussion

2.5.1 Migration of the nucleus and polar organisers to the basal pole results in the first asymmetric division

The single-celled spore begins the multicellular haploid stage of *M. polymorpha*'s lifecycle. In this chapter I show that the first division of the spore is asymmetric, generating a large apical cell and small basal cell, and is the result of the asymmetric placement of the nucleus. The nucleus starts roughly in the cell centroid but then migrates to the basal cortex. Nuclear migration leading to an asymmetric division is a common feature of cell polarisation, as seen in fern spores, angiosperm zygotes and stomatal cells (Edwards & Roux, 1998; Kimata *et al.*, 2016; Muroyama *et al.*, 2020). However, the mechanism driving and directing nuclear migrations can vary. In *M. polymorpha* spores, I show that the polar organisers (PO) - the MTOCs of liverworts - are tightly associated with the nucleus and they migrate together during spore polarisation. One PO always leads this migration and eventually docks at the basal cortex (**Summary Figure 2.1**). My data suggests that acentrosomal MTOCs are involved in spore polarisation, potentially by directing nuclear migration.

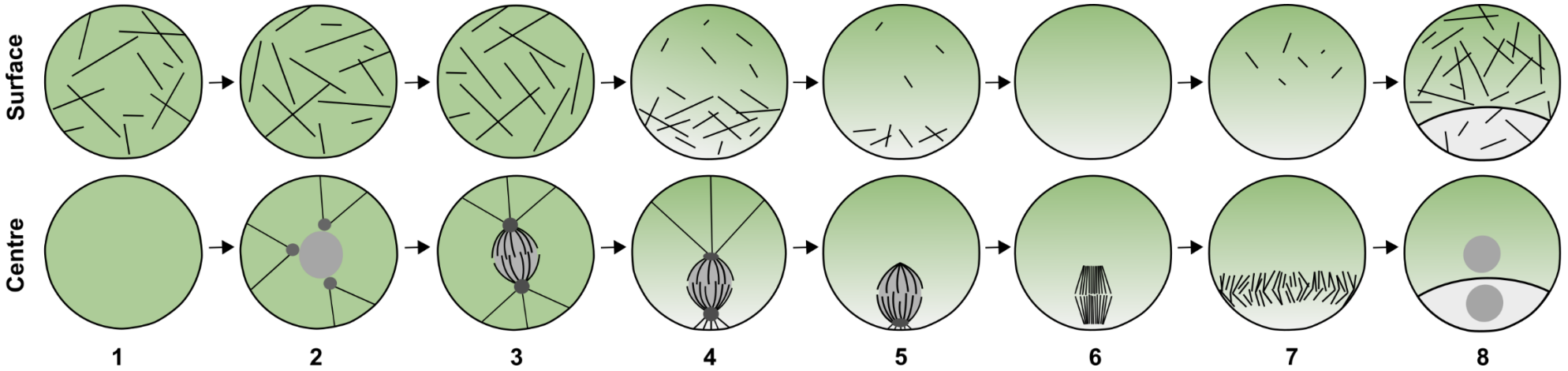

Summary Figure 2.1: Organisation of microtubules at the surface and in the centre of a *Marchantia polymorpha* spore during polarisation and the first asymmetric division

Diagram of microtubule and nucleus reorganisation during *M. polymorpha* spore development, with views of both the cell surface and a slice through the cell centre. Microtubules (black lines), nucleus (light grey circles) and polar organisers (dark grey circles).

Spore surface: **(1, 2, 3)** Random cortical microtubules. **(4)** Reduction in cortical microtubules from apical pole and accumulation at basal pole. **(5)** Further reduction in cortical microtubules. **(6)** No cortical microtubules. **(7)** Re-establishment of cortical arrays. **(8)** Random cortical arrays in apical and basal cells.

Spore centre: **(1)** No microtubule structures. **(2)** Microtubule foci around the nucleus. **(3)** Polar organisers with peri-nuclear microtubules (microtubule basket) around the central nucleus and astral arrays. **(4)** Nucleus and microtubule basket near the basal cortex. **(5)** Disintegration of polar organisers and change in microtubule basket shape. **(6)** Mitotic spindle. **(7)** Phragmoplast. **(8)** Divided cell

I propose that the mechanism driving the PO - nucleus migration is linked to the dense astral array that is nucleated from the basal PO and polymerises out towards the basal cortex. In *M. polymorpha* epidermal cells, astral arrays interact with the cortex and the pre-prophase band (PPB) to stabilise and position the POs and nucleus in the cell centre (Buschmann *et al.*, 2016). During the PO-nucleus migration in spores, the interaction of the astral arrays with the basal cortex could provide; a) directionality and/or b) a physical pulling force. I will explore both aspects in this discussion.

2.5.2 Does a polar protein domain direct nuclear migration in spores?

Organelle migration requires a direction, which in polarised cells is accomplished by a polar protein domain. In *M. polymorpha* spores, the nucleus appears to migrate towards a specific cell cortex not in a random direction. This is evidenced by the rotation of POs to orient the direction of nuclear migration and by the first spore division being oriented by light (Rötzer *et al*., unpublished). I hypothesise that a polar protein domain marks the basal membrane in spores to anchor the astral arrays and guide the nuclear migration.

Here I will propose a potential mechanism for interaction between a polarity domain and microtubules to direct the nuclear migration in spores. After PO formation, the plus ends of astral microtubules search the membrane. A few astral arrays from the ‘basal-most’ PO find and anchor to the basal polar domain, starting PO rotation. Now the basal PO is positioned nearest the polar domain and nucleates more microtubules which rapidly polymerise towards the polar domain where they are stabilised. This forms the dense astral array between the nucleus and basal cortex and aligns the PO axis with the apical-basal cell axis, setting the direction for PO migration. A similar system of MTOC rotation and nuclear alignment occurs in Fucoid zygotes, where astral arrays from the basal-most centrosome anchor to adhesion sites at the basal cortex (Bisgrove & Kropf, 2001). However, despite the investigation of well-

known candidates, no polar proteins have yet been identified in spores. Thus, the formation and the components of a spore polar domain remain elusive.

2.5.3 The link to light: how does light influence the nuclear migration?

Light, specifically blue wavelengths, orients the first division of *M. polymorpha* spores to form the basal cell away from the light source (Rötzer *et al*., unpublished). The blue light receptor phototropin is hypothesised to be involved. But what is mechanistic link between blue light, microtubules, and nuclear migration in spores? One hypothesis is that blue light signalling directs polar proteins to the basal membrane to form a polar domain, as I previously theorised.

A complementary hypothesis is that blue light signalling triggers microtubule severing and depolymerisation in the apical hemisphere. In *A.thaliana* hypocotyls, blue light perceived by phototropin can initiate microtubule severing via the enzyme katanin to reorient microtubule arrays (Lindeboom *et al.*, 2013; Nakamura, 2015). In spores, increased depolymerisation of astral arrays in the apical hemisphere would weaken the attachment of the nucleus to the apical cortex. Now the nucleus could be easily pulled towards the basal domain.

2.5.4 Polar organisers and astral arrays: guiding or pulling the nucleus?

In combination with directionality, nuclear migration also requires a physical pulling force. An actin-myosin system could generate such power, as I will explore in Chapter 3. Alternatively astral microtubules, in combination with microtubule motor proteins, may generate the force required. Budding yeast may provide a comparable system. At the yeast bud site, dynein localises to the microtubule plus ends, sliding the microtubules relative to cortex and pulling the spindle poles and nucleus towards the cell edge (Moore *et al.*, 2009). Land plants, including *M. polymorpha*, do not possess cytoplasmic dynein but instead have expanded kinesin families, some of which take on dynein's minus-end directed functions (Gicking *et al.*, 2018; Nebenführ & Dixit, 2018) (**Supplementary Figure 2.3.A**). In particular, the Kinesin

with a Calponin-Homology domain (KCH) from the expanded kinesin-14 family has roles in nuclear migration in both rice and moss (Frey *et al.*, 2010; Yamada & Goshima, 2018). In spores, many kinesins are expressed in the first 30 hours after germination (unpublished data by Radka Slovak) (**Supplementary Figure 2.3.B**). As nuclear migration occurs at 28 to 32 hours after spore germination, this is consistent with the hypothesis that a kinesin acts on astral microtubules to pull the nucleus towards the basal cortex.

2.5.5 Spore polarity may become fixed on polar organiser migration

Fixation of polarity is the point at which a cell cannot repolarise to new cues (Fowler & Quatrano, 1995). In spores, polar organisers can reorientate prior to their migration but once the basal PO is docked at the basal cortex, no further reorientation or movement was ever observed. Subsequently the spore always divided at this basal plane. This suggests that polarity is fixed once the basal PO docks at the basal cortex, typically between 28 and 32 hours after germination. Consistent with this hypothesis, the timepoint at which reversal of the light direction no longer reverses the orientation of spore division is 28 hours after germination (Rötzer *et al*., unpublished).

2.5.6 Cortical microtubule depletion may be linked to polar organiser migration

Migration of the nucleus is correlated with rearrangement of the cortical microtubules. Spores have a dynamic cortical array which is randomly distributed upon PO formation but depletes from the apical hemisphere as the POs and nucleus repositions to the basal pole (**Summary Figure 2.1**). Cortical microtubule redistribution is also seen in Fucoid zygotes, where cortical arrays deplete from the apical zone and accumulate at the future rhizoid outgrowth site (Corellou *et al.*, 2005). The mechanism behind cortical microtubule depletion and the resulting asymmetry is unclear.

One hypothesis is that microtubule-associated proteins destabilise microtubules in the apical hemisphere. A major candidate is the microtubule severing enzyme, katanin, which is known

to cut microtubules in response to blue light resulting in microtubule depolymerisation (Lindeboom *et al.*, 2013; Nakamura, 2015). There is also a variety of proteins which can reduce plus end polymerisation rate, increase catastrophe rates, or decrease minus-end stability. An example is BASL/BRXf which locally destabilises microtubules to generate a depleted cortical zone in stomatal cells (Muroyama *et al.*, 2023). This in turn prevents PPB formation and division within the BASL/BRXf domain. If a similar zone of depolymerisation is present in the spore apical hemisphere, this may the reduce cortical array density and prevent division in this region. To narrow down the possible mechanisms, microtubule polymerisation and depolymerisation rates could be measured in each spore hemisphere.

Another potential mechanism is that the rate of cortical microtubule nucleation is lower in the apical hemisphere. This could result from fewer independent foci or from the PO migration. In *M. polymorpha*, it is unknown if all cortical microtubules are nucleated from independent foci or if a sub-population are nucleated at the PO and released into the cortex. In spores, I show EB1 tracks extending from the basal PO into the basal cortex. This suggests that some microtubules nucleated from POs polymerise into the cortex, although it was unclear if these microtubules were severed and released to join the cortical microtubule population. Based on these data, I hypothesise that as the POs migrate to the basal pole, more microtubules are fed into the basal cortex. By contrast, less microtubules are fed into the apical cortex, and this results in the overall cortical microtubule asymmetry.

2.5.7 The biological function of the cortical microtubule asymmetry is unclear

The biological function of the cortical microtubule asymmetry is another uncertainty. Cortical microtubules typically act to control the direction of cell growth in plants via cellulose deposition (Burk & Ye, 2002). However, the spore stays spherical and does not change shape during polarisation. Alternatively, depolymerisation of microtubules could release αβ-tubulin dimers to enable polymerisation of the dense astral array from the basal PO. In this

theory, all cortical microtubules could be subject to depolymerisation but only the basal cortical microtubules are re-established from the basal PO.

One final hypothesis is that the basal cortical array acts as a rudimentary PPB, depositing proteins at the cell cortex to guide the expanding phragmoplast. The PPB in *M. polymorpha* epidermal cells is a tight band of parallel microtubules at the cortex aligning with the nucleus in the cell centre (Buschmann *et al.*, 2016). In spores, after the depletion of microtubules in the apical cortex, the remaining microtubules in the basal cortex roughly align with the centre of the docked nucleus. However, the density and orientation of these microtubules is highly variable and does not mirror the PPB in epidermal cells. Such structural variability would prove unreliable in determining the future division plane. Overall, there are many possible functions for the development of cortical microtubule asymmetry in spores, but which is true remains unclear.

2.5.8 Conclusion

To summarise this chapter, the nucleus migrates towards the basal cortex to orient the first asymmetric division of the spore and to define the first apical-basal body axis of *M. polymorpha*. This migration is led by an acentrosomal MTOC nucleating a dense astral array which polymerises towards the basal cortex. Polar localisation of the nucleus, MTOC and microtubules are now the first known signs of polarity in *M. polymorpha* spores.

2.6 Supplementary Data

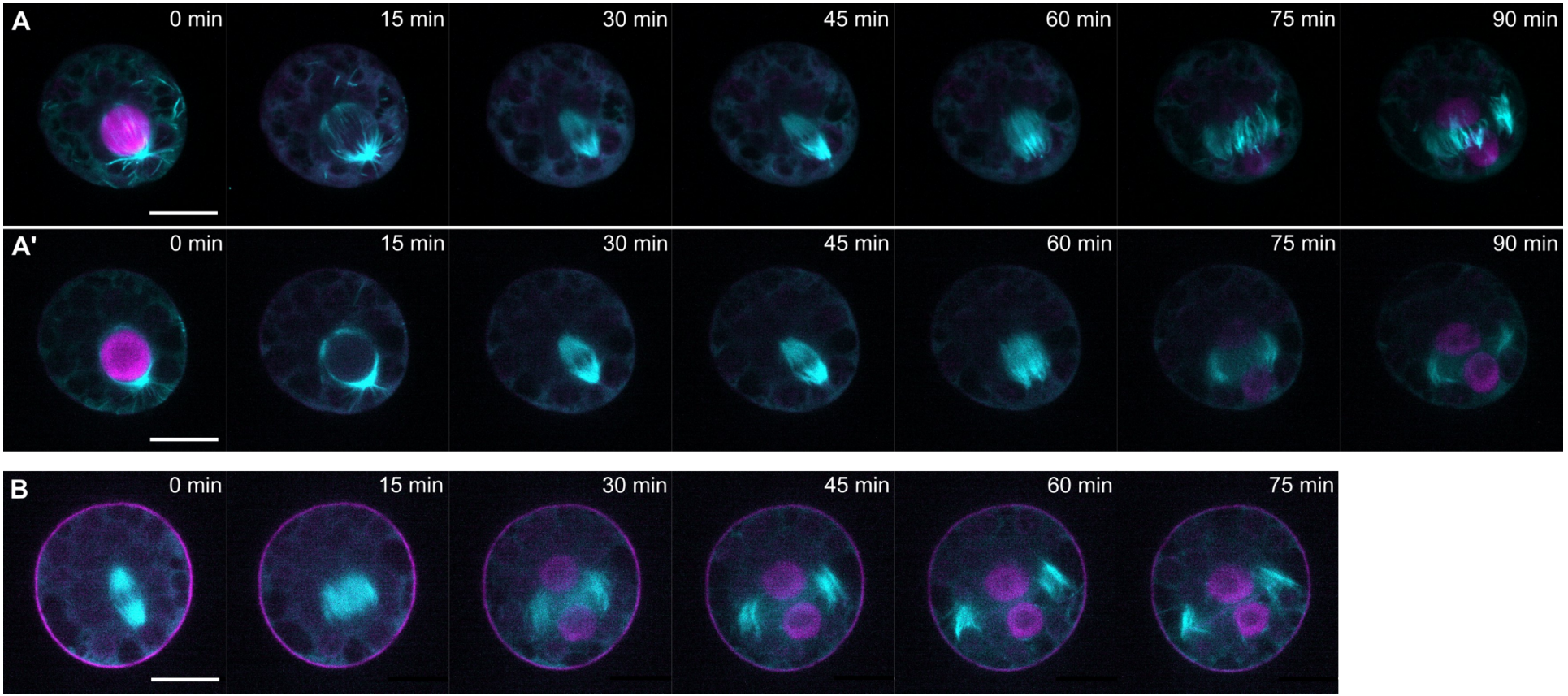

Supplementary Figure 2.1: The nuclear localised signal disappears on mitosis and reappears in the two daughter cells
(A - B) Timelapses of spores expressing *p*Mp*EF1α:GFP*-Mp*TUB1 (*cyan) and *p*Mp*ROP:mScarletI-N7* - *p*Mp*UBE2:mScarletI*-At*LTI6b* (magenta) at 29 hours after germination. Presented are Z-projections (A) and central planes in XY (A', B). **(A)** Nucleus within a microtubule basket near the basal pole followed by disappearance of the nuclear localised signal, then mitosis, phragmoplast expansion and appearance of two daughter nuclei. **(B)** Phragmoplast expansion resulting in two daughter cells each with a nucleus. Scale bars, 10 µm.

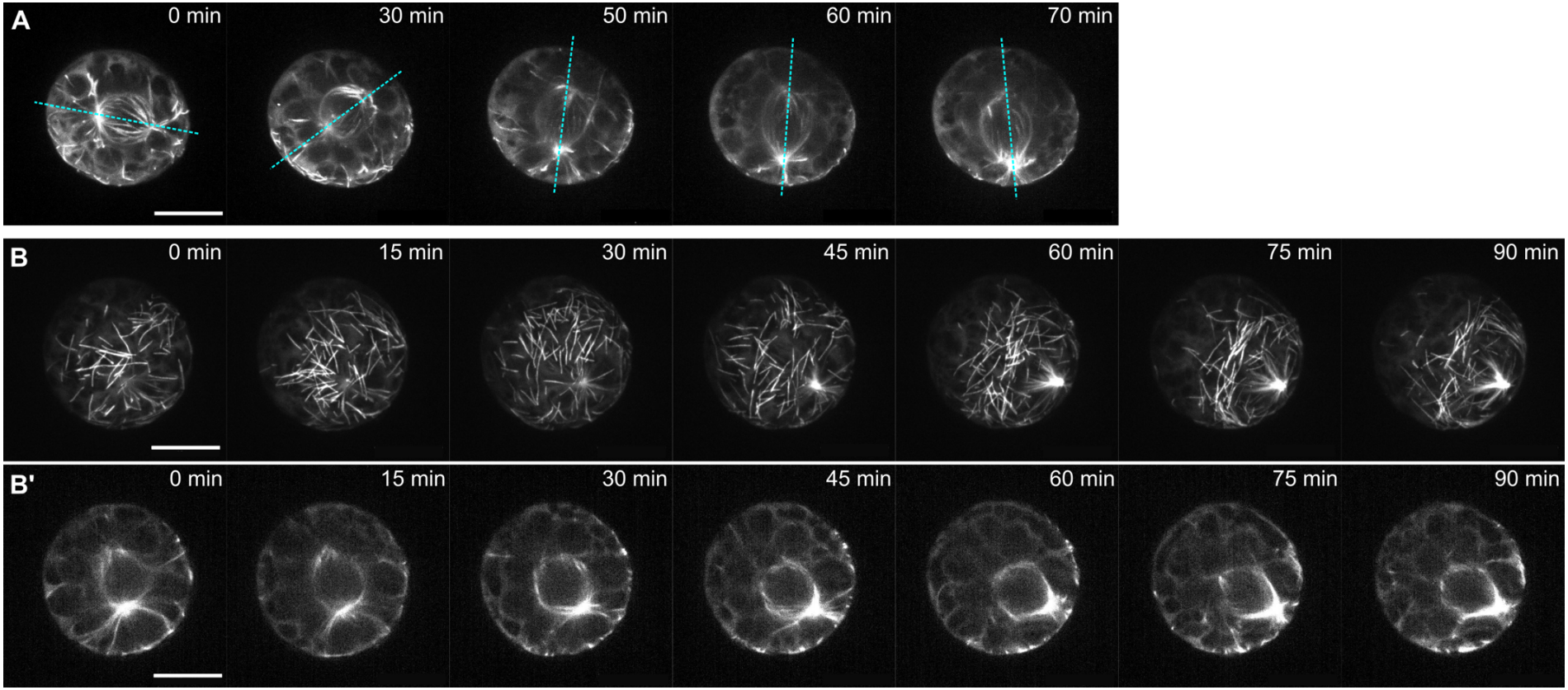

Supplementary Figure 2.2: Polar organisers rotate prior to migration, and cortical microtubules deplete from the apical hemisphere
(A - B) Timelapses of spores expressing *p*Mp*EF1α:GFP*-Mp*TUB1* at 29 hours after germination. Presented are Z-projections of the central slices (A), full Z-projections (B) and central slices in XY (B'). **(A)** Timelapse of polar organisers rotating in three dimensions before migration to the cell cortex. Dotted cyan lines mark the polar organiser axis. **(B)** Timelapse of cortical microtubule reduction from the apical pole during polar organiser migration. A ring of microtubules forms near the basal pole at 75 to 90 minutes. Scale bars, 10 µm.

A

Kinesin Family	Subfamily	*A. thaliana*	*P. patens*	*M. polymorpha*	Acronym
Kinesin-ARK	ARK	3	4	1	
	ARK-like	0	1	0	
Kinesin-1	I	1	0	0	
Kinesin-2	I	0	1	1	
Kinesin-4	I	3	5	1	FRA1
	II	0	3	1	
Kinesin-5	I	4	4	1	KRP125c
Kinesin-6	I	1	0	0	
Kinesin-7	I	5	2	1	MKRP1/2
	II	8	3	1	NACK1/2
	III	1	1	1	
	IV	1	1	1	
Kinesin-8	I	1	2	1	
	II	1	1	1	
Kinesin-9	I	0	3	1	
Kinesin-10	I	1	1	1	PAKRP2
	II	2	0	1	
Kinesin-12	I	3	15	1	POK1/2
	II	3	3	1	PAKRP1
Kinesin-13	I	2	3	1	
Kinesin-14	I	4	2	1	ATK
	II	9	4	1	KCH
	III	3	2	1	
	IV	2	1	0	
	V	2	2	1	KAC
	VI	1	4	1	KCBP

B

Gene ID	Kinesin subfamily	0 hours	15 hours	30 hours	Mean
Mapoly0114s0009	ARK	265.94	390.20	534.68	396.94
Mapoly0016s0024	Kin2	12.71	23.38	18.77	18.29
Mapoly0005s0208	Kin4-I (FRA1)	371.07	223.33	451.30	348.56
Mapoly0051s0102	Kin4-II	7.02	10.03	7.79	8.28
Mapoly0087s0035	Kin5 (KRP125)	27.94	54.43	649.40	243.92
Mapoly0019s0177	Kin7-I (MKRP)	121.69	273.41	364.00	253.04
Mapoly0025s0108	Kin7-II (NACK)	863.76	23.51	278.79	388.69
Mapoly0060s0012	Kin7-III	36.50	51.57	254.09	114.05
Mapoly0034s0119	Kin7-IV	7.49	60.01	268.84	112.11
Mapoly0026s0062	Kin8-I	640.97	188.64	187.42	339.01
Mapoly0093s0013	Kin8-II	471.77	93.80	116.56	227.38
Mapoly0040s0110	Kin-9	5.68	4.09	14.89	8.22
Mapoly0051s0002	Kin10-I (PAKR2P)	139.67	25.44	162.30	109.14
Mapoly0065s0078	Kin10-II	55.97	50.63	155.63	87.41
Mapoly0029s0045	Kin12-I (POK)	67.21	21.32	142.18	76.90
Mapoly0001s0076	Kin12-II (PAKRP1)	1.14	0.51	163.94	55.19
Mapoly0061s0132	Kin13	224.41	187.59	317.56	243.19
Mapoly0030s0095	Kin14-I (ATK1/5)	96.67	76.85	359.26	177.59
Mapoly0065s0070	Kin14-II (KCH)	1132.61	323.96	323.91	593.49
Mapoly0098s0032	Kin14-III	12.60	0.00	168.88	60.49
Mapoly0022s0156	Kin14-V (KCA)	317.37	323.72	491.38	377.49
Mapoly0012s0174	Kin14-VI (KCBP/ZWI)	636.64	954.74	1119.75	903.71

Supplementary Figure 2.3: Presence of kinesin motor protein family members in *M. polymorpha* and their expression levels in developing spores

(A) Table of kinesin families and subfamilies and their copy number in *Arabidopsis thaliana*, *Physcomitrium patens* and *Marchantia polymorpha*. Data from Richardson *et al.*, 2006; Shen *et al.*, 2012 and from BLAST searches of sequences against the *M. polymorpha* genome.

(B) Expression levels of each identified *M. polymorpha* kinesin in spores at 0, 15 and 30 hours after germination. Presented is RNA seq data collected and analysed by Radka Slovak. Level at each timepoint represent the mean of two samples. The overall mean represents the mean across all timepoints.

Chapter 3: Actin filament organisation during the polarisation of *Marchantia polymorpha* spores.

3.1 Abstract

Microtubules and actin filaments play distinct but complementing roles to generate cell asymmetry. Despite this, their respective dynamics and functions are rarely characterised in the polarisation of plant cells, particularly in the single cells – spores and zygotes – which give rise to the multicellular haploid and diploid phases of the land plant lifecycle respectively. My previous work established that the spores of the liverwort, *Marchantia polymorpha*, polarise by migration of the nucleus towards the cell cortex led by a microtubule organising centre and dense astral array (Chapter 2). Here, I aim to describe the dynamics of actin filaments as polarity develops in the spore. By imaging live spores expressing actin filament and nucleus reporters, I discovered that an actin filament network forms between the migrating nucleus and the basal cortex. On disruption of actin filaments in spores, I show evidence that rhizoid formation is prevented, and spores often divide symmetrically. Altogether my data supports the hypothesis that actin filaments are required for nuclear migration during the polarisation of *M. polymorpha* spores.

3.2 Introduction

Actin filaments are dynamic polymers which organise into a variety of structures from fine webs to thick bundles. By interacting with motor proteins, which hydrolyse ATP to generate force, actin filaments can move organelles and traffic vesicles to develop cell asymmetry. Using fluorescent reporters, live actin filament dynamics can be captured in plant cells and their role in polarity characterised (Era *et al.*, 2009; Vidali *et al.*, 2009). In this chapter I will investigate the dynamics of actin cytoskeleton in the polarisation of *M. polymorpha* spores.

In the single isolated cells which give rise to multicellular organisms, polarity – the asymmetric distribution of components within a cell – is generated along an apical-basal or posterior-anterior axis. This cellular axis orients the first asymmetric cell division (ACD) to pattern organism development. Actin filaments can establish this axis in animal and algal zygotes through a variety of mechanisms. In the *C. elegans* embryo, a contractile actin web forms across the anterior end to push cortical components to the posterior end (Munro *et al.*, 2004). Whilst in *Fucus* zygotes an actin patch forms at the basal cortex to target vesicles to this domain (Alessa & Kropf, 1999; Hable & Kropf, 2005). Each of these mechanisms requires a complex network of actin filaments. To generate these networks, actin filaments are tightly regulated by accessory proteins which can nucleate filaments at specific membrane domains, modulate their depolymerisation or cross link filaments into bundles (Pollard, 2016). In summary, actin filaments and accessory proteins are involved in the establishment of polarity at the one-cell stage in diverse organisms.

Actin filament dynamics are less well characterised in the single cells from which land plants develop. Land plants have two multicellular lifecycle phases - the diploid sporophyte and haploid gametophyte - each of which develop from a polarised single cell - the diploid zygote and haploid spore. For zygotes, there is gathering evidence that actin filaments are required during polarisation. In *A. thaliana* zygotes, an apical actin cap and longitudinal actin cables reorganise the vacuoles and direct the nucleus to the elongating cell apex (Kimata *et al.*, 2016, 2019). Such migration of organelles, especially of the nucleus and chloroplasts, is a function carried out by actin filaments in many plant cell types (Higa *et al.*, 2014). On the other hand, the role of actin filaments in the polarisation of spores is little known.

Actin filaments can generate a polar axis in preparation for an asymmetric cell division but can also generate a single polarised point for cell outgrowth. Formation of a localised domain enriched in actin filaments followed by targeted vesicle trafficking is a common mechanism used in tip-growing cells. In root hairs, highly-mobile fine actin webs form at the apex and dense stable cables stretch along the cell axis to ferry vesicles to the growing tip

(Era *et al.*, 2009). Similarly in pollen, an actin 'collar' forms at the germination site and the pollen tube subsequently outgrows by actin-mediated exocytosis (Liu *et al.*, 2018; Zhang *et al.*, 2023). Polarised growth not only occurs in tip-growing cells but also to a lesser extent in plant zygotes. Both angiosperm and brown algae zygotes undergo polar growth prior to asymmetric division, the latter by a basal actin patch directing exocytosis (Goodner & Quatrano, 1993; Lau *et al.*, 2012). Generation of cell polarity and changes in cell shape are therefore often intertwined making their respective mechanisms hard to distinguish.

The haploid spore of the liverwort, *M. polymorpha*, provides an ideal system to study actin filament dynamics during cell polarisation. Spores are single cells which polarise and divide asymmetrically to establish the plant's first apical-basal axis (Shimamura, 2016). Unlike *A. thaliana* zygotes, the spore stays spherical and does not undergo polarised growth or shape change prior to the first division. Polarity is established entirely internally involving the migration of the nucleus from the spore centroid to the basal cortex (Chapter 2). By studying the dynamics of actin filaments in polarising spores, I can uniquely test the role of actin filaments in establishing cell polarity independent of their role in generating morphology asymmetry. My prediction is that actin filaments and microtubules will function together to move the nucleus. In summary, my research uses a novel plant system to expand our understanding of the actin mechanisms which generate polarity from a non-polar state.

To investigate the role of actin filaments in the polarisation of *M. polymorpha* spores, I conducted live microscopy of actin filaments and nuclei in spores. I demonstrate that an actin network forms between the nucleus and basal cortex during spore polarisation. On actin inhibition, spores often divided symmetrically. Taken together, I speculate that actin filaments function to pull or anchor the nucleus to the basal pole during spore polarisation.

3.3 Materials and Methods

3.3.1 Plant lines, growth conditions and crossings

The wild type *M. polymorpha* accessions, the growth conditions, the method of crossing plants and spore sterilisation were the same as previously described in Chapter 2.3.1/ 2.3.2.

3.3.2 Reporter constructs

The *p*Mp*ROP:mScarletI-N7* - *p*Mp*UBE2:mScarletI-LTI6b* double reporter, labelling the nucleus and plasma membrane, was cloned by Hugh Mulvey as described in Chapter 2.3.3.

The *p*Mp*WDL:GFP-LifeAct* (GFP-LifeAct) fluorescent reporter labelling actin filaments is a unpublished construct which was cloned and kindly given by Clément Champion. The construct is composed of a LifeAct sequence – ATGGGTGTCGCAGATTTGATCAAGAAAT TCGAAAGCATCTCAAAGGAAGAA - fused to GFP expressed under the promotor of the *M. polymorpha WAVE-DAMPENED-LIKE* gene (Champion *et al.*, 2021).

3.3.3 Transformation of *M. polymorpha*

Constructs were transformed into *Agrobacterium* and then into *M. polymorpha* following the methods in Chapter 2.3.4/2.3.5. GFP-LifeAct transformants were selected by their resistance to 10 µg/mL G418 and checked for fluorescence using confocal microscopy.

3.3.4 Stereomicroscope imaging of plants

Spores grown on media plates were imaged using a Keyence VHX-7000 digital microscope equipped with a VHX-7020 camera and VH-ZST lens.

3.3.5 Spinning disk imaging of subcellular structures in gemmae

Gemmae expressing GFP-LifeAct were setup and grown in imaging chambers for 1 day following the method in Chapter 4.3.12. The actin filaments in the gemmae were imaged

using an Olympus IX3 Series (IX83) inverted microscope equipped with a Yokogawa W1 spinning disk, Hamamatsu ORCA-Fusion CMOS camera and 10x/0.4 NA air and 100x/1.45 NA oil objectives. Samples were excited at 488 nm and emission captured at 525 nm.

3.3.6 Spinning disk imaging of subcellular structures in spores

Spores for fluorescence imaging were setup in chambers and grown for 29 or 50 hours using the same method as described in Chapter 2.3.7. Spores were derived from crosses between plants expressing *p*Mp*WDL:GFP-LifeAct* and plants expressing *p*Mp*ROP:mScarletI-N7* - *p*Mp*UBE2:mScarletI*-At*LTI6b* or Tak-2.

Spores were imaged using an Olympus IX3 Series (IX83) inverted microscope equipped with a Yokogawa W1 spinning disk, Hamamatsu ORCA-Fusion CMOS camera and a 100x/1.45 NA oil objective. Imaging used the same method as described in Chapter 2.3.8.

3.3.7 Image presentation and analysis

Z-projections and central slices were converted in ImageJ Fiji (Schindelin *et al.*, 2012). Temporal projection of short interval timelapses were also generated in ImageJ Fiji.

The signal intensity profiles of GFP and mScarlet fluorophores around the spore perimeter were generated in ImageJ Fiji, using a script written by Tomas Lendl from the BioOptics Facility at the Vienna BioCenter. A sum-of-slices projection of a 5.2 µm region surrounding the medial plane was created for each spore. The perimeters were outlined using the segmented line tool set at spline 5, starting at 12 o'clock and moving clockwise. The script then applied background subtraction, scaled the two fluorophore intensities to the mean, and normalised the relative signal intensities. The resultant fluorophore intensity profiles, ranging from 0 to 1, were plotted against the distance around cell perimeter (µm) from the starting point. Plots were automatically generated using the ImageJ Fiji script.

3.3.8 Latrunculin B drug treatment on spores

Gamborg media plates containing Latrunculin B (LatB), dissolved in DMSO, were made to the final LatB concentrations: 0.01 µM, 0.03 µM, 0.1 µM, 0.33 µM, 1 µM and 5 µM. 1% DMSO was used as a control. Wild type spores, derived from crossing Tak-1 and Tak-2, were sterilised and spread on the media containing LatB. Sporeling were grown in the conditions set in Chapter 2.3.1 and imaged at 2, 3 and 4 days using the Keyence microscope as stated in Chapter 3.3.4.

3.4 Results

3.4.1 Actin filaments form a highly dynamic mesh at the spore cortex

To investigate the organisation and dynamics of actin filaments during spore development, I labelled live actin filaments using the *p*Mp*WDL:GFP-LifeAct* (GFP-LifeAct) reporter, made by Clément Champion. LifeAct is a short protein known to label actin filaments in *A. thaliana* and *M. polymorpha* (Riedl *et al.*, 2008; Era *et al.*, 2009). The *p*Mp*WDL:GFP-LifeAct* reporter is composed of a LifeAct sequence fused to GFP and expressed under the constitutive *p*Mp*WDL* promotor. Labelling of actin filaments by GFP-LifeAct was first confirmed in *M. polymorpha* epidermal cells (**Figure 3.1.A-C**). Plants expressing GFP-LifeAct were then crossed to wild type to produce spore populations in which half expressed the reporter.

To gain initial insights into the actin filament organisation in spores, spores expressing GFP-LifeAct were imaged at 29 hours after germination. A multi-layered, dense meshwork of filaments was present at the spore surface (**Figure 3.1.D, E**). These filaments were randomly organised and varied in length and density between spores. Timelapses with 3-second interval revealed that the cortical filaments were highly dynamic, constantly polymerising and altering organisation (**Figure 3.1.F**). In conclusion, there is a dynamic actin cortex in spores which is successfully labelled by GFP-LifeAct.

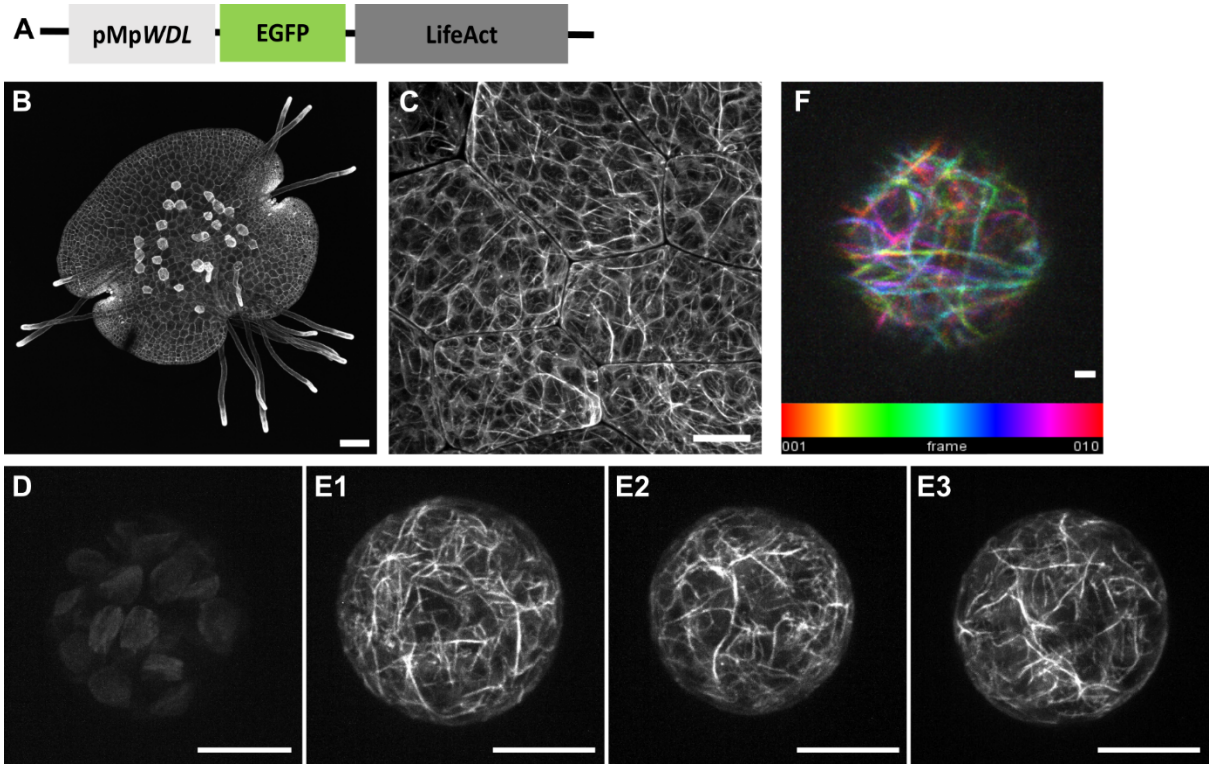

Figure 3.1: GFP-LifeAct labels dynamic cortical actin filaments in *M. polymorpha* spores
(A) Schematic of the actin filament reporter, *p*Mp*WDL:GFP-LifeAct.*
(B) Actin filaments are labelled in all the cells of a 1-day-old gemma expressing *p*Mp*WDL:GFP-LifeAct*, especially at the rhizoid tips. Scale bar, 100 µm.
(C) Actin filaments are labelled at the cortex of epidermal cells in a 1-day-old gemma expressing *p*Mp*WDL:GFP-LifeAct*. Scale bar, 10 µm.
(D) GFP autofluorescence of a wild type spore at 29 hours after germination. Scale bars, 10 µm.
(E) Actin filaments are labelled at cortex of three spores (E1 - E3) expressing *p*Mp*WDL:GFP-LifeAct* at 29 hours after germination. Scale bars, 10 µm.
(F) Temporal projection of actin filaments polymerising across the cortex of a spore expressing *p*Mp*WDL:GFP-LifeAct* at 30 hours after germination. Timelapse captured the top 5 µm of the spore with 3 seconds intervals. Z-projections were generated before temporal projection. Scale bar, 1 µm.

3.4.2 Actin filaments form a network between the nucleus and basal cortex

In Chapter 2, I showed that the nucleus migrates from the cell centroid to the basal cortex prior to the first division in spores. Nucleus location therefore indicates whether a spore is non-polar (central nucleus) or polarised (basal nucleus). To test if actin filaments reorganise during spore polarisation, I compared the actin organisation in spores with a central nucleus to spores with a basal nucleus. For this analysis, spores were generated by crossing plants expressing GFP-LifeAct to plants expressing *p*Mp*ROP:mScarletI-N7* – *p*Mp*UBE2:mScarletI-*At*LTI6b*. In spores with a central nucleus, actin filaments were randomly distributed across

the cortex and no filaments were observed near the nucleus (**Figure 3.2.A**). In spores with a basal nucleus, there was a network of fine actin filaments located between the nucleus and the basal cortex (**Figure 3.2.B**). In timelapses, this actin network persisted throughout the time when the nucleus was near the basal cortex (0 - 45 minutes) (**Figure 3.2.C**). Whilst the cortical actin filaments appeared randomly distributed at every timepoint with no clear asymmetry. Overall, actin filaments form a network between the nucleus and the basal cortex during spore polarisation.

To verify the presence of an actin network at the basal pole of polarised spores, the signal intensity of RFP (plasma membrane) and GFP (actin filaments) around the cell perimeter was quantified in spores expressing mScarletI-AtLTI6b and GFP-LifeAct reporters. In spores with a central nucleus, the GFP signal varied around the spore perimeter in a similar pattern to the RFP signal (**Figure 3.2.D, Figure 3.3.A**). Occasional spikes in GFP intensity correlated to actin bundles in the cortex. In spores with a basal nucleus, the intensity patterns were similar except for the GFP intensity was greatly increased compared to the RFP intensity for a 10 µm region between 28 and 38 µm distance (**Figure 3.2.E**). This 10 µm region represents the half-way point around the spore perimeter and is the closest region to the basal nucleus e.g., the basal pole. Seven spores with a basal nucleus were analysed, and in all spores the GFP intensity was consistently higher than the RFP intensity at the region correlating to the basal pole, typically between 30 and 40 µm distance (**Figure 3.3.B**). There was however variability in the intensity, distance, and appearance of the GFP signal at this region; sometimes appearing as one clear peak, as multiple high peaks, or as low scattered peaks (**Figure 3.3.B**). This may reflect the dynamic nature of actin filaments. Overall, the data indicates that there is a heightened GFP signal, and therefore actin filament density, at the basal pole of polarised spores which is absent in non-polar spores.

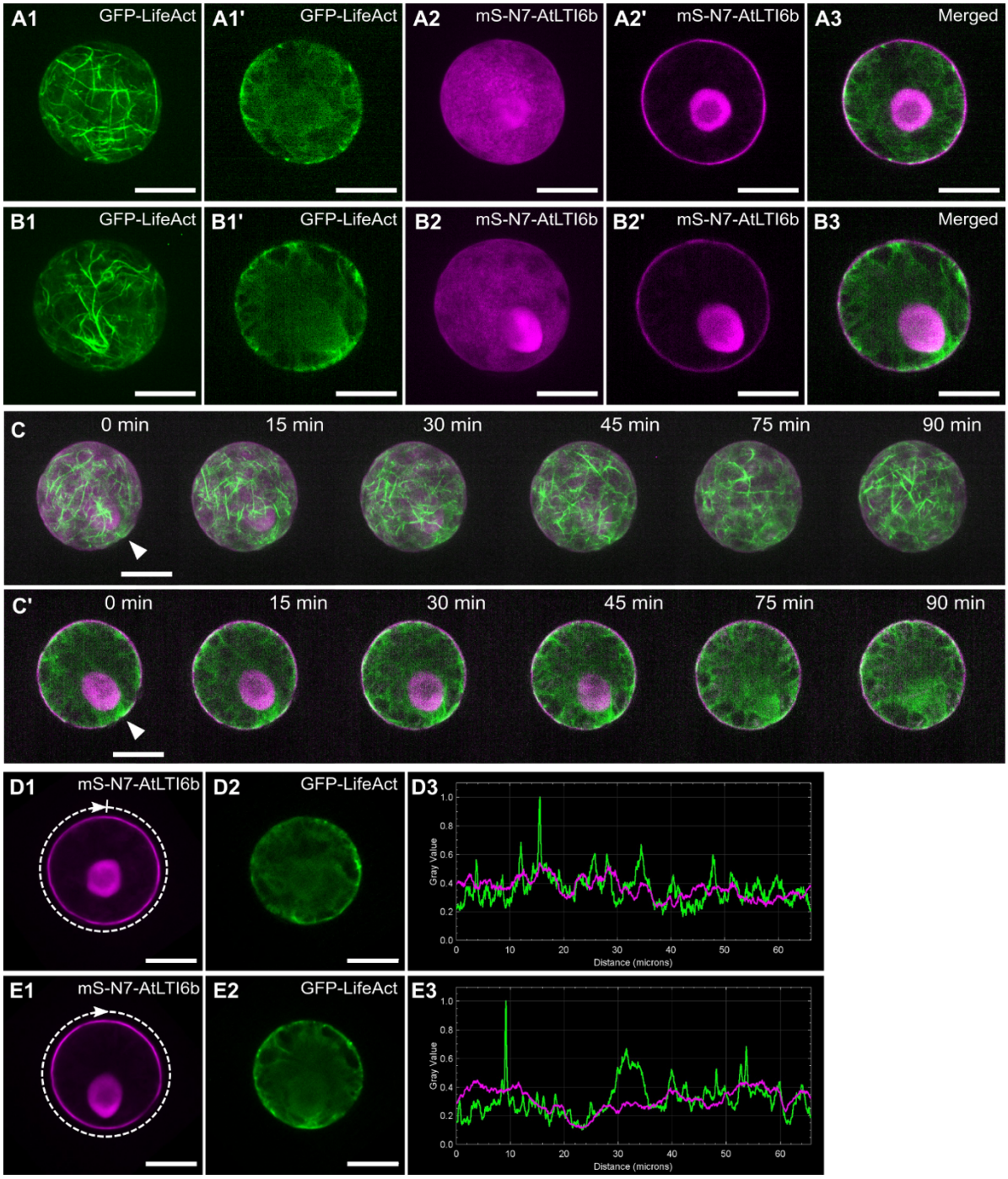

Figure 3.2: An actin filament network forms between the nucleus and basal cortex
(A - B) Actin organisation in a spore with a central nucleus **(A)** and basal nucleus **(B)** expressing *p*Mp*WDL:GFP-LifeAct* (green) and *p*Mp*UBE2:mScarletI*-At*LTI6b - p*Mp*ROP:mScarletI-N7* (magenta) at 29 hours after germination. Presented are Z-projections of GFP (A1, B1) and mScarlet (A2, B2) and central XY slices of GFP (A1', B1') and mScarlet (A2', B2'). Scale bars, 10 µm.
(C) Timelapse of actin filament organisation in a spore expressing *p*Mp*WDL:GFP-LifeAct* (green) and *p*Mp*UBE2:mScarletI*-At*LTI6b - p*Mp*ROP:mScarletI-N7* (magenta) starting at 29 hours after germination. Presented are Z-projections of the merged channels (C) and central slices in XY of the merged channels (C'). An actin network is present between the basal nucleus and basal cortex at 0 - 45 minutes, indicated by a white arrow. Scale bars, 10 µm.
(D - E) Comparison of the RFP (plasma membrane) and GFP (actin) signal intensity around the circumference of a spore with a central nucleus **(D)** and a spore with a basal nucleus **(E)** expressing

*p*Mp*WDL:GFP-LifeAct* (green) and *p*Mp*UBE2:mScarletI*-At*LTI6b* - *p*Mp*ROP:mScarletI-N7* (magenta) at 29 hours after germination. Presented are sum-of-slices projections of the central 2.6 µm section in RFP (D1, E1) and GFP (D2, E2). Arrows indicate the start point and direction that intensity was measured. Graphs present the normalised intensity value (grey value) for each point (distance, µm) around the spore perimeter. Scale bars, 10 µm.

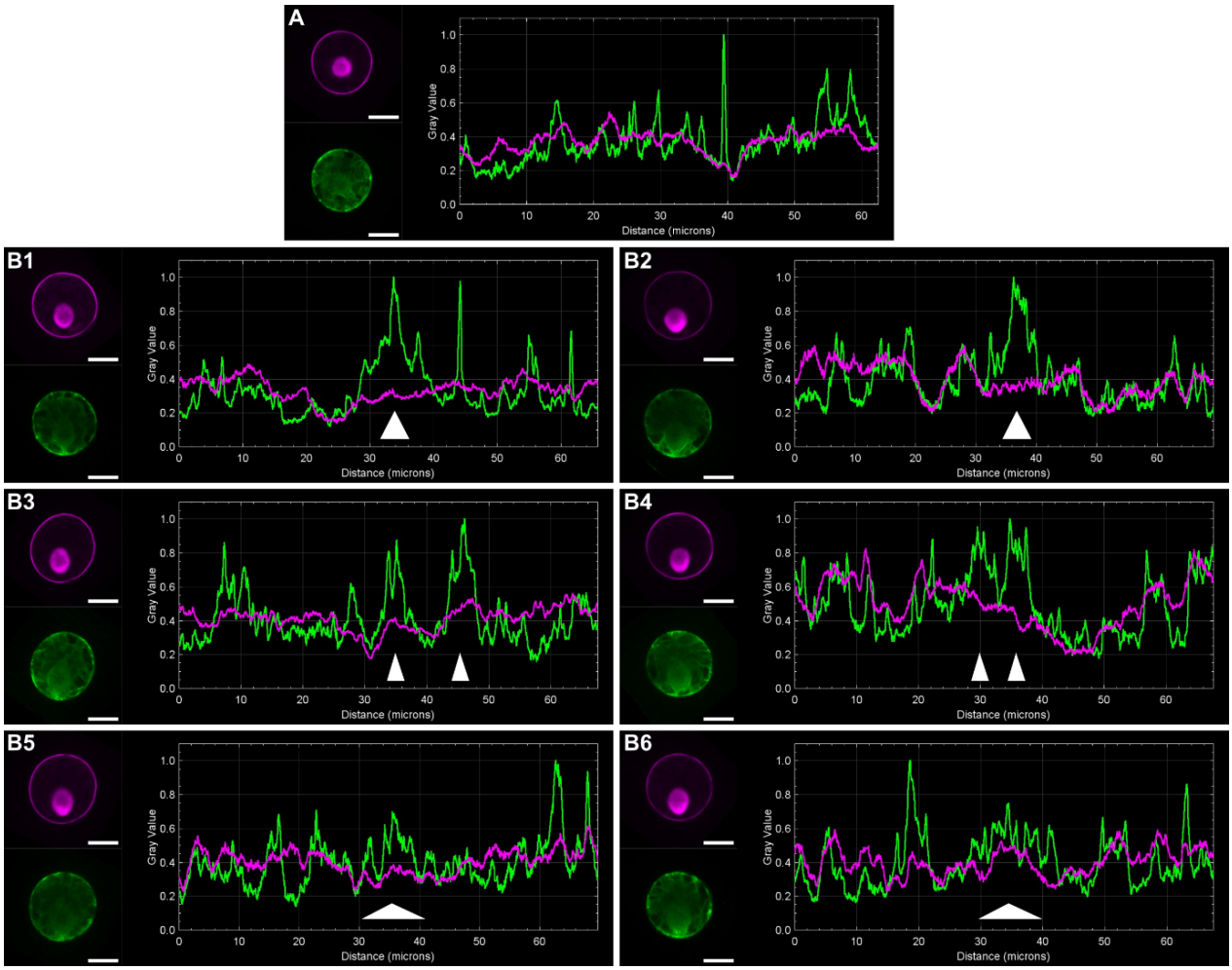

Figure 3.3: Variability in the intensity and area of the actin filament network at the basal pole
Intensity of GFP (actin) and RFP (plasma membrane) signal around of the circumference of a spore with central nucleus **(A)** and six spores with a basal nucleus **(B1 - B6)** expressing *p*Mp*WDL:GFP-LifeAct* (green), and *p*Mp*UBE2:mScarletI*-At*LTI6b* (magenta) are 29 hours after germination. Images present the sum-of-slices Z-projections of a central 2.6 µm region of each cell in GFP and RFP. Scale bars, 10 µm. Plots present the grey value (signal intensity value scaled to the mean and normalised) around the distance (µm) of the spore perimeter, proceeding clockwise from the start point (12 o'clock). 30 - 40 µm typically represents the basal pole. Regions of increased GFP signal at the basal pole are indicated by white arrows.

3.4.3 Cortical actin filaments are asymmetrically distributed during cytokinesis

To investigate if actin filaments reorganise during the first division or if the basal actin network is retained, spore populations expressing GFP-LifeAct were imaged at 29 hours after germination. A small proportion of spores had a short, dense plane of actin filaments predicted to be the phragmoplast (**Figure 3.4.A1-A3**). In these dividing cells, long cortical actin cables were present in the apical hemisphere (future apical cell), whereas short fine actin filaments filled the basal pole (future basal cell). Overall, actin has distinct organisations in the apical and basal domains of spores during cytokinesis.

3.4.4 Actin filaments accumulate at the growing tip of the basal daughter cell

The first spore division forms two cells, each with a different fate. To investigate if the actin filament organisation differs between the apical and basal daughter cells, divided spores were imaged at 29 and 50 hours after germination. In newly divided two-celled spores, cortical actin bundles were present in the apical cell and finer actin arrays in the basal cell (**Figure 3.4.B**). In mature two-celled spores, both apical and basal cells had a cortical actin mesh but at a higher density in the basal cell (**Figure 3.4.C**). In two-celled spores with elongated basal cells - now a differentiated rhizoid - a network of fine actin filaments was present at the rhizoid tip (**Figure 3.4.D**). This tip-localised network likely acts to direct endocytosis for polarised tip-growth. Overall, the apical and basal cells generated from the first asymmetric cell division have distinct actin organisations.

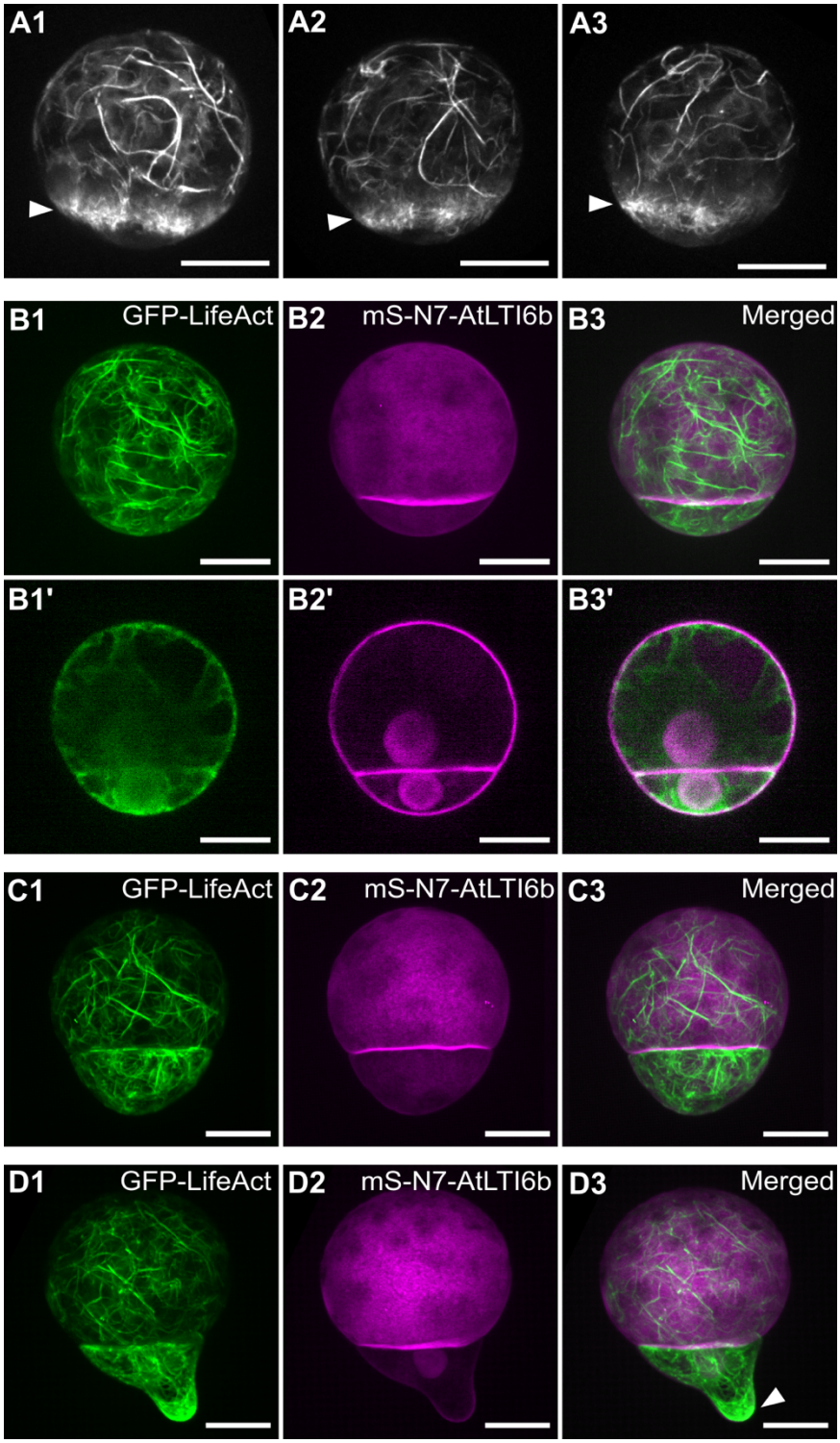

Figure 3.4: Distinct actin filament organisations form in the apical and basal daughter cells
(A) Actin filaments organisation during cytokinesis of spores expressing *p*Mp*WDL:GFP-LifeAct* at 29 hours after germination. Presented are Z-projections of three individual spores (A1-A3). White arrows indicate the phragmoplast. Scale bars, 10 µm.
(B - D) Actin filament organisation in two-celled spores expressing *p*Mp*WDL:GFP-LifeAct* (green) and *p*Mp*UBE2:mScarletI-*At*LTI6b* - *p*Mp*ROP:mScarletI-N7* (magenta) captured at 29 hours (B) or 50 hours (C, D) after germination. Presented are the GFP (B1-D1), RFP (B2- D3) and merged channels (B3-D3) as Z-projections (B-D) and as central XY planes (B'). A white arrow indicates the actin network at the rhizoid cell tip. Scale bars, 10 µm.

3.4.5 Inhibition of actin filaments prevents rhizoid formation in spores

I have shown that a basal actin network forms during spore polarisation. I hypothesise that actin filaments are required for spore polarisation and that on inhibition of actin filaments spores would not polarise and therefore divide symmetrically. To test this hypothesis, actin filament polymerisation was inhibited in spores using Latrunculin B (LatB).

To identify a LatB dose which inhibited actin filaments but still enabled the first division, wild type spores were grown on increasing concentrations of the LatB for 2 days and the number of divided spores was quantified. Overall, division rates decreased as the LatB concentration increased (**Figure 3.5.A, C**). When grown on the DMSO control and 0.01 µM LatB, 57.8% and 53.8% of spores had divided at least once. On 0.03 µM LatB, 43.8% of spore had divided and on 0.1 µM LatB only 11.7% had divided. Although the exact division plane was hard to quantify in this setup, on DMSO and 0.01 µM LatB most divisions appeared asymmetric. By contrast, on 0.1 µM LatB many divisions appeared symmetric forming two green cells of similar size. In conclusion, high doses of LatB (> 0.1 µM) lowers the rate of spore division and potentially increases symmetrical divisions.

The first asymmetrical division of the spore generates a small basal cell which differentiates into a rhizoid. To determine if actin inhibition prevents rhizoid cell formation, sporeling morphology was characterised after 3 and 4 days of growth on LatB. When grown on DMSO and 0.01 µM LatB, spores had divided multiple times in a linear pattern and had elongated rhizoids (**Figure 3.5.A, B**). On 0.03 µM LatB, spores had divided multiple times to form a cluster of chloroplast-filled cells (**Figure 3.5.A, B**). A few sporelings had one short rhizoid but most had no rhizoids. This may result from inhibition of rhizoid cell formation or inhibition of tip growth. On 0.1 µM to 5 µM LatB, sporeling had a mixture of phenotypes: dead, single-celled, multi-celled, or multi-celled with one dead cell (**Figure 3.5.A, B**). Of the divided sporelings, none had rhizoids and many divisions were symmetric. In conclusion, inhibition of actin filaments prevents rhizoid formation and/or outgrowth, and appears to induce more

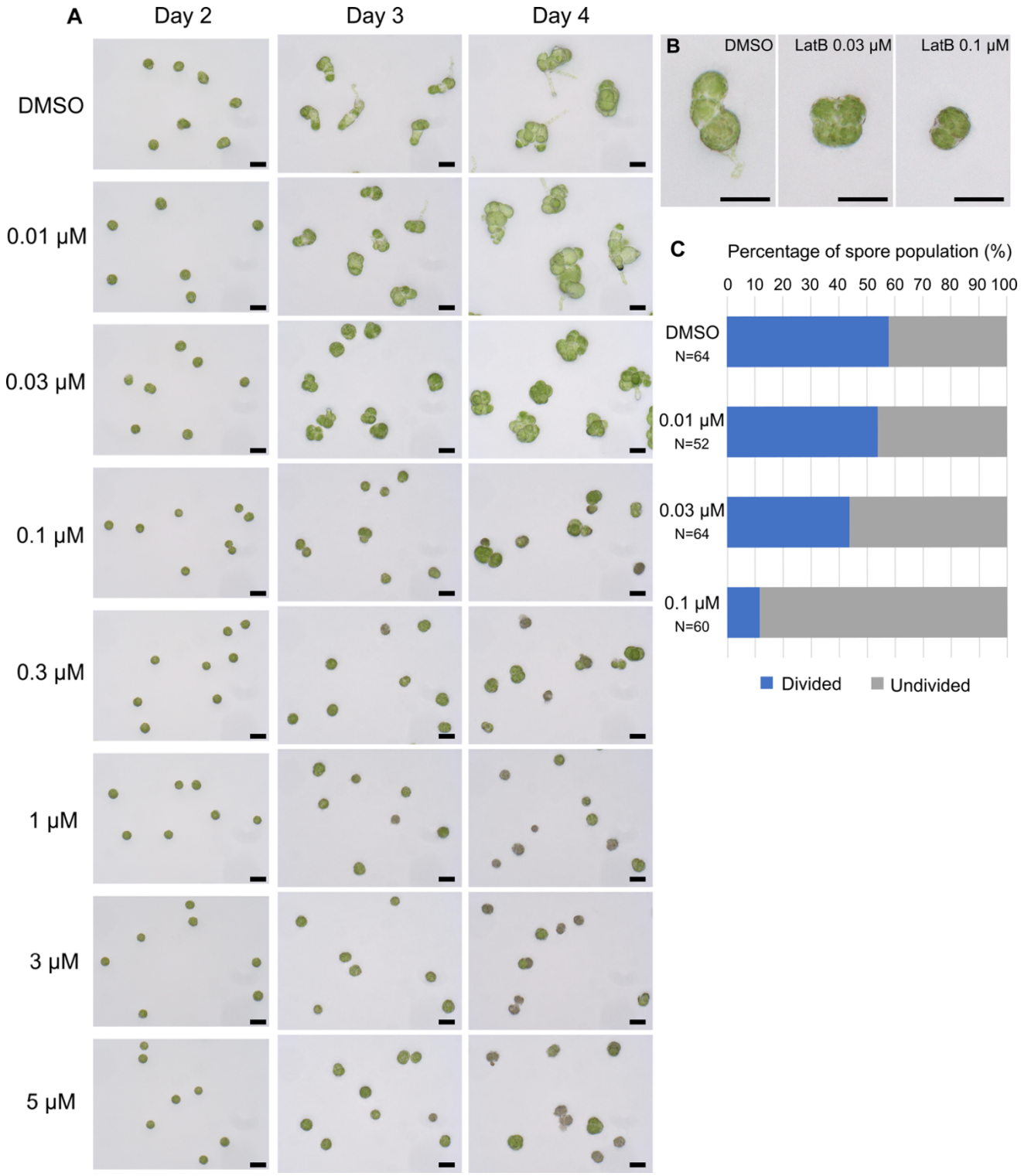

Figure 3.5: Latrunculin B disrupts rhizoid formation and appears to induce more symmetrical divisions in spores

(A-B) Development of wild type spores grown on increasing doses of oryzalin and a DMSO control. Presented are representative spores from the population at 2, 3 and 4 days after germination on Gamborg media containing 0.01 µM to 5 µM LatB or DMSO **(A)**. Enlarged images of representative spores grown on DMSO, 0.03 µM and 0.1 µM LatB for 3 days **(B)**. Scale bars, 50 µm.

(C) Percentage of divided and undivided spores in populations grown on 0.01 µM, 0.03 µM and 0.1 µM LatB and DMSO for 2 days. N is the number of spores quantified.

symmetrical cell divisions. This is consistent with the hypothesis that actin filaments are required for spore polarisation and the first ACD.

This data defines a dose of LatB (0.1 μM) at which actin filaments are inhibited but spores still divide. The next steps to test if actin filaments are required for spore polarisation would be to treat spores expressing a nuclear-plasma membrane reporter with 0.1 μM LatB and then to quantify the position of the nucleus and the first division plane.

3.5 Discussion

3.5.1 An actin network forms between the nucleus and basal cortex in polarising *M. polymorpha* spores

In Chapter 2, I established that during the development of *M. polymorpha* spores, the nucleus migrates from the cell centroid to the basal cortex resulting in an asymmetric cell division. In this chapter, I discovered that actin filaments reorganise as the nucleus migrates. When the nucleus is central, no actin filaments were associated with the nucleus. On repositioning of the nucleus to the basal pole, an actin network forms between the nucleus and basal cortex and there is an enrichment of actin filaments at the basal cortex (**Summary Figure 3.1**). Formation of an enriched actin domain is a common mechanism used to mark specific poles in polarised cells. An ‘actin patch’ is positioned at basal cortex of brown algae zygotes during polarity establishment (Alessa & Kropf, 1999). Further an ‘actin cap’ marks the apical cortex in polarising *A. thaliana* zygotes and an ‘actin collar’ forms at the germination site of pollen (Kimata *et al.*, 2016; Liu *et al.*, 2018). Through quantification of the GFP-LifeAct reporter intensity around the perimeter of multiple spores, I revealed variability in the width and density of the enriched actin domain. This may be due to the dynamic nature of actin filaments or may represent different stages of domain enrichment. One hypothesis is that actin accumulates over a large area and then narrows overtime.

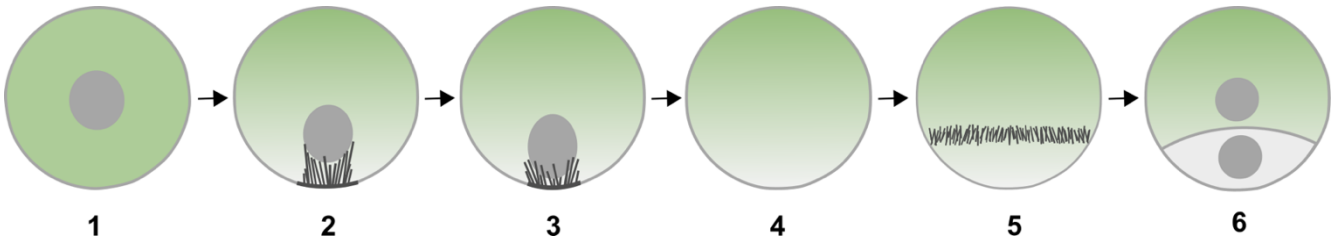

Summary Figure 3.1: Organisation of actin filaments in the centre of a *Marchantia polymorpha* spore during polarisation and the first asymmetric division
Diagram of actin filament organisation and nucleus position during the development of a *M. polymorpha* spore, viewed as a slice through the cell centre. Actin filaments (dark grey lines) and nucleus (light grey circles). **(1)** Nucleus in cell centre with no associated actin filaments. **(2-3)** An basal actin network forms as the nucleus nears the basal pole. **(4)** No internal actin filament arrays during mitosis. **(5)** Actin filaments within the phragmoplast. **(6)** Divided cell.

From the actin-enriched cortical domain, a network of fine actin filaments polymerises inwards towards the nucleus base. To generate this network requires actin-nucleating proteins. Formins nucleate unbranched parallel actin filaments capable of bundling into cables, as seen at the germination site of *A. thaliana* pollen (Thomas *et al.*, 2009; Liu *et al.*, 2018). By contrast, nucleation by Actin-Related-Protein (ARP) complexes leads to branched actin webs as seen at the basal domain of *Fucus* zygotes (Hable & Kropf, 2005). I speculate that ARP complexes generate the fine actin network at the basal pole of polarising spores.

There are actin filaments throughout the cell cortex which are not associated with the basal actin network that forms during spore polarisation. These cortical filaments appeared randomly organised in non-polar and polar spores alike. With no clear evidence of asymmetry this suggests that cortical actin filaments are not involved in cell polarisation.

3.5.2 Does the basal actin network function to pull the nucleus?

What is the role of the basal actin network formed during spore polarisation? Actin filaments often direct endocytosis to specific domains to alter the membrane properties and change cell shape. For example, the rhizoid pole of *Fucus* zygotes elongates via actin-directed vesicle fusion (Hable & Kropf, 1998; Hadley *et al.*, 2006). By contrast, spores stay spherical

throughout polarisation and division. The actin network therefore does not target vesicles for directional growth but may still deliver proteins to sustain a basal polar protein domain.

An alternative hypothesis is that actin network is pulling and/or anchoring the nucleus to the basal pole. Nucleus positioning via actin filaments is a common mechanism used in tip-growing cells, such as root hairs and pollen tubes (Vidali & Hepler, 2001; Ketelaar *et al.*, 2002). This also occurs in *A. thaliana* zygotes, with actin cables reorganising the vacuoles and guiding the nucleus to the elongating apex (Kimata *et al.*, 2016, 2019). In *M. polymorpha* spores, the actin network appears to polymerise from the basal cortex to contact the base of the nucleus (**Summary Figure 1.3**). I have also shown evidence that spores divide symmetrically on inhibition of actin polymerisation. These two observations are consistent with the hypothesis that actin filaments are required for nuclear migration during spore polarisation. I further speculate that actin filaments are the main cytoskeletal element pulling and anchoring the nucleus to the basal pole, whilst microtubules guide the way.

If actin filaments do physically pull the nucleus, then the mechanical force is likely generated by myosin motor proteins undertaking ATP hydrolysis. There are two myosin families in plants: XI and VIII. Myosin XI proteins function in organelle movement whereas myosin VIIIs function in endocytosis (Nebenführ & Dixit, 2018). In particular, myosin-XI-I has been implicated in nuclear positioning after the asymmetric division of stomata progenitor cells (Muroyama *et al.*, 2020). Unlike other land plants, where there are multiple families with several members in each myosin class, the myosin XI and VII families of *M. polymorpha* contain a single member each (Duan *et al.*, 2020) (**Supplementary Figure 3.1A**). Both myosins are highly expressed in spores in the first 30 hours after germination (unpublished data by Radka Slovak) (**Supplementary Figure 3.1B**). This is consistent with the hypothesis that myosin proteins aid nuclear migration which typically occurs between 28 and 32 hours after germination. Taken together, the action of myosin-XI on actin filaments could provide a mechanism for nuclear migration in spores.

3.5.3 The link to light: how does light direct the formation of the actin network?

Blue light orients the first asymmetric cell division in *M. polymorpha* (Rötzer *et al*., unpublished). Blue light must therefore directly or indirectly control the direction of nuclear movement and positioning of the actin network at the basal pole. On the detection of light by plant cells, including blue light wavelengths, actin filaments are triggered to reorganise and reposition chloroplasts (Sakurai *et al.*, 2005; Kong & Wada, 2011). However, the mechanistic link between actin filament reorganisation, blue light and nuclear migration is more obscure. One study showed that detection of blue light by phototropin triggers nuclear migration along actin filaments to the anticlinal walls of leaf cells (Iwabuchi *et al.*, 2007, 2010). A different study proposed that this nuclear movement is a result of nuclear-associated plastids moving along actin filaments, rather than a direct actin-nucleus interaction (Higa *et al.*, 2014). In summary there is evidence, although limited, that directional organelle transport mediated by actin filaments can be integrated with blue light signalling via phototropin in plants. I speculate that blue light directs actin reorganisation and network formation at the basal pole of the spore to directly capture and pull the nucleus to this pole.

3.5.4 Actin filament reorganisation is associated with cell shape change at later stages of sporeling development

Polarised cells often undergo directional cell growth prior to an asymmetrical cell division. Examples of this include budding yeast and the zygotes of brown algae and angiosperms (Hable & Kropf, 1998; Slaughter *et al.,* 2009; Wang *et al.,* 2019). By contrast, the *M. polymorpha* spore grows isotopically in the first 24 hours then stays spherical throughout polarisation and the first asymmetric division as shown in Chapter 2. At this one-cell stage, actin filaments only generate internal asymmetry not external asymmetry.

In later sporeling development, the function of actin filaments appears to change to polarised cell growth. After the first spore division, there is an enrichment of actin filaments at the tip of the basal cell. This is predicted to direct endocytosis for tip growth enabling elongation of the

basal cell and its terminal differentiation into a rhizoid, as seen in root hairs (Baluška *et al.*, 2000). The actin enrichment in the basal rhizoid cell appears as a dense cortical cap at the cell tip. By contrast the actin enrichment in polarising spores appears as a fine network which extends from the basal cortex to the nucleus. This difference in organisation may reflect the different functions of the actin filaments in these two scenarios: one in endocytosis and cell shape, and the other in nuclear migration and force generation.

3.5.5 Conclusion

To summarise this chapter, actin filaments form a network between the basal cortex and nucleus during spore polarisation. On inhibition of actin polymerisation, spores often divided symmetrically. This is consistent with the hypothesis that actin filaments generate force for nuclear movement in *M. polymorpha* spores necessary for the first asymmetric division.

3.6 Supplementary Data

A

Myosin Family	Evolutionary group	Gene Name	*Arabidopsis* Gene ID	*Marchantia* Gene ID
MYO-XI	Group F	MYOXI-F	AT2G31900	Mapoly0012s0190
	Group G	MYOXI-2	AT5G43900	
		MYOXI-B	AT1G04160	
			AT2G20290	
		MYOXI-G	AT2G20290	
		MYOXI-H	AT4G28710	
		MYOXI-A	AT1G04600	
		MYOXI-D	AT2G33240	
	Group I	MYOXI-I	AT4G33200	
	Group J	MYOXI-C	AT1G08730	
		MYOXI-E	AT1G54560	
		MYOXI-J	AT3G58160	
	Group K	MYOXI-K	AT5G20490	
		MYOXI-1	AT1G17580	
MYO-VIII	Group A	MYOVIII-1	AT3G19960	Mapoly0024s0124
		MYOVIII-A	AT1G50360	
	Group B	MYOVIII-2	AT5G54280	
		MYOXVIII-B	AT4G27370	

B

Gene ID	Myosin family	0 hours	15 hours	30 hours	Mean
Mapoly0012s0190	MYOXI	922.9	773.9	815.0	837.2
Mapoly0024s0124	MYOVIII	895.8	705.7	656.2	752.6

Supplementary Figure 3.1: Presence of myosin motor protein family members in *M. polymorpha* and their expression levels in developing spores
(**A**) Table of kinesin families and subfamilies and their gene ID in *Arabidopsis thaliana* and *Marchantia polymorpha*. *A. thaliana* groups taken from Peremyslov *et al.*, 2011 with gene IDs from TAIR10. *M. polymorpha* sequences identified from BLAST search with gene IDs from genome v3.1.
(**B**) Expression levels of Mp*MYO-XI* and Mp*MYO-VIII* in spores at 0, 15 and 30 hours after germination. Presented is the RNA seq data collected and analysed by Radka Slovak. Level at each timepoint represent the mean of two samples and the overall represents the mean across all timepoints.

Chapter 4: The role of katanin in microtubule organisation, dynamics, and polar organiser formation in *Marchantia polymorpha*

4.1 Abstract

Cytoskeleton dynamics are tightly controlled by a suite of associated proteins. By severing microtubules, the enzyme katanin reorients cortical and mitotic arrays in plant cells thereby orienting cell growth and division. However, our knowledge of katanin's function in plants derives solely from one species, the angiosperm *Arabidopsis thaliana.* An alternative model species is the liverwort, *Marchantia polymorpha*, which uniquely forms two acentrosomal microtubule organising centres (MTOCs), termed the polar organisers. Here, I take a reverse genetic approach to investigate katanin's function in *M. polymorpha*. I show that Mp*ktn* mutants have disordered cortical arrays and form supernumerary polar organisers which nucleate disorganised astral arrays. Further, I demonstrate that mitotic spindles are elongated, misoriented, and can rotate in the Mp*ktn* mutant. This ultimately leads to misoriented cell divisions. I conclude that katanin severing regulates microtubule dynamics throughout the cell cycle in *M. polymorpha*. Moreover, katanin severing is required for acentrosomal MTOC formation representing a novel function for katanin in land plants.

4.2 Introduction

In Chapter 2, I established that the polarisation of *M. polymorpha* spores involves migration of the nucleus towards the basal cortex led by a polar organiser and a dense microtubule array. Microtubule dynamics and polar organiser formation must therefore be tightly controlled during spore development. A variety of microtubule accessory proteins are known to regulate plant microtubule dynamics, but it is unknown what proteins regulate polar

organiser formation and function. One protein I predict to be involved in both microtubule and polar organiser dynamics is the microtubule severing enzyme, katanin.

Katanin, 'the cutting sword', is a highly conserved enzyme in eukaryotes which severs microtubules at cross-over and branch points resulting in microtubule depolymerisation (McNally & Vale, 1993). Katanin activity maintains dynamic microtubule arrays and enables rapid microtubule rearrangement. In plants, katanin acts on cortical microtubules to form parallel arrays, reduce branching, promote bundling, prune older microtubules and reorientate arrays in response to external cues (Zhang *et al.*, 2013; Deinum *et al.*, 2017). The arrangement of cortical arrays subsequently orients cellulose deposition and ultimately directs cell growth (Bichet *et al.*, 2001; Burk & Ye, 2002). In summary, katanin is essential for cortical array organisation, dynamics, and anisotropic cell growth in plants.

The role of katanin in plant cell growth is well characterised, but its exact role in plant cell division is still ambiguous. Katanin localises to the pre-prophase band, mitotic spindle poles and distal phragmoplast in plant cells (Sasaki *et al.*, 2019). Furthermore a number of *A. thaliana* katanin mutants (At*ktn*) have misoriented cell divisions (Bichet *et al.*, 2001; Webb *et al.*, 2002). By tubulin immunostaining, spindles with supernumerary poles were identified in two At*ktn* mutants (Panteris *et al.*, 2011). In a later study, timelapse imaging of an At*ktn* mutant did not show spindle multipolarity but did note increased spindle rotation and abnormal pre-prophase bands (PPB) compared to wild type (Komis *et al.*, 2017). These studies proposed two different methods by which katanin orients cell divisions: first by the regulation of the spindle bipolarity, and second by regulating spindle stability and PPB formation. These proposed functions are distinct but not mutually exclusive; katanin's combined regulation of both spindle structure and dynamics may orient division planes. Investigation of katanin in additional plant species could clarify this mechanism and its conservation across plants. As the organisation of microtubules differs between plant species, I suspect that katanin's role in plant cell division may also differ.

Microtubule organisation is partly dependent on the site of nucleation. In animal and algal cells, nucleation occurs at the centrosomes - microtubule organising centres (MTOC) containing centrioles. By contrast, the only MTOCs in land plants are the acentrosomal MTOCs in bryophytes. Liverworts have two unique MTOCs - the polar organisers - which nucleate peri-nuclear and astral arrays (Brown & Lemmon, 1990). Unlike centrosomes, polar organisers are not inherited but form *de novo* in each cell. The current model of polar organiser formation in *M. polymorpha* proposes that small microtubule foci aggregate around the nucleus and fuse to form two larger foci (Buschmann *et al.*, 2016). Although much is still unclear about this mechanism, it is likely that dynamic microtubules are required. I therefore hypothesise that katanin is involved. Katanin's role in MTOC formation has never been investigated and studying bryophytes such as *M. polymorpha* gives us this opportunity.

Katanin acts on individual microtubules but has major implications at the level of the cell, tissue and ultimately the whole organism. Katanin has been linked to plant growth, organ development and fertility in *A. thaliana* (Burk *et al.*, 2001; Webb *et al.*, 2002; Luptovčiak *et al.*, 2017). These pleiotropic effects are likely a result of katanin's fundamental role in cell growth and division. However, this pleiotropy makes it difficult to distinguish if katanin has any additional functions in development. Studying katanin in a plant with a simple morphology and few cell types could clarify katanin's role in plant morphogenesis.

The thalloid liverwort*, M. polymorpha,* is an ideal plant to study katanin function. Firstly, *M. polymorpha* has a simple morphology for investigation of tissue morphogenesis, cortical microtubule organisation and cell division orientation (Shimamura, 2016). Secondly, *M. polymorpha* forms polar organisers which enable studies on MTOC formation and function (Brown & Lemmon, 1990; Buschmann *et al.*, 2016). Combined with these biological traits, *M. polymorpha* has an abundance of beneficial genetic traits and technical resources (Bowman *et al.*, 2022). Overall *M. polymorpha* proves to be an innovative system to examine the role of katanin in a range of developmental plant processes.

To investigate katanin's role in plant morphogenesis, microtubule organisation and MTOC formation in *M. polymorpha*, I generated and characterised loss of function *katanin* mutants (Mp*ktn)*. Mp*ktn* mutants were defective in plant growth, organ formation, tissue development, cortical array organisation and bundling. Mp*ktn* mutants also had supernumerary polar organisers which nucleated dense, disordered astral arrays. Further, timelapse imaging of dividing Mp*ktn* cells showed that the mitotic spindle axis was misaligned and rotated overtime. From these data, I speculate that katanin regulates MTOC formation and orients the cell division plane through stabilising the mitotic spindle.

4.3 Materials and Methods

4.3.1 Sequence alignments and generation of phylogenetic trees

To identify katanin sequences, the protein sequence for the *A. thaliana* katanin p60 subunit, AT1G80350, was used as the query sequence in a BLASTp search against the *M. polymorpha* proteome. The top hit, Mapoly0116s0028, was then used as the query for BLASTp searches in the proteome databases of 20 plant and algal species (**Table 4.3.1**). In each species, except two *Osterococcus* species, protein sequences scoring above E-87 were identified and selected.

Protein sequences were aligned using MAFFT version 7 employing the L-INS-i method (Katoh *et al.*, 2002). Sequences from three species - *Anthoceros punctatus, Salvinia cucullata* and *Picea abies* - were subsequently removed due to suspected mis-annotation of one or more exon-intron boundaries, or because the sequences were incomplete. For one species – *Azolla filiculoides* – a new coding sequence was proposed after I suspected mis-annotation of the exon-intron boundary, which was confirmed by examining the *Azolla* transcriptome. Sequences from the 15 remaining species were realigned and trimmed using BioEdit software to the conserved AAA ATPase and Vsp4C domains. These domains were identified using the SMART protein domain dataset (Letunic & Bork, 2018)

Species	Lineage (common name)	Genome database	Genome BLAST server	Proteome database	Proteome BLAST server	Gene identified	Issues with sequences	Resolution
Arabidopsis thaliana	Angiosperm (Thale Cress)	TAIR10	phytozome	TAIR10 primary proteins	phytozome	AT1G80350		
Amborella trichopoda	Angiosperm		phytozome	proteins v1.0, 2013	marchantia.info	evm_27.model.AmTr_v1.0_scaffold00122.30		
Oryza sativa	Monocot (Rice)	v7_JGI	phytozome	v7_JGI	phytozome	LOC_Os01g49000.1		
Zea Mays	Monocot (Maize)	PH207 v1.1 (or Ensembl-18)	phytozome	PH207 v1.1 (or Ensembl-18)	phytozome	Zm00008a032285_T01 Zm00008a014130_T01		
Picea abies	Gymnosperm (Norway spruce)	Pabies1.0-MC-gene (or transcript v1.0, 2015)	congenie.org (or phytozome)	Pabies1.0-MC-pep v1.0, 2015 (no hits in 1.0-HC-prep)	marchantia.info	MA_10429958g0030 MA_165281g0010	Partial alignment only First exons not sequenced	Removed Removed
Pinus taeda	Gymnosperm (Loblolly pine)	v1.0	congenie.org	Predicted from v1.0 genome	congenie.org	PITA_000022979		
Azolla filiculoides	Fern (Water Fern)	genome v1.2, CDS v1.1 (or transcript_HC/LC, v1.1, 2018)	fernbase.org (or phytozome)	protein v1.1	fernbase.org	Azfi_s0008.g011502 Azfi_s0019.g015159	Mislabelled exons/introns	Proposed new CDS. Confirmed with NCBI transcriptome (GBTV01.1.fas_nt.gz/.)
Salvinia cucullata	Fern (Asian watermoss)	genome v1.2, CDS v1.2 (or transcript_HC/LC, v1.1, 2018)	fernbase.org (or phytozome)	proteins v1.2	fernbase.org	Sacu_v1.1_s0030.g010496 Sacu_v1.1_s0091.g018832	Mislabelled exons/introns Mislabelled exons/introns	No transcriptome to confirm CDS. Removed. No transcriptome to confirm CDS. Removed.
Selaginella moellendorffii	Lycophyte (Spike moss)		phytozome	primary proteins v1.0, 2014	marchantia.info	Smoe78692		
Marchantia polymorpha	Bryophyte (Liverwort)	v3.1, 2015	phytozome, marchantia.info	primary proteins v3.1, 2015	marchantia.info	Mapoly0116s0028.1		
Physcomitrium patens	Bryophyte (Earth moss)		phytzome	primary proteins v3.0,2014	marchantia.info	Pp3c15_10930V3.4 / Phpat015G04500 Pp3c9_3800V3.1 / Phpat009G015600		
Sphagnum fallax	Bryophyte (Peat moss)	v0.5	phytozome	v0.5	phytozome	Sphfalx0057s0060.1 Sphfalx0002s0132.1		
Anthoceros agrestis	Bryophyte (Hornwort)	v1, 2020 (Oxford strain)	Evo.plants BLAST server	v1, 2020 (Oxford strain)	Evo.plants BLAST server	AagrOXF_evm.model.utg000118l.68.1		
Anthoceros punctatus	Bryophyte (Hornwort)	v1, 2020	Evo.plants BLAST server	v1, 2020	Evo.plants BLAST server	Apun_evm.model.utg000141l.49.1	Mislabelled intron/exons	No transcriptome to confirm CDS. Removed.
Chlamydomonas reinhardtii	Chlorophyte algae		phytozome	primary proteins v5.5, 2014		Cre10.g427600.t1.2		
Ostreococcus tauri	Chlorophyte algae		phytozome	proteins 2012	marchantia.info	No protein fully aligned		
Ostreococcus lucimarinus	Chlorophyte algae		phytozome	primary proteins v2.0, 2014	marchantia.info	No protein fully aligned		
Micromonas pusilla	Chlorophyte algae	CMP1545 v3.0	phytozome	CMP1545 v3.0	phytozome	MCM_CCM16445		
Volvox carteri	Chlorophyte algae	v2.1	phytozome	v2.1	phytozome	Vocar.0005s0308.1		
Klebsormidium nitens	Streptophyte algae	v1.1	plantmorphogenesis.bio.titech	proteins v1.0, 2014	marchantia.info	kfl00352_0030		

Table 4.3.1: The genome and proteome databases used to identify katanin sequences in a range of land plant and algal species.

Maximum likelihood trees were generated using MEGA-X 10 software utilising all amino acid sites and bootstrap values were calculated from 500 replicates (Kumar *et al.*, 2018).

4.3.2 Plant lines and growth conditions and crossings

The wild type *Marchantia polymorpha* accessions used were Takaragaike-1 (Tak-1) and Takaragaike-2 (Tak-2). All constructs were transformed into the wild type progeny derived from crossing Tak-1 and Tak-2. The media, soil and growth conditions for plants and induction of reproductive organs were the same as in Chapter 2.3.1/2.3.2. Methods for crossing plants and sterilising sporangium were the same as in Chapter 2.3.2

4.3.3 Design and cloning of a katanin fluorescent reporter

Cloning of the *p*Mp*KTN:GFP*-Mp*KTN* construct was performed by the Protein Technologies Facilities at Vienna BioCenter Core Facilities (VBCF) using the GreenGate cloning system (**Figure 4.3.1**) (Lampropoulos *et al.*, 2013). For the promotor, a 3.5 kb genomic sequence upstream of the Mp*KTN* start codon was synthesised with internal BsaI sites altered. The Mp*KTN* (Mapoly0116s0028) genomic sequence was cloned from genomic DNA extracted from Tak-1 tissue. A GFP linker fluorophore was placed at the N-terminus of the Mp*KTN* sequence.

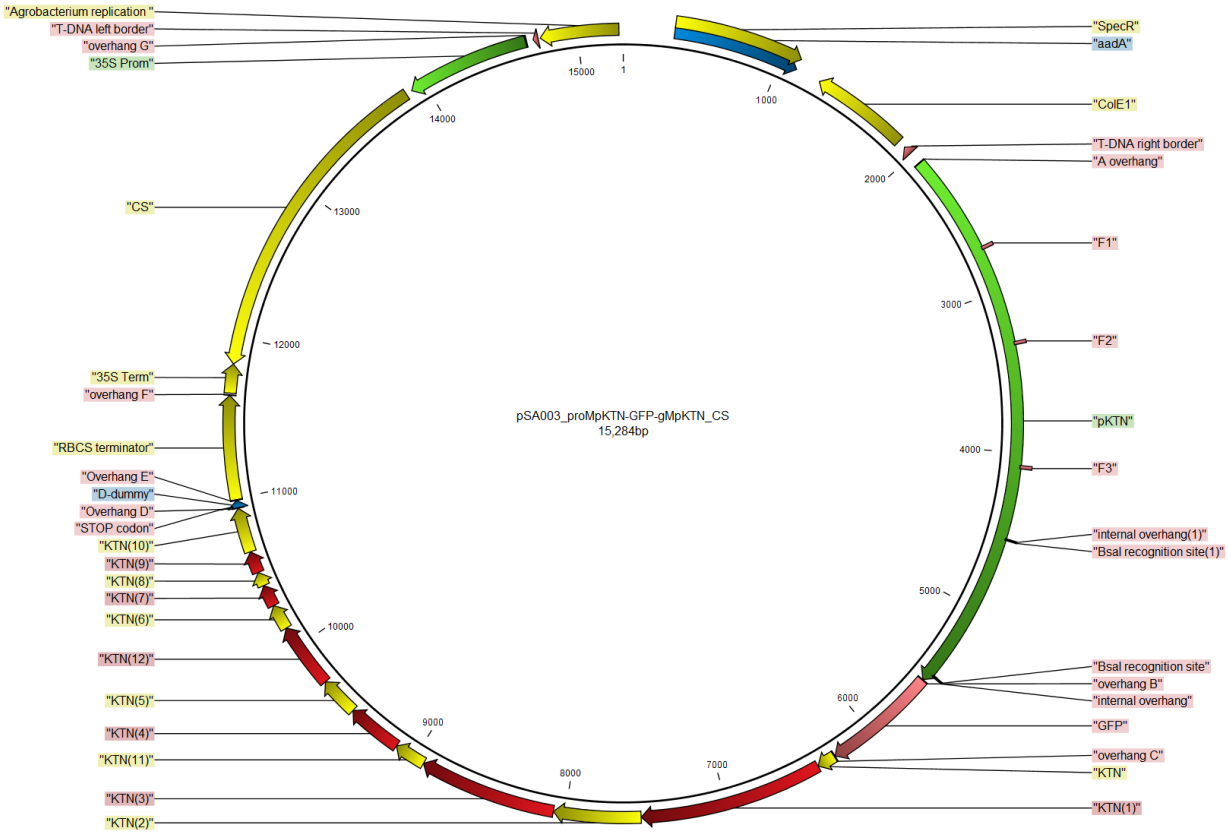

Figure 4.3.1: Vector map of the *p*Mp*KTN:GFP*-Mp*KTN* construct labelling katanin

4.3.4 sgRNA design for CRISPR/Cas9 mutagenesis

sgRNAs, consisting of 20 nucleotides followed by a (NGG) sequence, were designed to target the Mp*KTN* (Mapoly0116s0028) gene. To identify sgRNAs with high target efficiency and low off-target effects, I used the CRISPR-P software (Lei *et al.*, 2014). Candidate sequences were BLAST against the *M. polymorpha* genome v4 (marchantia.info) to check potential off-target hits. The final two selected sgRNAs sequences were:

- sgRNA-K3: TACGTTGGCCTCCAAATGGA(GGG).
- sgRNA-K5: GGAGCTTGCCAGACGTACAG(AGG).

The sgRNAs respectively target the AAA ATPase domain in exon 4 and the slightly upstream of the VSP4C domain in exon 7 of Mp*KTN*. A CTCG overhang was added to the 5' end of the sgRNA-K3 sequence prior to cloning.

4.3.5 Cloning of CRISPR/Cas9 plasmids

Two cloning methods were used to generate the sgRNA-Cas9 plasmids. Cloning of the sgRNA-K5 Cas9 plasmid was performed by the Protein Technologies Facility at Vienna BioCenter Core Facilities (VBCF) using vectors from the OpenPlant toolkit and following the protocol published in Sauret-Güeto *et al.*, 2020.

Cloning of the sgRNA-K3 Cas9 plasmid used the vectors and protocol presented in Thamm *et al.*, 2020 adapted from Sugano *et al.*, 2014. First the sgRNA primers were annealed and amplified to create double-stranded oligos. 2 µL forward and reverse primers (100 µM stock), 5 µL T4 DNA ligase buffer, 1 µL T4 PNK and 40 µL ddH2O were mixed and incubated at 37 °C for 30 minutes then 95 °C for 5 minutes. The temperature was then decreased by 5 °C every 30 seconds until 20 °C was reached.

The sgRNA plasmid (pMpGE-En03 single) was restriction digested to open the vector. 500 ng plasmid, 1 µL BsaI, 2 µL CutSmart Buffer (10x) and water up to 20 µL were mixed. The reaction was incubated for 2 hours at 37 °C then inactivated at 65 °C for 30 minutes. To isolate the digested vector, the samples were run on a 1% agarose gel, extracted, and eluted water. The vector's digested ends were dephosphorylated by mixing 1 µg vector, 1 µL Antarctic Phosphatase, 2 µL Antarctic Phosphatase buffer (10x) and ddH2O up to 20 µL. The reaction was incubated for 30 minutes at 37 °C then inactivated at 80 °C for 2 minutes.

Into the digested vector, the sgRNAs were now ligated. 50 - 100 ng digested vector, 0.66 ng annealed sgRNA oligos, 1 µL T4 ligase, 2 µL T4 ligase buffer (10x) and ddH20 up to 20 µL were mixed. The reaction was incubated for 1 hour at room temperature then inactivated at 65 °C for 10 minutes. The ligated vector was heat-shock transformed into *E. coli* then isolated using the GeneJet Plasmid Mini Prep kit, following the methods in Chapter 2.3.4. As the ligation reaction is low efficiency, multiple colonies were taken for colony PCR and the products run on 1% agarose gel to check for the presence of band. Successfully transformed colonies were selected, and the vector isolated and sequenced using the M13R primer.

A gateway reaction recombined the sgRNA vector into the Cas9 vector (pMpGE010). 100 ng sgRNA vector, 150 ng Cas9 vector, 0.5 µL LR Clonase II and TE buffer up to 10 µL were mixed and incubated for 1 hour at 25 °C. The reaction was terminated by addition of 1 µL proteinase K and incubation for 10 minutes at 37 °C. The ligated vector was heat-shock transformed into *E.coli*, following the method in Chapter 2.3.4. As this reaction is high efficiency, the Cas9-sgRNA plasmid was directly isolated from *E.coli* and sequenced using primers CACCTCTCTTTGGTTATGTCTTGA and GCAAGACCGGCAACAGGATTC.

4.3.6 Transformation of *M. polymorpha*

Each construct was amplified in *E. coli* and then transformed into *Agrobacterium tumefaciens* following the protocol described in Chapter 2.3.4. *Agrobacterium*-mediated transformation of wild type sporelings followed the method in Chapter 2.3.5. Transgenic plants were selected by their resistance to 10 µg/mL hygromycin or 10 µg/mL chlorsulfuron.

4.3.7 Genotyping of *M. polymorpha* plants

Two methods of DNA extraction and amplification were used to identify mutations at the sgRNA site of CRISPR/Cas9 mutagensied plants, using the PCR primers in **Table 4.3.2**.

The first method used the Phire Plant Direct PCR kit (ThermoFisher Scientific). The samples were run by gel electrophoresis and DNA extracted using the GeneJet Gel Purification kit (ThermoFisher Scientific). In the second method, 3 x 3 mm pieces of plant tissue were ground within 100 µL of extraction buffer (100 mM Tris HCl, pH 9.5, 1 M KCl, 10 mM EDTA). Samples were incubated at 65 ºC for 10 minutes before dilution in 500 µL MonoQ water. DNA was PCR amplified using 2x HS Taq Polymerase (2x Hot Start MM, 0.5 µM forward primer, 0.5 µM reverse primer, 1 µL DNA, 7 µL Nuclease free water). The PCR products were purified using an ExoSAP treatment. 2 µL ExoSAP mix (0.04 µL Exonuclease I, 0.4 µL Shrimp Alkaline Phosphatase, 1.56 µL Storage solution) was added to each 20 µL PCR reaction. The reaction was incubated at 37 ºC for 30 minutes, before deactivation at 80 ºC

for 10 minutes. Isolated DNA was Sanger sequenced using the Seq primers in **Table 4.3.2**. Sequences were aligned against the Tak-1 genome sequence using Geneious or CLC Genomics Workbench to identify mutations near the sgRNA PAM site.

Primer	Direction	Sequence
K3 sgRNA	Forward	(CTCG)TACGTTGGCCTCCAAATGGA
K3 PCR	Forward	TGTCTGTGGCTACCCTGAAC
K3 PCR	Reverse	ATCCAAACTACGGCCAGTGC
K3 Seq	Forward	ATACAGGGCATTCGTCGACC
K3-Cas9 plasmid	Forward	CACCTCTCTTTGGTTATGTCTTGA
K3-Cas9 plasmid	Reverse	CAGGAAACAGCTATGAC
K5 sgRNA	Forward	GGAGCTTGCCAGACGTACAG(AGG)
K5 PCR	Forward	ACATTCCTTTGCCGAACGAG
K5 PCR	Reverse	GAACCAAACTCTGCCAACCA
K5 Seq	Forward	ACATTCCTTTGCCGAACGAG
K5-Cas9 plasmid	Forward	CTCATCGAGACAAACGGTGA
K5-Cas9 plasmid	Reverse	ATCAGCCCTTGAATCACCAC

Table 4.3.2: sgRNA sequences used to target Mp*KTN* for mutagenesis, primers for sequencing Mp*KTN* gene and primers to test for Cas9 presence in transformed plants.

4.5.8 Generation and selection of CRISPR/Cas9 mutants expressing reporters

The Mp*katanin* (Mp*ktn*) mutants generated by CRISPR/Cas9 mutagenesis were crossed to plants expressing *p*Mp*EF1α:GFP*-Mp*TUB1* (GFP-MpTUB1) (**Figure 4.3.2**). The resulting F1 progeny were grown, genotyped, tested for the presence/absence of the Cas9 plasmid and then screened for GFP-MpTUB1 reporter fluorescence.

For genotyping, DNA was extracted and sequenced at the mutation site following the method in Chapter 4.5.7. To test for the presence of the Cas9 plasmid, DNA was extracted, and PCR amplified using the Cas9 primers (**Table 4.3.2**). PCR products were run on a 1% agarose gel with a band indicating the presence of the Cas9 plasmid. Samples from parental plants were used as negative and positive controls. To test for the expression of the GFP-MpTUB1, gemma of Cas9-free lines were grown on Gamborg media with and without 10 µg/mL hygromycin. Resistance indicated that plants had inherited GFP-MpTUB1, which was confirmed by fluorescence imaging. Cas9-free wild type (wildtype-TUB) and Mp*ktn* (Mp*ktn*-TUB) siblings expressing the GFP-MpTUB1 reporter were selected.

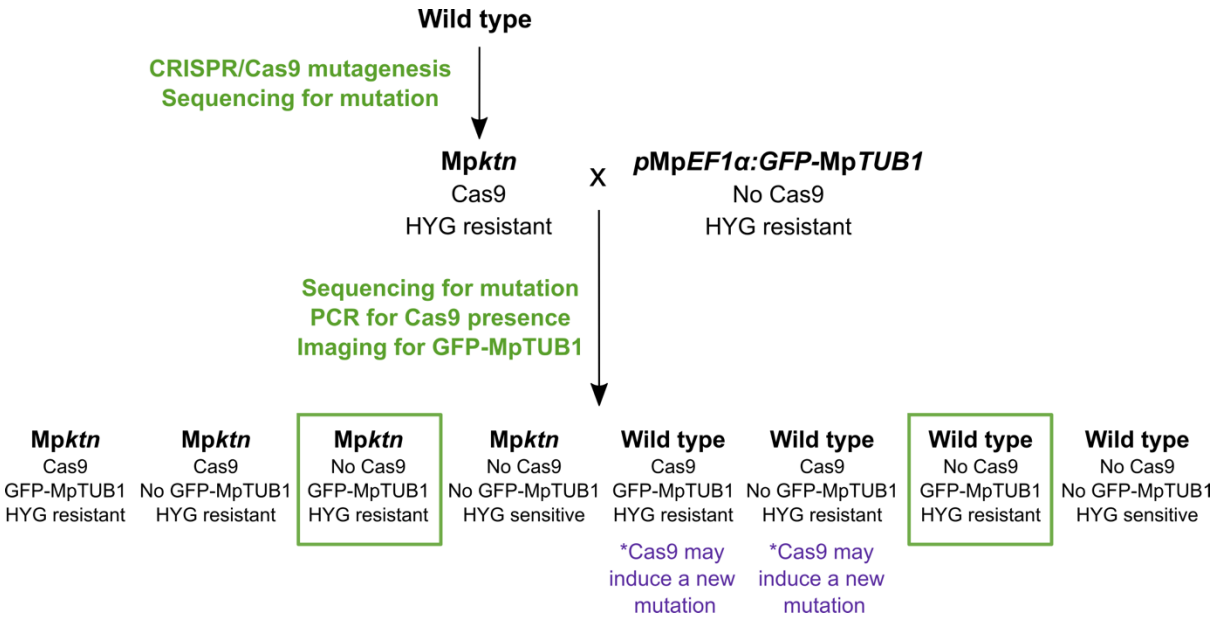

Figure 4.3.2: CRISPR/Cas9 mutagenesis and crossings were used to generate Mp*ktn* mutants expressing a microtubule reporter
Diagram showing the generation of Cas9-free Mp*ktn* mutants expressing a microtubule reporter. Wild type spores were mutagenized using CRISPR/Cas9 to generate Mp*ktn* mutants. The mutants were crossed to plants expressing the microtubule reporter, *p*Mp*EF1α:GFP*-Mp*TUB1* (GFP-MpTUB1). Eight different potential genotypes were created. Progeny were sequenced for mutations in the Mp*KTN* gene and tested for Cas9 presence using PCR. Cas9-free progeny were selected and tested for expression of GFP-MpTUB1 using hygromycin (HYG) resistance and confocal imaging. Cas9-free Mp*ktn* and wild type siblings expressing GFP-MpTUB1 were selected (green boxes).
Note that both the Cas9 plasmid and GFP-MpTUB1 confer hygromycin resistance.

4.3.9 Stereomicroscope imaging of plant tissues and organs

Gemmalings were imaged with the Leica MZ16FA stereomicroscope equipped with the Leica DFC300 FX camera. Mature plants and tissues were imaged with the Keyence VHX-7000 digital equipped with a VHX-7020 camera and VH-Z00R/T and VH-ZST lenses.

4.3.10 Imaging and analysis of plant tissue area

Gemmalings were imaged with the Berthold NightOwl II LB 983 *In Vivo* Imaging system which detects chlorophyll autofluorescence of living tissue after exposure to 120 seconds of white light. The tissue area was detected and quantified using the indiGo software package. A growth curve was generated using ggplot2 and drc packages in R (Wickham, 2009).

4.3.11 Staining and confocal imaging of gemmae

0-day-old gemmae were treated with 5 µg/µL propidium iodide (PI) for 10 minutes to stain the cell walls before washing three times with water. The stained gemma were imaged with a Zeiss LSM780 confocal microscope equipped with a 10x/0.3 NA air objective. Samples were excited with a 561 nm lazer and the emission was captured at 680 - 700 nm for chlorophyll autofluorescence and at 570 - 645 nm for the PI signal.

4.3.12 Spinning disk imaging of microtubules and katanin in epidermal cells

Gemma for fluorescence imaging were setup within imaging chambers designed in Kirchhelle and Moore, 2017. A breathable gum boarder (Carolina Observation gel) was filled with a Gamborg media slab and layered with cellophane soaked in liquid Gamborg media (½-strength B5 Gamborg's medium without agar). Perfluorodecalin was added to the chamber and 0-day-old gemmae were transferred onto the media surface. A cover slip sealed the chamber. Gemmae were grown for 1 or 2 days prior to imaging.

Gemmae were imaged using an Olympus IX3 Series (IX83) inverted microscope equipped with a Yokogawa W1 spinning disk, Hamamatsu ORCA-Fusion CMOS camera and a 100x/1.45 NA oil objective. For GFP, samples were excited at 488 nm and emission captured at 525 nm. For chlorophyll, samples were excited at 640 nm and emission captured at 685 nm. Z-stacks with 0.26 µm slices were taken, unless otherwise stated. GFP-MpKTN and GFP-MpTUB1 labelled cortical arrays were imaged in central epidermal cells. GFP-MpTUB1 labelled mitotic arrays were imaged in dividing cells near the meristem.

4.3.13 Deconvolution and conversion of spinning disk images

Deconvolution of selected images was done using Huygens software (Scientific Volume Imaging). Z-projections and central slices were converted for presentation using ImageJ Fiji (Schindelin *et al.*, 2012). For temporal projections, each image slice was first deconvolved in

Huygens then maximum projections were generated for each timepoint in ImageJ Fiji before temporal projection in ImageJ Fiji.

4.3.14 Analysis of microtubule organisation

Cortical microtubule analysis was done using the ImageJ LPX package published in Higaki *et al.*, 2010 following the steps in Higaki, 2017. From Z-projections of the central epidermis, individual cells were outlined using the Freehand Tool in ImageJ Fiji. Microtubules were skeletonised using the LPX Filter2d with the Otsu method and a line extract value of 5. This image was masked by the cell outlines, and the skeletonised microtubules in each cell were analysed using the LPX script. Statistical analysis used Excel and graphs were done in R.

To quantify polar organiser number, polar organisers were manual counted from Z-projections of individual cells. Spindle length was measured in ImageJ Fiji using the Line tool. Spindle position was quantified by identifying the central points of the cell and spindle in ImageJ, then calculating the distance between these points. Statistical analysis used Excel.

4.4 Results

4.4.1 *Marchantia polymorpha* has a single *KATANIN* gene

To investigate the role of katanin in *M. polymorpha* development, I first confirmed the presence and number of copies of the katanin gene in *M. polymorpha.* The protein sequence for the katanin p60 subunit gene in *A. thaliana,* AT1G80350, was used as a query sequence for a BLASTp search against the *M. polymorpha* proteome. This identified Mapoly0116s0028 as the most similar sequence. To confirm Mapoly0116s0028 as *M. polymorpha*'s only copy of katanin, I searched for similar sequences in the proteome of *M. polymorpha* and 19 other land plant and algal species using Mapoly0116s0028 as a query sequence. In every proteome searched, except for two *Osterococcus* species, one or two highly similar proteins

(>E-100) and many lower similarity proteins (>E-87) were identified (**Table 4.3.1**). Using sequences which scored above E-87, a phylogenetic tree was generated to distinguish between katanin and katanin-like sequences. First, sequences from three species were removed as I suspected mis-annotation of one or more exon-intron boundaries, or because the sequences were incomplete (**Table 4.3.1**). For the remaining 15 species, sequences were aligned and trimmed to the homologous AAA ATPase domain and a maximum likelihood tree was generated (**Supplementary Figure 4.1.A**). The tree revealed two distinct clades with strong support values at each base (**Figure 4.1.A**). One clade contained known katanin orthologs and all the sequences with high similarity scores (>E-100). The second clade contained the low similarity sequences (E-100>E-87), predicted to be katanin-like proteins. Overall, katanin is present in most land plant and algal species as one or two copies. *M. polymorpha* had a single gene present in the katanin clade, Mapoly0016s0028, now referred to as Mp*KATANIN* (Mp*KTN*).

To investigate the evolution of katanin in land plants and algal species, a second tree was formed using sequences from the katanin clade (>E-100). Sequence alignment showed high amino acid similarity across the entire protein, particularly at the highly conserved AAA and VSP4C domains (**Supplementary Figure 4.1.B**). The protein alignment was trimmed to these two domains and used to construct a maximum likelihood tree (**Figure 4.1.B**). By increasing the number of conserved sequences used, better resolution is given to the katanin tree topology. The gene tree closely reflected the known evolutionary relationship between plant species, apart from the positioning of the lycophytes and monilophytes. Overall, the katanin protein is highly conserved across land plants and algae.

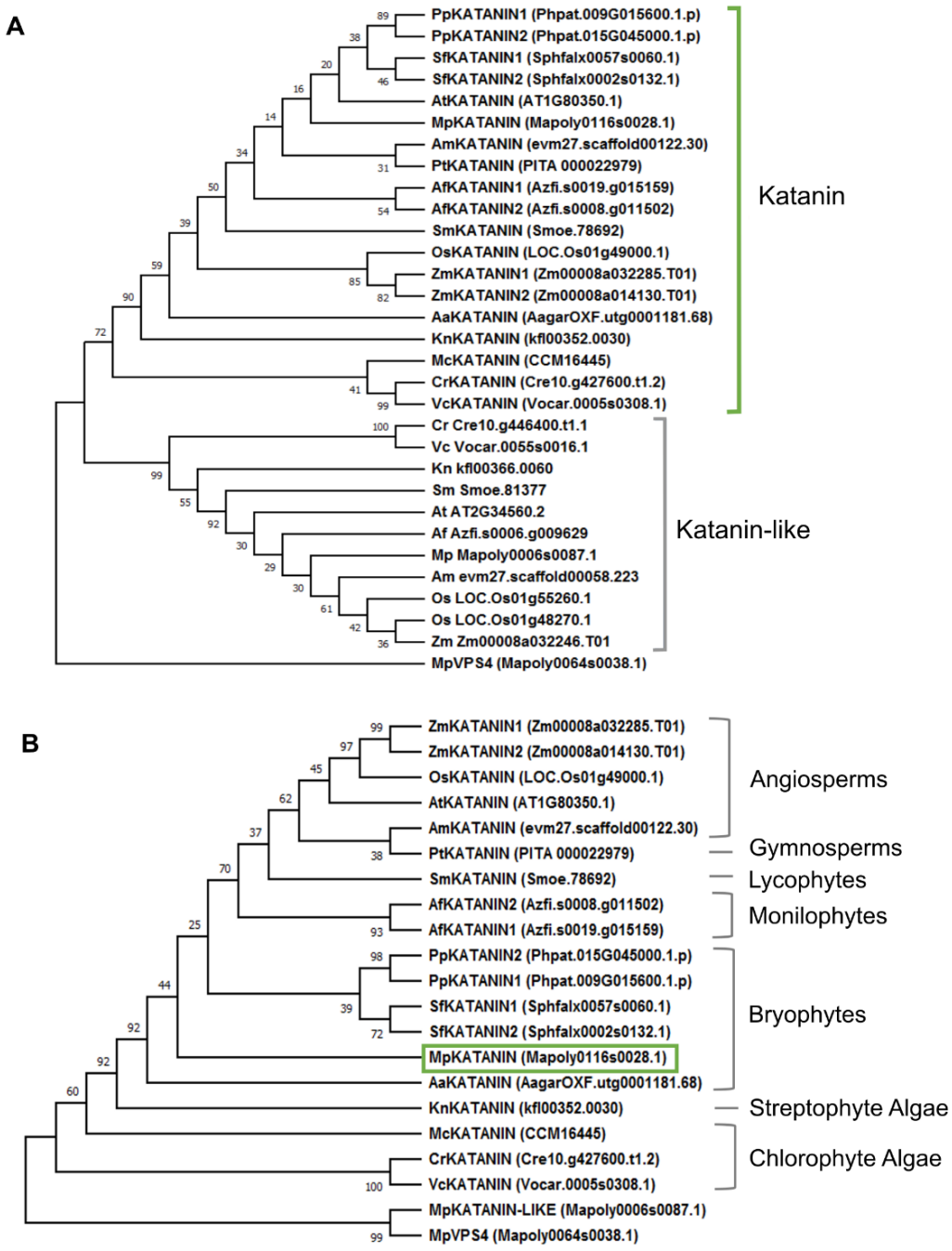

Figure 4.1: *Marchantia polymorpha* has a single *KATANIN* gene
(A) Maximum likelihood tree of the KATANIN and KATANIN-LIKE proteins from 15 land plant and algal species. The tree uses the full protein sequence alignments, and MpVSP4 (Mapoly0064s0038) as an outgroup. The katanin and katanin-like clades are labelled.
(B) Maximum likelihood tree of KATANIN protein from 15 plant and algal species. The tree uses an alignment of only the AAA domain sequences and includes the MpVSP4 (Mapoly0064s0038) and MpKATANIN-LIKE (Mapoly0006s0087) protein sequences. The major plant lineages are labelled and the single *M. polymorpha* KATANIN (Mapoly0116s0028) is indicated (green box).
At, *Arabidopsis thaliana.* Am, *Amborella trichopoda.* Os, *Oryza sativa.* Zm, *Zea mays*. Pt, *Pinus taeda.* Af, *Azolla filiculoides.* Sm, *Selaginella moellendorffi.* Mp, *Marchantia polymorpha.* Pp, *Physcomitrium patens.* Sf, *Sphagnum fallax.* Aa, *Anthoceros agrestis*. Cr, *Chlamydomonas reinhardtii.* Mc, *Micromonas pusilla.* Vc, *Volvox carteri*. Kn, *Klebsormidium nitens.*

4.4.2 Generation of Mp*ktn* mutants using CRISPR/Cas9 mutagenesis

To investigate the role of katanin in *M. polymorpha* development, I undertook CRISPR/Cas9 mutagenesis to generate loss-of-function katanin mutants. I designed two sgRNA constructs to induce mutations in the Mp*KTN* gene. sgRNA-K3 targeted the catalytic AAA ATPase domain and sgRNA-K5 targeted slightly upstream of the VSP4C oligomerisation domain (**Figure 4.2.A**). The sgRNAs were each cloned into a Cas9 vector, then transformed into *M. polymorpha* using *Agrobacterium*. Successful transformants were selected by their hygromycin resistance and sequenced at the sgRNA site. Thirteen Mp*katanin* (Mp*ktn*) mutants were generated using sgRNA-K3 (**Figure 4.2.B**). The mutations were predicted to result in amino acids substitutions or frameshifts leading to premature stop codons within the catalytic AAA ATPase domain (**Figure 4.2.C**). A further three Mp*ktn* mutants were generated using sgRNA-K5 (**Figure 4.2.B**). The mutations were predicted to result in frameshifts leading to altered amino acid sequences or stop codons before the VSP4C domain (**Figure 4.2.C**). Each mutation was expected to alter the katanin protein sequence and consequently disrupt the microtubule severing ability of katanin.

A

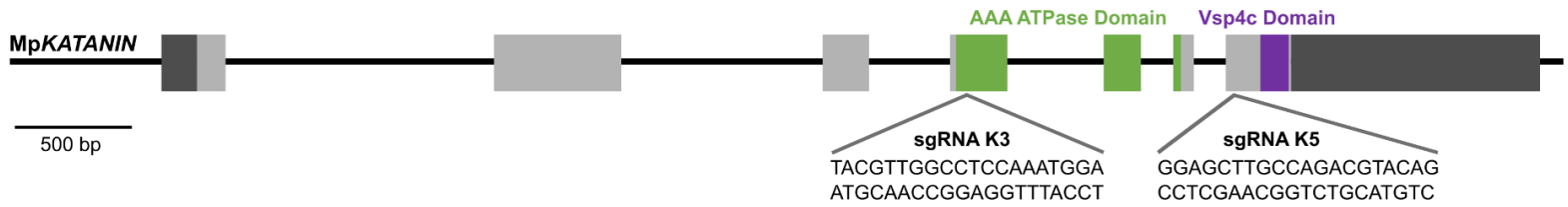

B

Plant line	Location	Gene sequence	Genetic consequence	Predicted protein sequence	Predicted protein consequence
Wild type	Exon 4	ACGTTGGCCTCCAAATGGAGGGGTGAG		TLASKWRGE	
K3-8	Exon 4	ACGTTGGCCTCCAAACGTAGGAGGGGTG	3 bp insertion and T>A substitution	TLASKRRGE	Trp>Arg substitution and additional Arg
K3-9	Exon 4	ACGTTGGCCTCCAAATGGAGGGGTG	1 bp insertion	TLASKWEG*	Frameshift, truncation 3 AA downstream
K3-32	Exon 4	ACGTTGGCCTCCAAACAAACAACCCAAGCCTCTCATGGAGGGGTGAG	21 bp insertion	TLASKQTNPSLSWRGE	Insertion of QTNPSLS, no frameshift
K3-37	Exon 4	ACGTTGGCCTCCAACGAACGGAGGGGTGAG	3 bp insertion and T>C substitution	TLASNERRGE	Lys >Asn & Trp>Arg substitutions and additional Glu
K3-50	Exon 4	ACGTTGGCCTCCAA-GGGAGGGGCCAG	1bp deletion and substitutions T>G, TG>CC	TLASKGG…*	Frameshift, truncation 15 AA downstream
K3-66	Exon 4	ACGTTGGCCTCGTA--GGAGGGGTGAG	CA>GT substitution and 2 bp deletion	TLAS*	STOP codon formed, immediate truncation
K3-85	Exon 4	ACGTTGGCCTCCAAATTGGAGGGGTGAG	1 bp insertion	TLASKLEG*	Frameshift, truncation 4 AA downstream
Wild type	Exon 7	GAGGAGCTTGCCAGACGTACAGAGGGT		EELARRETG	
K5-15	Exon 7	GAGGAGCTTGCCAGACGTATAGCTTGCCAGAGGGT	8 bp insertion	EELARRIA…*	Frameshift, truncation 11 AA downstream
K5-45	Exon 7	GAGGAGCCCTTGCCA----------	169 bp deletion	EEPLPKFHA...	Large deletion, frameshift
K5-58	Exon 7	GAGGAGCTTGCCAGA--------GGGT	8 bp deletion	EELARGL*	Frameshift, truncation 2 AA downstream

C

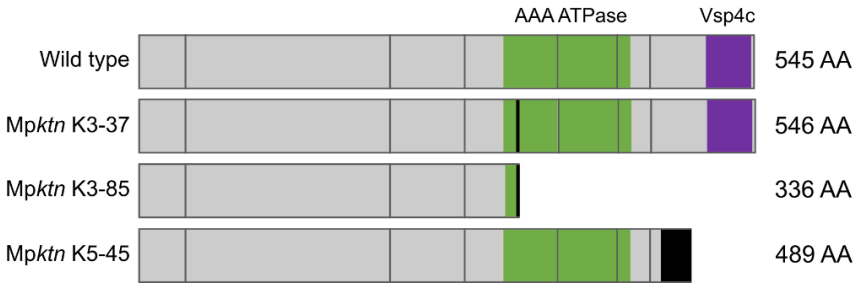

Figure 4.2: Generation of Mp*katanin* (Mp*ktn*) mutants with a range of mutations using CRISPR/Cas9 mutagenesis
(A) Schematic of the Mp*KTN* gene indicating the location and sequences of the two sgRNAs (K3 and K5). Light grey boxes indicate exons and dark grey boxes indicate untranslated regions. Green regions represent the AAA ATPase domain, and the purple region indicates the Vsp4c domain. Scale bar, 500 bp.
(B) Table of Mp*ktn* mutants including their mutated gene sequences and predicted protein sequences. K3 lines were generated with sgRNA-K3 targeting the exon 4, and K5 lines were generated with sgRNA-K5 targeting exon 7. Presented are 10 out of the 16 Mp*ktn* lines generated.
(C) Diagram of the MpKTN protein structure and length in wild type and three selected Mp*ktn* mutants. Grey boxes indicate exons. Green regions indicate the AAA ATPase domain, and purple regions indicate the Vsp4c domain. Black regions indicate mutated regions.

4.4.3 Mutations in katanin result in defective organ development, tissue morphogenesis, plant growth and fertility in *M. polymorpha*

To define the function of katanin in *M. polymorpha* gametophyte development, I characterised the development of Mp*ktn* mutants throughout their lifecycle, starting with the mature thallus. The dorsal surface of the *M. polymorpha* thallus is composed of air chambers containing an air pore for gas exchange (outlined in **Figure 4.3.B**). Upon the dorsal surface are gemma cups - organs which contain gemmae. In wild type plants, the dorsal thallus was flat and had a uniform arrangement of air chambers with small central air pores (**Figure 4.3.A, B**). The gemma cups were round, protruding structures with serrated edges (**Figure 4.3.C**). By contrast, the Mp*ktn* mutants had undulating thalli with 'crinkled' edges (**Figure 4.3.A, B**). The air chambers in Mp*ktn* were non-uniform in their shape, size, arrangement and spacing, and occasionally the air pore apertures were enlarged or elongated. Further in Mp*ktn* mutants, the gemma cups were enlarged, flat structures with lobed edges and uneven serration (**Figure 4.3.C**). This abnormal phenotype was consistent across all the Mp*ktn* mutants, irrespective of if the mutation was in the AAA ATPase domain or before the VSP4C domain (**Supplementary Figure 4.2.A-C**). Overall, mutations in katanin lead to defects in the morphology of the thallus, gemma cups and air chambers. This indicates that katanin is required for correct organ development and tissue morphogenesis in *M. polymorpha*.

The mature *M. polymorpha* gametophyte develops asexually from a gemma. Gemma development therefore defines the thallus morphology. To characterise katanin's role in gemma development, wild type and Mp*ktn* gemmalings were grown over 11 days. Wild type gemmalings had two symmetrical lobes. At 5 days, the first air chambers appeared and by 7 days the dorsal thallus was uniformly covered by air chambers (**Figure 4.4.A**). By contrast, Mp*ktn* gemmalings had two asymmetrical lobes and crinkled edges. Air chambers started to form at 7 days and by 11 days the dorsal thallus had non-uniform patches of air chambers. At every timepoint, Mp*ktn* gemmalings were smaller than wild type reflecting a slower growth

rate (**Figure 4.4.B**). This growth rate may explain the delayed air chamber development in Mp*ktn* gemmalings but does not explain the patchy air chamber distribution. Overall, this data indicates that katanin is required for timely air chamber formation, correct gemma development and to sustain the growth rate of *M. polymorpha*.

To investigate if katanin activity influences *M. polymorpha* reproduction, Mp*ktn* mutants were grown on soil under far-red light to induce reproductive development. Liverworts are dioicous, with males producing antheridiophores and females producing archegoniophores. Ten of the Mp*ktn* mutants were male and six were female (**Supplementary Figure 4.2.D**). Male wild type plants produce wide, flat antheridiophores with lobed edges (**Figure 4.3.D**). By contrast, the male Mp*ktn* mutants produced small flat antheridiophores with crinkled, un-lobed edges and abnormal outgrowths (**Figure 4.3.D**). Female wild type plants produce 'umbrella-like' archegoniophores with symmetrical fonds (**Figure 4.3.E**). By contrast, the female Mp*ktn* mutants produced small archegoniophores with short asymmetrical fonds and thick stems (**Figure 4.3.E**). Overall, this indicates that katanin is required for both male and female reproductive organ development in *M. polymorpha*.

To investigate if these defects in reproductive structures lead to fertility defects in the Mp*ktn* mutants, each mutant was crossed to wild type plants expressing a microtubule reporter. Only five Mp*ktn* mutants produced sporangia after crossing, unlike wild type crosses which are mostly successful (**Supplementary Figure 4.2.D**). These five crossable Mp*ktn* mutants were all male. Each successful cross only produced a few dark yellow sporangia compared to the many healthy yellow sporangia produced in wild type crosses. Overall, mutations in katanin reduce the fertility of *M. polymorpha* plants, particularly females, thereby reducing spore production. This could result from defects in reproductive development, sperm or egg production, fertilisation, or meiosis of the sporocyte.

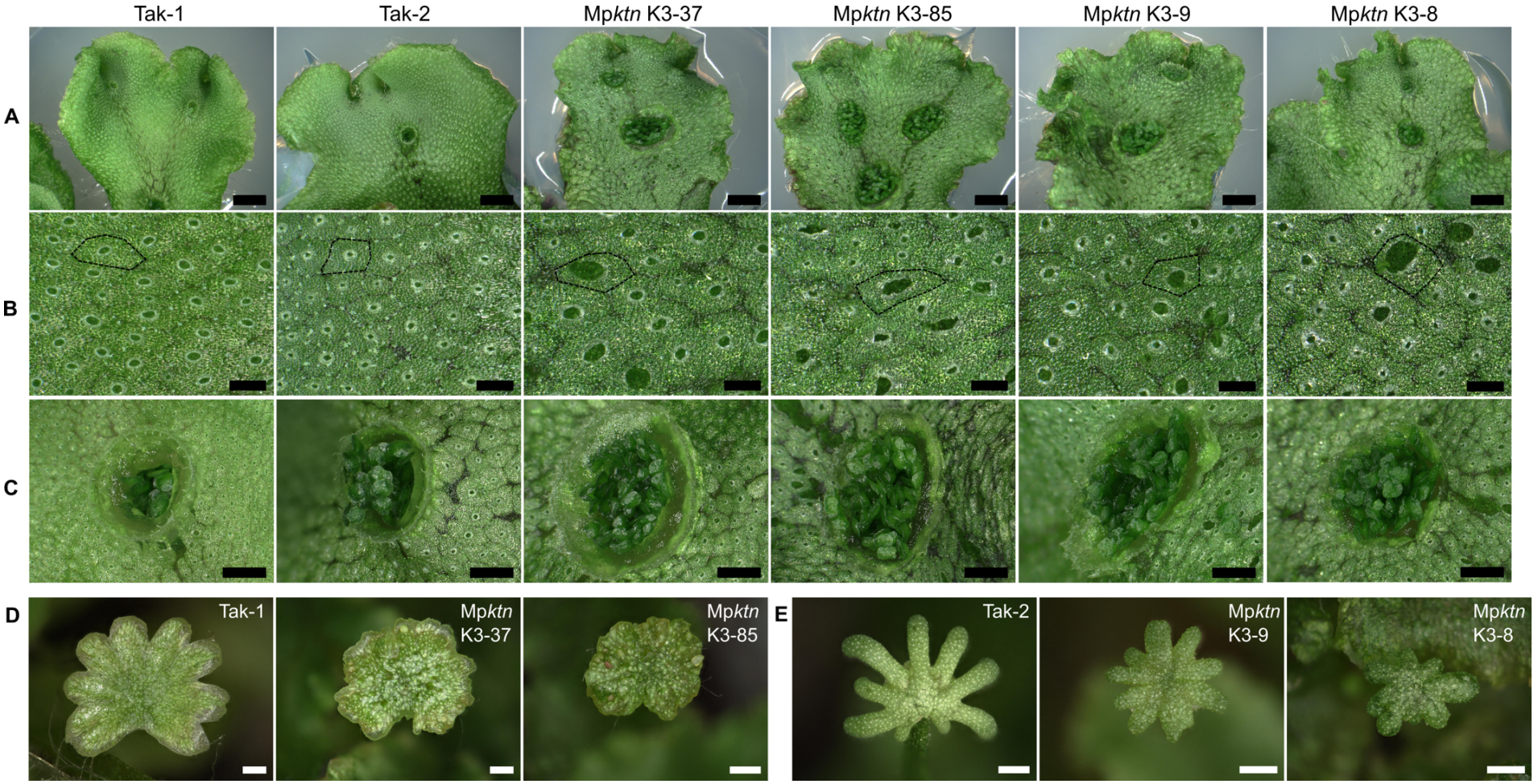

Figure 4.3: Mp*ktn* mutants develop a crinkled thallus, disorganised tissues and abnormal organs

(A) Dorsal thallus of wild type (Tak-1, Tak-2) and four Mp*ktn* mutant plants. Scale bars, 2 mm.

(B) Dorsal epidermal surface of wild type (Tak-1, Tak-2) and four Mp*ktn* mutant plants. One air chamber outlined in each image. Scale bars, 300 µm.

(C) Gemma cups on the dorsal thallus surface of wild type (Tak-1, Tak-2) and four Mp*ktn* mutant plants. Scale bars, 1 mm.

(D) Antheridiophores of wild type (Tak-1) and two male Mp*ktn* mutants (K3-37, K3-85) grown under far-red light. Scale bars, 1 mm

(E) Archegoniophores of wild type (Tak-2) and two female Mp*ktn* mutants (K3-9, K3-8) grown under far-red light. Scale bars, 1 mm.

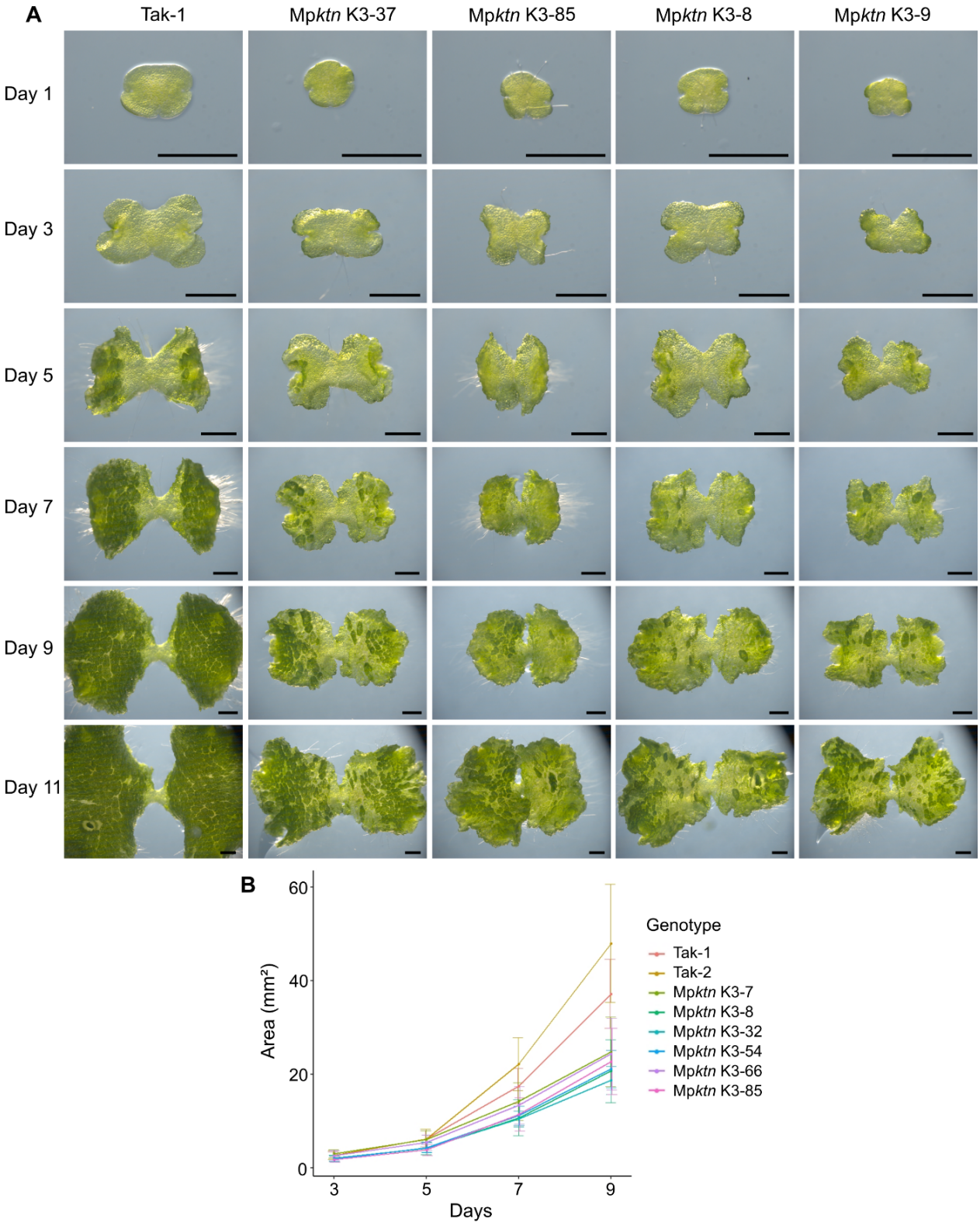

Figure 4.4: Development of Mp*ktn* mutant gemmalings is delayed and defective
(A) Development of wild type (Tak-1) and four Mp*ktn* mutant gemmalings on Gamborg media. Plants grown from 0-day-old gemma and imaged every 2 days over 11 days. Scale bars, 1 mm.
(B) Plot of gemmaling tissue area over 9 days growth for wild type (Tak-1, Tak-2) and six Mp*ktn* mutants. Tissue area was calculated from chlorophyll autofluorescence. 9 plants per genotype were measured every 2 days. Presented is the mean area (mm²) and standard error at each timepoint.

4.4.4 Mutations in katanin result in defective cell patterning in gemma

The plant and tissue defects in Mp*ktn* mutants may result from defects in cell patterning – the organisation of cells with distinct sizes, shapes, and identities within a tissue. To determine if katanin controls the patterning of cells in *M. polymorpha*, 0-day-old wild type and Mp*ktn* gemma were stained with propidium iodide to visualise the walls of each cell. Wild type gemmae were symmetrical in shape with smooth edges (**Figure 4.5.A**). Rhizoid initial cells (chlorophyll devoid cells) and large epidermal cells and were positioned in the gemma centre, leading to smaller cells and regularly spaced oil bodies at the gemma periphery. By contrast, Mp*ktn* gemmae was often asymmetrical in shape, with abnormal lobes and crinkled edges (**Figure 4.5.B-E**). Gemma morphology was highly variable even within the same Mp*ktn* mutant line (**Figure 4.5.B-C**). Rhizoid initial cells and large epidermal cells were positioned both in the gemma centre and at the gemma periphery (seen clearly in **Figure 4.5.B, E**). Oil bodies were variably positioned around the gemma periphery. Overall, this indicates that katanin is required for correct cell patterning and to regulate gemma morphology in *M. polymorpha*. I speculate that this may stem from katanin functioning in cell growth and division.

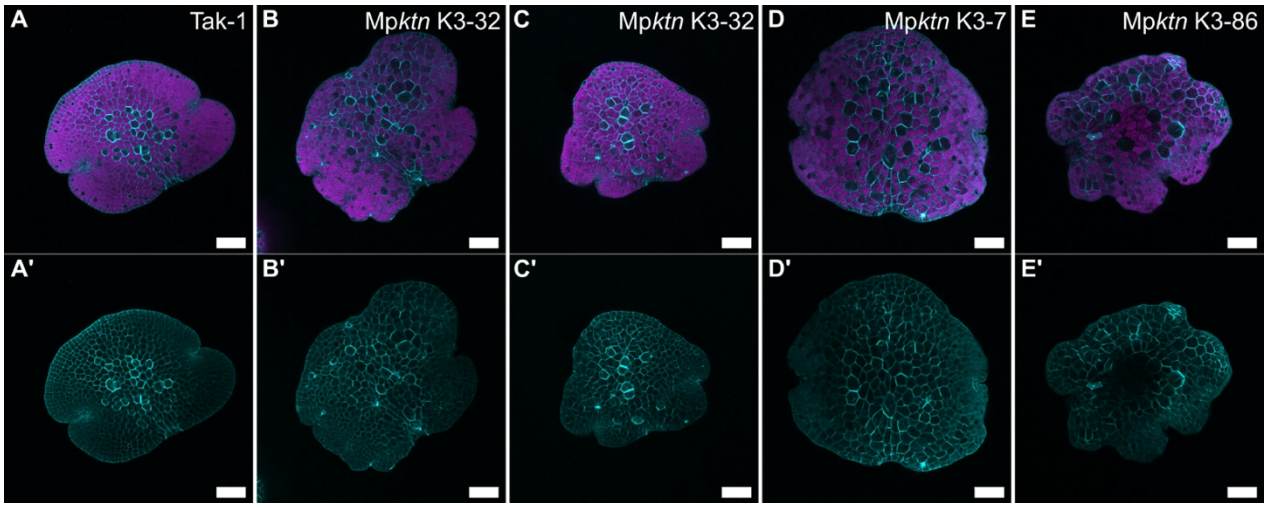

Figure 4.5: Gemmae morphology is variable and cell patterning defective in the Mp*ktn* mutants
Organisation of cells in 0-day-old gemmae from wild type Tak-1 **(A)** and three Mp*ktn* mutants **(B - E)** stained with the cell wall dye, propidium iodide. Both propidium iodide (cyan) and chlorophyll autofluorescence (magenta) signals were captured. Presented are Z-projections of the merged channels (A - E) and propidium iodide only channel (A' - E'). Scale bars, 100 µm.

4.4.5 Katanin activity promotes the parallel organisation and bundling of cortical microtubules

Katanin is a microtubule severing enzyme which cuts arrays to alter the microtubule architecture within a cell (McNally & Vale, 1993). To investigate the role of katanin in the regulation of microtubules in *M. polymorpha*, microtubule dynamics and organisations were observed in the Mp*ktn* mutants using a microtubule reporter. To integrate the reporter into the Mp*ktn* mutants, Mp*ktn* mutants were crossed to plants expressing *p*Mp*EF1α:GFP-*Mp*TUB1* (GFP-MpTUB1). Wild type (wildtype-TUB) and mutant (Mp*ktn*-TUB) progeny which lacked Cas9 and expressed the GFP-MpTUB1 reporter were then selected (**Figure 4.3.2**). This was done for three independent mutant lines (K3-37, K3-85, K5-45). In this chapter, I used wildtype-TUB and Mp*ktn*-TUB siblings derived from crossing the Mp*ktn* K3-37 mutant.

To determine if katanin regulates the organisation of the cortical array in *M. polymorpha*, I imaged microtubules in the cortex of the central epidermal cells in wild type and Mp*ktn* gemma. In wild type, there was a mixture of cells with parallel arrays and others with non-parallel arrays (**Figure 4.6.A**). In Mp*ktn,* all cells had dense, non-parallel microtubule arrays (**Figure 4.6.B**). This suggests katanin regulates cortical arrays in a cell-specific manner. To then quantify the differences in microtubule parallelness, bundling and density between wild type and Mp*ktn* cells, I used an image analysis methodology described in Higaki, 2017. My study segmented and quantified microtubules in 108 wild type cells and 107 Mp*ktn* cells from 10 gemmae each. I will now separately explore each parameter quantified.

Microtubule parallelness is the orientation of microtubules relative to one another within a cell. This is measured by the distribution of angles formed by microtubules (NormAvgRad) which ranges from 0 non-parallel to 1 parallel. Wild type had a mixture of cells with random organisations and cells with parallel organisations. This was reflected by a high parallelness score but with high variability (0.338 ± 0.148) (**Figure 4.6.B, C**). By contrast, in the Mp*ktn* mutant most cells had non-parallel, random cortical arrays and almost no cells had parallel

organisations. This consistent randomness was reflected by a significantly lower parallelness score and lower variability in Mp*ktn* (0.172 ± 0.101) than wild type.

Microtubule bundles are formed from arrays of overlapping microtubules. Bundling is measured as the skewness in the intensity distribution of segmented microtubules, with higher intensity values indicating higher bundling. Bundling was significantly higher and more variable in wild type (1.390 ± 0.303) than in the Mp*ktn* mutant (1.300 ± 0.228) (**Figure 4.6.B, D**). This may relate to microtubule parallelness, as wild type had more cells with parallel microtubules which are more likely to overlap and bundle together.

Microtubule density is the area of the cell surface covered by cortical microtubules. This is calculated as the number of segmented pixels in a cell divided by the cell area (npix/μm²). Density was significantly higher in the Mp*ktn* mutant (9.384 ± 1.612) compared to wild type (7.700 ± 1.864) however the variability was not significantly different (**Figure 4.6.B, E**). Therefore, Mp*ktn* cells consistently had more microtubules than wild type cells.

In summary, the results suggest that katanin activity increases the overall parallelness and bundling of cortical arrays in *M. polymorpha* and decreases cortical microtubule density.

4.4.6 Katanin activity orients cortical arrays but with little effect on cell growth

Cortical arrays can orient the direction of cell growth (Burk & Ye, 2002). To determine the effect of katanin regulated cortical microtubule organisation on cell growth, I quantified the area and circularity of the wildtype-TUB and Mp*ktn*-TUB cells used in the previous microtubule analysis. There was no significant difference in cell area between wild type (895.9 μm² ± 286.6 μm²) and the Mp*ktn* mutant (887.9 μm² ± 279.4 μm²) (**Figure 4.6.C**). The mean cell circularity was also similar between wild type (0.828 ± 0.04) and Mp*ktn* (0.815 ± 0.60). However, the variability of cell circularity was significantly higher in Mp*ktn*, indicating a wider range of cell shapes (**Figure 4.6.C, G**). As this analysis describes the mature cells in the gemma centre, which have stopped growth and division, their current microtubule

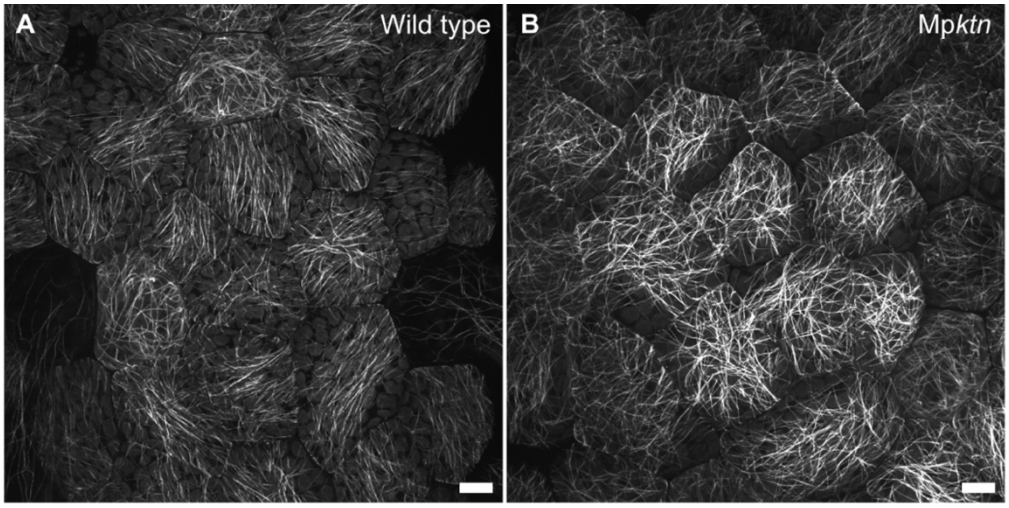

C

	Genotype	Mean	Standard deviation	T-test (Welch's, 2-tail)	F-test (2-tail)
Parallelness (NormAvgRad)	Wild type	0.338	0.148	4.33E-18 ***	0.0001 ***
	Mp*ktn*	0.172	0.102		
Bundling (skewness)	Wild type	1.389	0.303	0.0121 *	0.0032 ***
	Mp*ktn*	1.297	0.227		
Density (npix/µm²)	Wild type	7.700	1.612	2.18E-11 ***	0.1350
	Mp*ktn*	9.384	1.864		
Cell area (µm²)	Wild type	895.851	286.589	0.8367	0.7932
	Mp*ktn*	887.883	279.375		
Cell circularity	Wild type	0.828	0.040	0.0658	5.31E-05 ***
	Mp*ktn*	0.815	0.060		

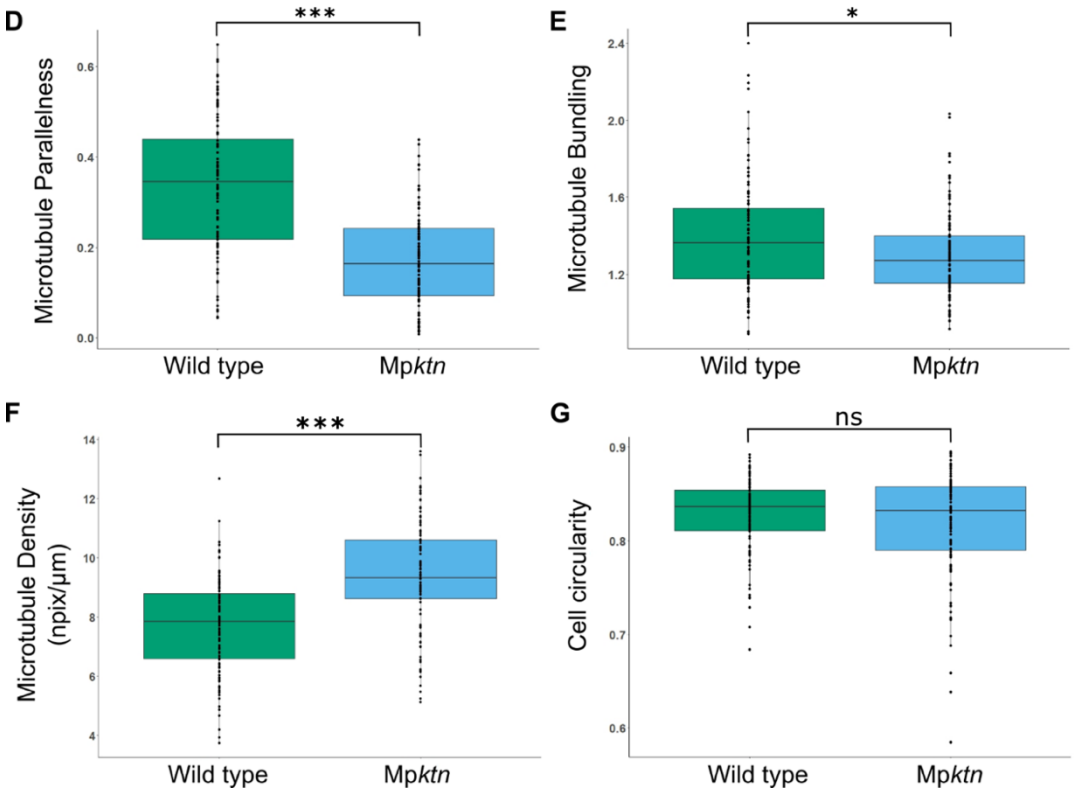

Figure 4.6: Cortical arrays are disordered, less bundled and denser in the Mp*ktn* mutant
(A - B) Cortical arrays in the central epidermal cells of wild type **(A)** and Mp*ktn* (K3-37) **(B)** 2-day-old gemmae expressing *p*Mp*EF1α:GFP*-Mp*TUB1.* Presented are Z-projections. Scale bars, 10 µm. **(C)** Quantification of the parallelness, bundling and density of cortical microtubules in wild type and Mp*ktn* (K3-37) epidermal cells from 2-day-old gemmae. N = 108 cells for wild type, N = 107 cells for

Mp*ktn* across 10 gemmae per genotype. Data was analysed using Welches 2-tail T-test and 2-tail F-test. (*) indicates a significant difference between the genotypes, P = 0.05.
(D - F) Boxplots of the parallelness **(D)**, bundling **(E)**, and density **(F)** of cortical microtubules in the wild type and Mp*ktn* cells quantified in (C).
(G) Boxplot of the circularity of the cells from wild type and Mp*ktn* quantified in (C).

organisation may not have directed previous cell growth. Overall, the results suggest that regulation of cortical arrays by katanin does not affect the average size or shape of gemma epidermal cells but may reduce variability in cell shape. One hypothesis is that katanin reorients arrays after cell growth has ceased.

4.4.7 Katanin localises to cortex of epidermal cells in *M. polymorpha*

I have demonstrated that cortical microtubules are less parallel in the Mp*ktn* mutant compared to wild type, suggesting that katanin severing generates parallel cortical arrays in *M. polymorpha.* To test this hypothesis, katanin was localised in *M. polymorpha* cells using the fluorescent reporter *p*Mp*KTN:GFP*-Mp*KTN* (GFP-KTN). This reporter is composed of the genomic DNA sequence of Mp*KTN* fused to a N-terminus GFP and expressed under the Mp*KTN* promotor (**Figure 4.3.1**). To visualise the katanin reporter in epidermal cells of *M. polymorpha*, GFP fluorescence was captured in 1-day-old gemma from wild type and GFP-MpKTN transformants. To distinguish the GFP-MpKTN signal at 488 nm excitation from chlorophyll autofluorescence, I also captured chlorophyll signal at 640 nm excitation and overlaid the channels. In multiple independent lines expressing GFP-MpKTN, distinct puncta were identified at the surface of the central epidermal cells (**Figure 4.7.B-D**). These puncta did not overlap with the chlorophyll autofluorescence. In wild type cells with no reporter expression, only chloroplast autofluorescence was observed and no surface puncta (**Figure 4.7.A**). In conclusion, the puncta represent the GFP-MpKTN signal and indicate that katanin is present at distinct sites in the cell cortex of *M. polymorpha.* This data is consistent with the hypothesis that katanin localises to, and severs, cortical microtubules at sites of cross over

and branching to generate parallel cortical arrays. To verify katanin localises to these sites would require an RFP-MpTUB1 reporter to be used in combination with GFP-MpKTN.

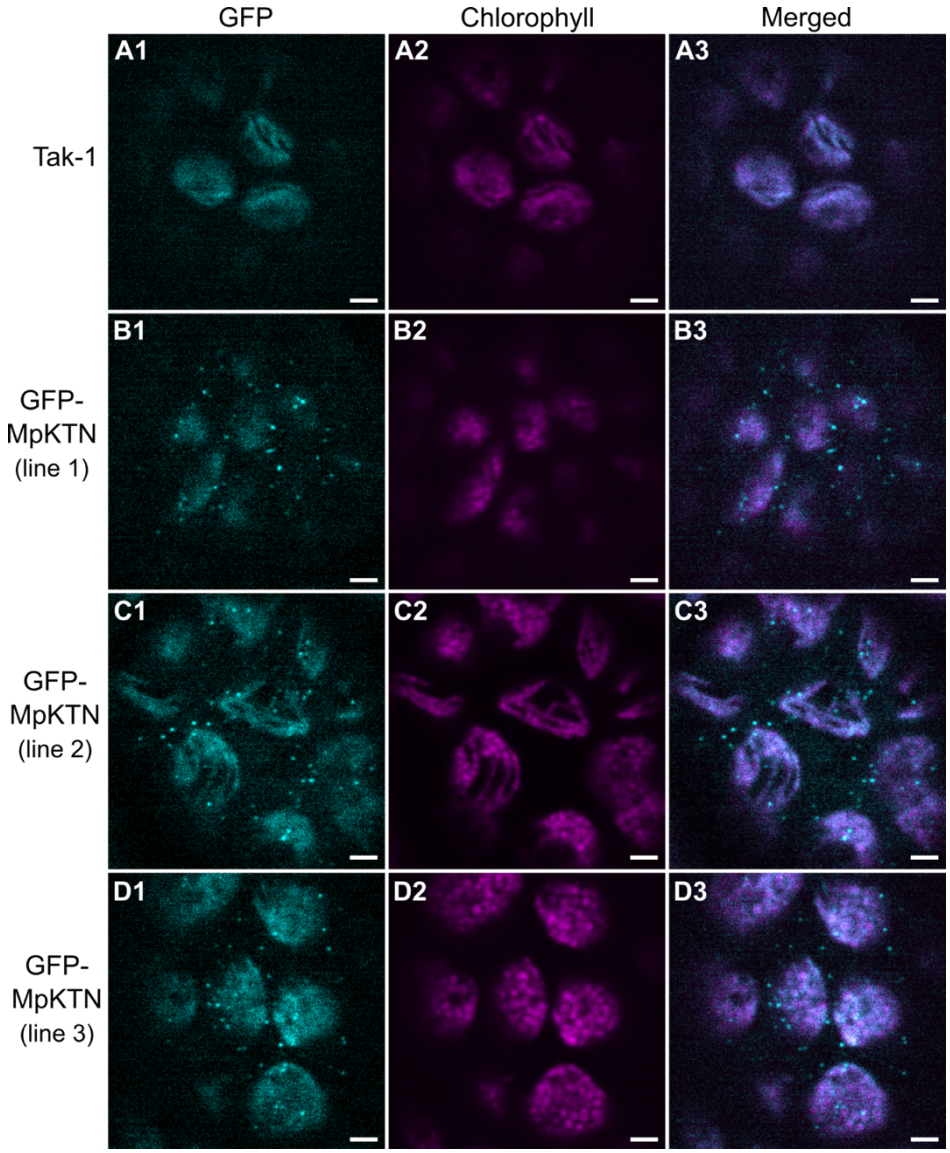

Figure 4.7: GFP-MpKTN localises to the cortex of *M. polymorpha* epidermal cells
Localisation of GFP-MpKTN in central epidermal cells of 1-day-old gemma from wild type Tak-1 **(A)** and three independent plant lines expressing *p*Mp*KTN:GFP*-Mp*KTN* **(B - D)**. Presented are single slices of the epidermal surface showing the GFP fluorescence signal (A1 - D1), chlorophyll autofluorescence (A2 - D2) and merged channels (A3 - D3). Scale bars, 2 µm.

4.4.8 Katanin aids the formation of polar organisers and astral arrays

Microtubule organising centres (MTOCs) nucleate and organise microtubules within cells. Liverworts are unique among land plants as they have two acentrosomal MTOCs – the polar organisers – which form *de novo* during prophase and nucleate astral and peri-nuclear

arrays (Buschmann *et al.*, 2016). I hypothesised that katanin is required for the formation of polar organisers and the dynamics of the nucleated microtubules in *M. polymorpha*.

To investigate katanin's role in polar organiser formation and structure, microtubules in dividing cells near the meristems of wildtype-TUB and Mp*ktn*-TUB gemma were imaged. Wild type cells had two defined polar organisers at opposing sides of the nucleus (**Figure 4.8.A**). The nucleated astral arrays radiated out symmetrically to the cortex. By contrast, Mp*ktn* cells had elongated and misshaped polar organisers positioned asymmetrically around the nucleus (**Figure 4.8.B**). The nucleated astral arrays radiated out asymmetrically to the cortex, often denser on one cell side. Most wild type cells with polar organisers had a pre-prophase band (PPB) (exemplified in **Figure 4.8.A1**). By contrast, PPB were never observed in Mp*ktn* cells with polar organisers. Overall, this indicates that katanin is required to define the polar organiser structure and for PPB formation in *M. polymorpha*.

Many Mp*ktn* cells appeared to have supernumerary polar organisers. I therefore quantified the number of polar organisers in 36 wild type cells and 35 Mp*ktn* cells (**Figure 4.8.C**). 83.3% of wild type cells had two polar organisers compared to 54.3% of Mp*ktn* cells. 16.7% of wild type cells had three polar organisers compared to 28.6% of M*pktn cells*. Often the three 'polar organisers' noted in wild type cells had low fluorescence intensity and may have been microtubule foci. 14.2% of Mp*ktn* cells had four polar organisers and wild type had none. Overall, the Mp*ktn* mutant had on average more polar organisers per cell than wild type. This indicates that katanin is required to regulate the number of polar organisers in each cell, potentially by regulating the formation of polar organisers from microtubule foci.

To investigate katanin's role in the dynamics of polar organisers and the astral arrays, short interval timelapses were captured. In wild type, the position of the polar organisers and astral arrays often moved between timepoints indicated by the range of colours in the temporal projections (**Figure 4.8.D**). In Mp*ktn*, the position of polar organisers and astral arrays often overlapped between timepoints, indicated by the white regions in the temporal projections

(**Figure 4.8.E**). This data, although limited, suggests that polar organisers are more mobile in wild type than in Mp*ktn,* and the astral arrays are more dynamic. One hypothesis is that katanin severing increases polar organiser mobility by controlling astral array dynamics.

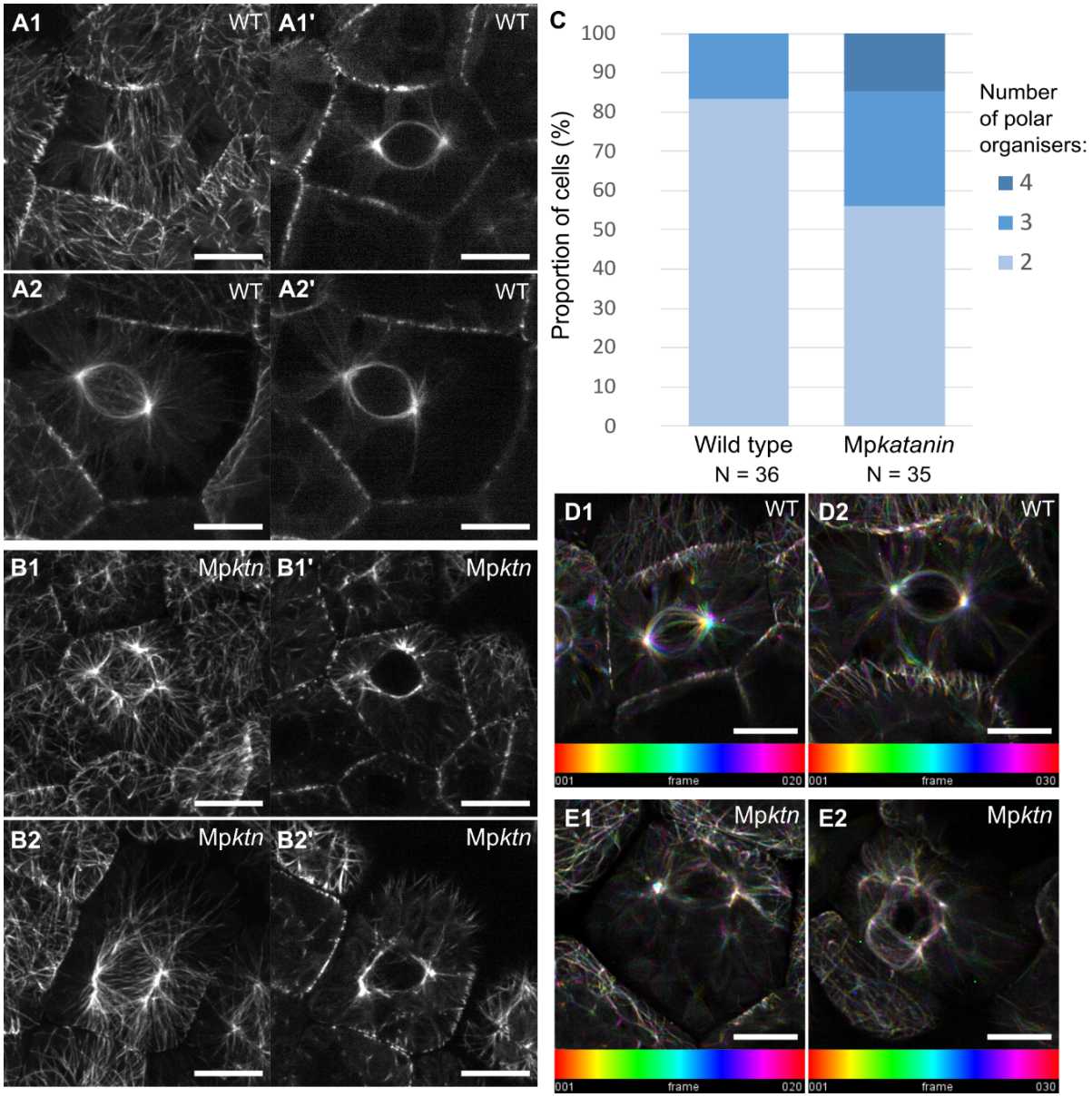

Figure 4.8: Supernumerary, disordered polar organisers form in Mp*ktn* cells
(A - B) Polar organisers and astral arrays in two representative wild type **(A1, A2)** and Mp*ktn* (K3-37) **(B1, B2)** cells from 2 day old gemmae expressing *p*Mp*EF1α:GFP*-Mp*TUB1.* Presented are Z projections (A, B) and central slices in XY (A', B'). Scale bars, 10 µm.
(C) The proportion of wild type and Mp*ktn* (K3-37) cells in 2-day-old gemmae with 2, 3 or 4 polar organisers. N = 36 cells for wild type, and N= 35 cells for Mp*ktn*.
(D - E) Temporal projections of polar organiser movement in two wild type **(D1, D2)** and two Mp*ktn* (K3-37) **(E1, E2)** cells from 2 day old gemmae expressing *p*Mp*EF1α:GFP*-Mp*TUB1.* Timelapses were taken with 8 seconds intervals for a total of 20 (D1, E1) or 30 (D2, E2) frames. Presented are temporal projections created from deconvolved Z-projections of 5 µm. Scale bars, 10 µm.

4.4.9 Katanin regulates the structure and positioning of the mitotic spindle and the phragmoplast within the cell

Polar organisers are known to disassemble at the onset of mitosis to form y-tubulin mini-poles which nucleate the mitotic spindle (Brown *et al.*, 2004). I hypothesised that, alongside polar organisers, katanin would also regulate mitotic spindle formation. To investigate this, the mitotic spindle structure and position was characterised in wildtype-TUB and Mp*ktn*-TUB cells undergoing mitosis. The spindles in wild type cells appeared short and box shaped (**Figure 4.9.A**). By contrast, the spindles in Mp*ktn* appeared elongated with tapered poles (**Figure 4.9.B**). This was reflected by a significantly higher and more variable spindle length in Mp*ktn* (15.5 µm ± 2.93 µm) compared to wild type (9.4 µm ± 0.69 µm) (**Figure 4.9.C**). Spindles were positioned centrally in wild type cells, but often near the edge of Mp*ktn* cells (**Figure 4.9.A, B**). The average distance between the cell centre and the spindle centre in Mp*ktn* (3.38 µm ± 1.4 µm) was significantly higher and more variable compared to wild type (0.87 µm ± 0.4 µm) (**Figure 4.9.D**). This indicates that spindles were consistently central in wild type cells but were variably position in Mp*ktn* cells. Overall, this data indicates that katanin is required to regulate mitotic spindle length and positioning in *M. polymorpha.*

The role of katanin in phragmoplast formation was likewise investigated. The early phragmoplast appeared similar in wild type and Mp*ktn* cells (**Figure 4.9.E, F**). The structure of expanded phragmoplast was overall similar in wild type and Mp*ktn* cells, but the phragmoplast arrays appeared more tilted and had wide gaps in the Mp*ktn* mutant(**Figure 4.9.G, H**). The phragmoplast typically cut straight across the central plane of wild type cells, to divide the cell across the shortest axis (**Figure 4.9.G).** By contrast, the phragmoplast in Mp*ktn* cells was variably positioned, often curved across the cell, and often not aligned with the shortest cell axis (**Figure 4.9.H**). Overall, this indicates that katanin maybe required to regulate the structure and orientation of the phragmoplast in *M. polymorpha.*

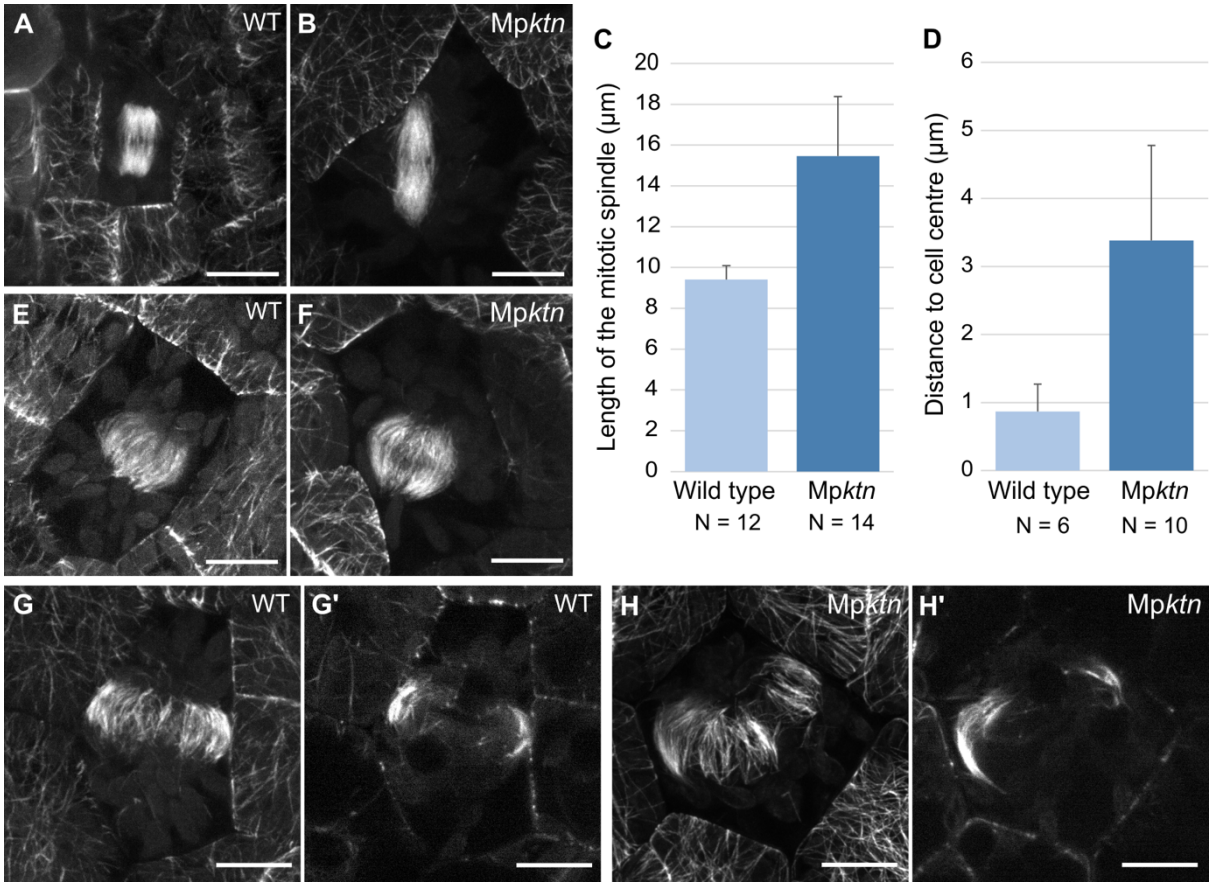

Figure 4.9: Elongated mitotic spindles and disordered phragmoplast arrays form in Mp*ktn* cells often in non-central positions

(A - B) The mitotic spindle in wild type **(A)** and Mp*ktn* (K3-37) **(B)** cells from 2-day-old gemmae expressing *p*Mp*EF1α:GFP*-Mp*TUB1*. Presented are Z-projections. Scale bars, 10 µm.

(C) Graph of the mitotic spindle length (µm) in wild type and Mp*ktn* (K3-37) cells. N is the number of spindles analysed.

(D) Graph of the distance (µm) between the centre of the mitotic spindle and the centre of the cell for wild type and Mp*ktn* (K3-37). N is the number of spindles analysed.

(E - F) The early phragmoplast in wild type **(E)** and Mp*ktn* (K3-37) **(F)** cells from 2-day-old gemmae expressing *p*Mp*EF1α:GFP*-Mp*TUB1*. Presented are Z-projections. Scale bars, 10 µm.

(G - H) The expanded phragmoplast in wild type **(G)** and Mp*ktn* (K3-37) **(H)** cells from 2-day-old gemmae expressing *p*Mp*EF1α:GFP*-Mp*TUB1*. Presented are Z-projections (G, H) and central slices in XY (G', H'). Scale bars, 10 µm.

4.4.10 The polar organiser axis and mitotic spindle axis are misaligned in the Mp*ktn* mutant during cell division

In *M. polymorpha*, the PPB and polar organisers are thought to determine the position of the mitotic spindle, phragmoplast and ultimately the plane of cell division (Buschmann *et al.*, 2016). I hypothesised that in Mp*ktn* mutant cells, the disordered polar organisers were the origin of the mispositioned mitotic spindles and phragmoplasts, and would ultimately result in abnormal cell division planes. To test this hypothesis, I captured timelapses of dividing wildtype-TUB and Mp*ktn*-TUB cells and compared the 'polar organiser axis' (e.g the axis between the two polar organisers) to the 'spindle axis' (e.g the axis between the two mitotic spindle poles) and the plane of phragmoplast expansion.

In the timelapse of a wild type cell, the microtubule basket was positioned in the cell centre with the polar organiser axis perpendicular to the PPB at 0 to 30 minutes (**Figure 4.10.A**). At 40 minutes the mitotic spindle formed in the cell centre. The spindle axis was identical to the polar organiser axis. At 60 minutes the phragmoplast formed in the cell centre and expanded in a plane perpendicular to the mitotic spindle, in the same plane as the PPB. The cell divided symmetrically and anticlinal to the epidermal surface. The same series of events were previously described in Buschmann *et al.*, 2016.

By contrast, in the two Mp*ktn* cell timelapses, the microtubule basket appeared tilted within the cell at 0 to 40 minutes (**Figure 4.10.B, C**). The polar organisers axis was hard to define and therefore was estimated as the axis between the two brightest foci. At 50 minutes, an indistinct bundle of microtubules formed at the location of the microtubule basket then at 60 minutes the mitotic spindle formed. In cell B, the mitotic spindle formed in a different axis to the polar organiser axis, clearly viewed from the X-axis (**Supplementary Figure 4.3.C, D**). In cell C, the mitotic spindle elongated and rotated over a 60-minute period (**Figure 4.10.C**). The spindle axis misaligned with the polar organiser axis. In both cells, the phragmoplast formed and expanded in a plane perpendicular to the last position of the mitotic spindle. Cell

B divided in a tilted plane, clearly viewed from the Y-axis (**Supplementary Figure 4.3.A, B**). Cell C divided asymmetrically. In summary, in the Mp*ktn* mutant the polar organiser axis and spindle axis did not align, the spindle could rotate overtime, and the phragmoplast expanded perpendicular to the final spindle axis. This is not consistent with my original hypothesis, that katanin orients cell division purely from regulating polar organisers formation. Instead, this data suggests that katanin orients cell division by aligning the mitotic spindle axis with the polar organiser axis and stabilising the mitotic spindle throughout mitosis.

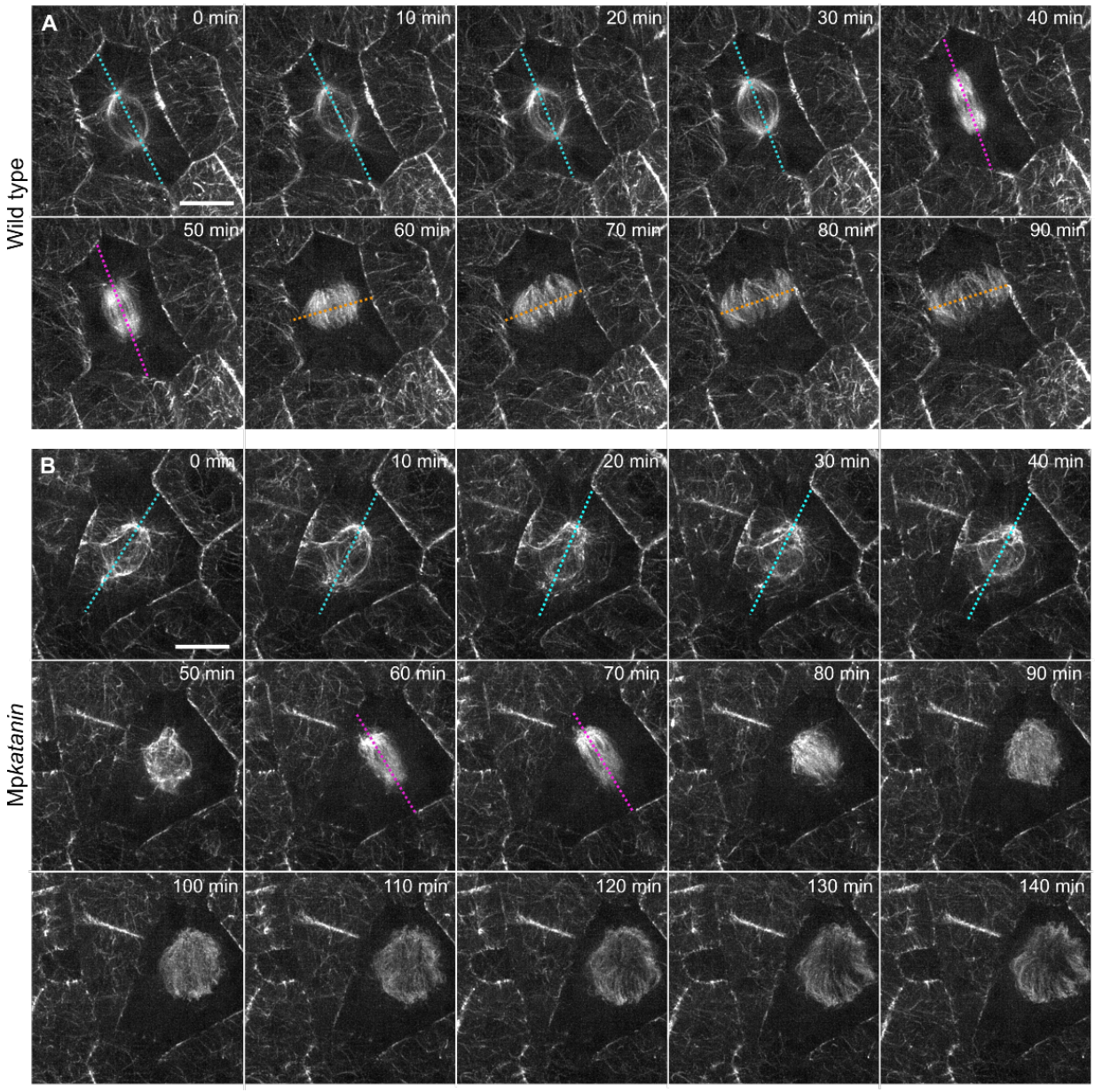

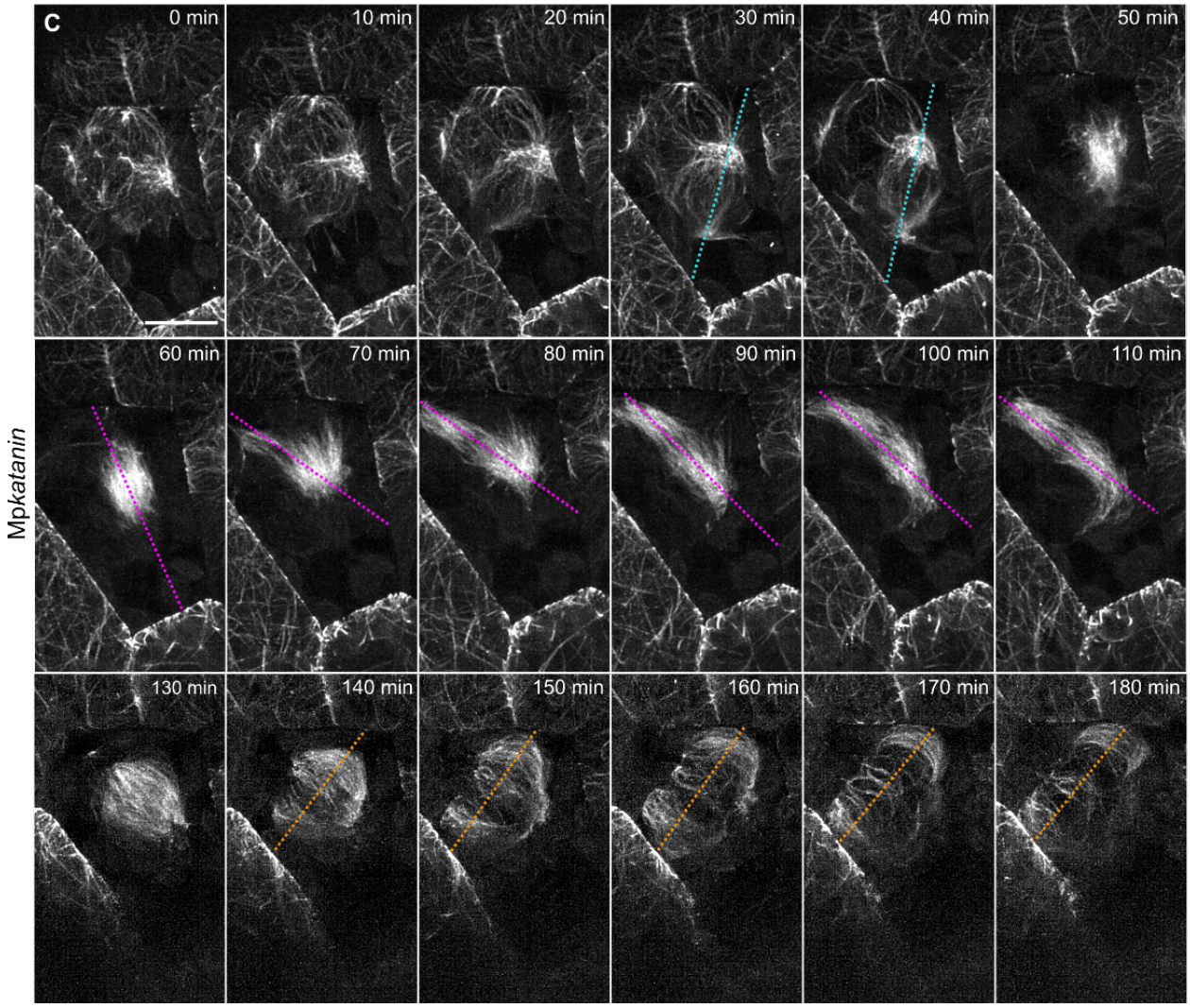

Figure 4.10: The polar organiser axis and mitotic spindle axis misalign during cell division in the Mp*ktn* mutant and the mitotic spindle can rotate overtime

Timelapses of a dividing wild type cell **(A)** and two Mp*ktn* (K3-37) cells **(B, C)** from 2-day-old gemmae expressing *p*Mp*EF1α:GFP*-Mp*TUB1*. Presented are deconvolved Z-projections taken at 10-minute intervals. Dotted cyan lines indicate the polar organiser axis, dotted magenta lines indicate the mitotic spindle axis and dotted orange lines indicate the phragmoplast axis. Scale bars, 10 µm.

4.5 Discussion

4.5.1 Katanin controls tissue morphogenesis in *M. polymorpha*

Katanin severs microtubules to regulate their organisation and dynamics (McNally & Roll-Mecak, 2018). In this chapter, I show that katanin is highly conserved across land plants and there is a single copy in *M. polymorpha* which controls gametophyte development. Across multiple Mp*ktn* mutants, I characterised defects in thallus morphology, air chamber formation, air pore size, gemma cup structure, reproductive development, fertility, and growth rate. These phenotypic defects were consistent across the Mp*ktn* mutants including both in-frame and frameshift mutations, in the AAA ATPase domain and in the VSP4C domain. This suggests that both domains and their highly conserved sequences are required for katanin function. Many of these traits are also characteristic of the *A. thaliana* katanin (At*ktn*) mutants for example defects in fertility, growth and organ development (Bichet *et al.*, 2001; Burk *et al.*, 2001; Webb *et al.*, 2002; Bouquin *et al.*, 2003; Luptovčiak, Samakovli, *et al.*, 2017; Ovečka *et al.*, 2020). In summary, katanin has pleiotropic effects at multiple stages of the plant lifecycle, suggesting that katanin functions in fundamental cellular processes which underpin multiple aspects of plant development.

4.5.2 Katanin orients and promotes bundling of the cortical arrays

Through severing microtubules, katanin can alter the microtubule architecture within a cell (McNally & Roll-Mecak, 2018). My data indicates that katanin promotes the formation of parallel, bundled cortical arrays in *M. polymorpha*. This is evidenced by the less parallel and less bundled cortical arrays in the Mp*ktn* mutant compared to wild type. Katanin also appears to regulate microtubule density, as microtubules were on average denser in the Mp*ktn* cells compared to wild type. One hypothesis is that katanin targets older arrays for severing which induces their depolymerisation and thereby regulating the number of microtubules per cell. This is consistent with studies in *A. thaliana*, which show that katanin severs microtubules at cross-over and branch points to maintain, re-organise, and promote

bundling of cortical arrays and prune older arrays (Stoppin-Mellet *et al.*, 2006; Zhang *et al.*, 2013). In summary, katanin severing is required to reorientate cortical arrays into parallel bundles and to lower microtubule density in *M. polymorpha* epidermal cells, likely by cutting at cross-over points. Consistent with this hypothesis, katanin was localised at foci in the cortex of *M. polymorpha* cells.

Variation in the cortical array organisation was observed between individual epidermal cells. Across wild type tissue, the average parallelness of the cortical array was high, but there was also high variability between individual cells e.g., some cells had highly parallel arrays whilst others had nonparallel arrays. By contrast, in all Mp*ktn* cells the arrays were consistently random. I hypothesise that during *M. polymorpha* development, katanin severing reorientates cortical microtubules from random to parallel arrays as a cell matures. In the absence of katanin activity, cortical arrays retain a random arrangement despite cell maturity. This could explain the variation in wild type - as arrays may be in the process of reorientation - compared to the invariance in the Mp*ktn* mutant.

The arrangement of cortical arrays directs cellulose deposition and controls the direction of plant cell growth (Burk & Ye, 2002). Random cortical arrays typically lead to isotropic cell growth, whilst parallel arrays lead to diffuse anisotropic growth. In wild type, reorientation of cortical arrays from nonparallel to parallel is predicted to alter growth from isotropic to anisotropic. Whereas in Mp*ktn* cells, isotropic cell growth is maintained. However, this hypothesis is opposed by my evidence that the wild type and Mp*ktn* cells analysed had similar sizes and shapes. An alternative hypothesis is that katanin reorients the cortical arrays after the cell has matured and stopped growth, therefore not affecting the cell growth direction. Further quantification of cell size and shape across the entire gemma at multiple timepoints for both wild type and the Mp*ktn* mutant could clarify if katanin plays a role in directional cell growth in *M. polymorpha*.

4.5.3 How does katanin regulate the size and shape of polar organisers?

Polar organisers are the acentrosomal microtubule organising centres (MTOCs) of liverworts, forming two points on opposing sides of the nucleus (Brown & Lemmon, 1990). Containing mostly y-tubulin, the polar organisers nucleate peri-nuclear arrays which encase the nucleus and astral arrays which polymerise to the cell cortex (Brown *et al.*, 2004; Buschmann *et al.*, 2016). My data indicates that katanin severing is required to define the polar organiser structure and to organise the nucleated arrays. Wild type polar organisers appear as distinct points which nucleate symmetrical arrays. Whilst polar organisers in Mp*ktn* cells appeared as elongated points nucleating scrambled dense arrays. Overall, my data is consistent with the hypothesis that katanin severing regulates the size and shape of polar organisers, and the density and organisation of the nucleated arrays in *M. polymorpha*.

I hypothesise that katanin severing, astral array density and polar organiser shape are tightly interlinked. Here I propose a model. When katanin is functional, the astral and peri-nuclear arrays are severed which initiates their depolymerization. This opens space at the polar organiser for new arrays to be nucleated and maintains the polar organiser size (**Summary Figure 4.1.A**). By contrast in the absence of katanin, arrays are not severed and remain stable. To nucleate new arrays, the polar organiser must increase in size by accumulating y-tubulin (**Summary Figure 4.1.A**). This forms a feedback loop with katanin at the core; the array dynamics determine the polar organiser structure which in turn determines the array organisation. To test this hypothesis, I established a katanin reporter (GFP-MpKTN) in *M. polymorpha.* In the future, this reporter - in combination with a microtubule reporter – could determine if katanin localises to, and severs, the astral arrays nucleated from the polar organisers.

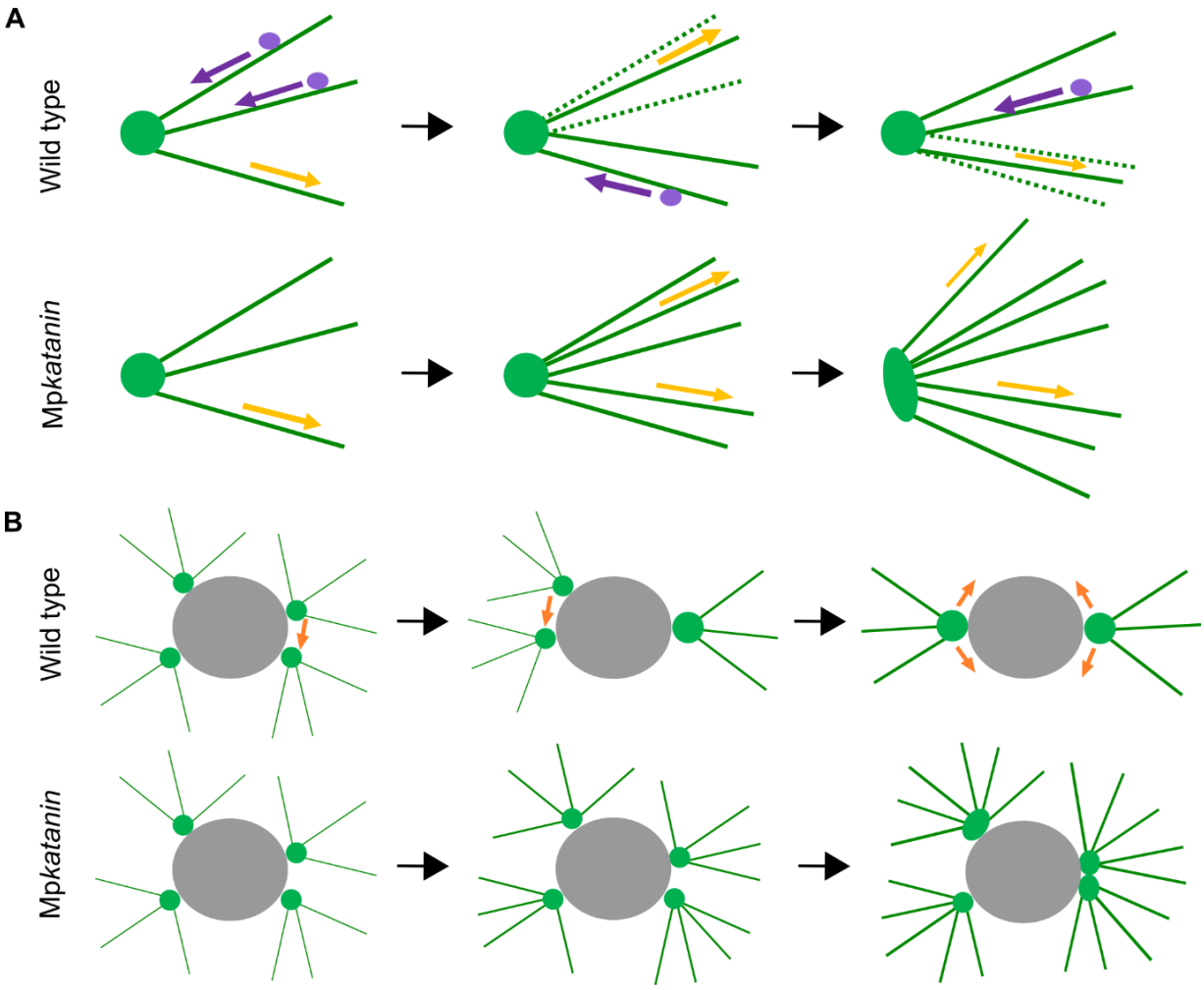

Summary Figure 4.1: Hypotheses for the role of katanin in astral microtubule dynamics, and the formation and mobility of polar organisers in *Marchantia polymorpha*

(A) Hypothesis for the dynamics of astral microtubule in wild type and Mp*ktn* mutants. Astral microtubules continuously polymerise from the polar organiser. In wild type, katanin cuts the astral arrays and causes their depolymerisation. The density of astral arrays stays stable. In Mp*ktn* mutants, no astral arrays are cut and depolymerised. The density of astral arrays increases over time, and the polar organiser expands to accommodate.

(B) Hypothesis for the formation and mobility of polar organiser in wild type and Mp*ktn* mutants. Multiple microtubule foci are positioned around the nucleus. In wild type, these foci can move and fuse to form two polar organisers, which are mobile. In Mp*ktn* mutants, these foci cannot move due to their stable astral arrays and cannot fuse. Multiple polar organisers form.

Microtubule (green line), microtubule foci/polar organiser (green circle), nucleus (grey circle). Katanin protein (purple circle). Microtubule polymerisation (yellow arrow), microtubule depolymerisation (purple arrow). Movement of microtubule foci/polar organisers (orange arrow).

4.5.4 Does katanin control polar organiser formation?

Two polar organisers form in each wild type *M. polymorpha* cell. By contrast Mp*ktn* mutants often had supernumerary polar organisers, consistent with the hypothesis that katanin controls polar organiser number. Two mechanisms of katanin activity could explain this: one is that katanin maintains two polar organisers (e.g without katanin the polar organisers form but then split), the alternative is that katanin aids in the formation of polar organisers.

Polar organisers are formed *de novo* by the bipolar aggregation of several small microtubule foci across the nuclear surface (Buschmann *et al.*, 2016). Here I propose a katanin-based mechanism for polar organiser formation. When katanin is active, astral arrays are continuously being cut, depolymerised and repolymerised. This enables microtubule foci to move freely around the nucleus and fuse into the final two polar organisers (**Summary Figure 4.1.B**). By contrast when katanin is inactive, the astral arrays are more stable and anchor the microtubule foci in place, reducing movement and preventing fusion. Each foci accumulates y-tubulin, grows, and nucleates more arrays and becomes a supernumerary polar organiser (**Summary Figure 4.1.B**). This hypothesis suggests that polar organiser formation is dependent on katanin controlling astral array dynamics. In summary, I propose a mechanism for *de novo* MTOC formation in *M. polymorpha,* and a novel function for katanin in this pathway.

4.5.5 Katanin controls pre-prophase band formation, but how?

The pre-prophase band (PPB) is a parallel band of microtubules at the cortex which aligns across the pre-mitotic nucleus and determines the future division plane in plant cells. In liverworts, the polar organisers form before the PPB (Brown & Lemmon, 1990; Buschmann *et al.*, 2016). In Mp*ktn* cells, no true PPB was ever observed and may be linked to the presence of supernumerary polar organisers. In one study, *M. polymorpha* cells treated with CIPC – a drug inducing additional MTOCs – had reduced PPB formation (Buschmann *et al.*, 2016). It was proposed that additional polar organisers influence activities at the cortex

which confuses PPB formation. My data agrees with this. Overall, one hypothesis is that katanin indirectly regulates PPB formation through regulation of polar organiser number.

An alternative hypothesis is that katanin directly regulate PPB formation. There are two steps to PPB formation: alignment then narrowing of cortical microtubules into a parallel array. Although no full PPB forms in Mp*ktn*, a dense microtubule array wrapping around one edge was often observed. This may resemble an extreme form of the one-sided PPB characteristic of At*ktn* mutants, which is attributed to katanin mediating PPB narrowing (Komis *et al.*, 2017). Overall, a second hypothesis is that katanin regulates PPB formation through directly aligning and narrowing arrays. In summary, katanin is required for PPB formation in *M. polymorpha*, but the role of katanin plays is still unclear.

4.5.6 Katanin regulates the mitotic spindle and phragmoplast in *M. polymorpha*

The mitotic spindle is a dynamic bipolar array of microtubules. In wild type *M. polymorpha*, mitotic spindles are box-shaped, centrally positioned in the cell and do not rotate. By contrast in Mp*ktn,* mitotic spindles were often non-central, tilted within the 3D cell volume and could rotate overtime. Similar rotation of the metaphase spindle was observed in At*ktn* mutants (Komis *et al.*, 2017). Furthermore, there were structural defects in Mp*ktn* spindles; they were elongated, bent, and had tapered poles which nucleated thin wavy astral arrays. Surprisingly, this mimics observations in animal cells. On katanin inhibition in *Xenopus tropicalis* sperm, the mitotic spindles became elongated with curly microtubule bundles protruding from the spindle poles (Loughlin *et al.*, 2011). Further, katanin inhibition in *C. elegans* prevented the shortening of the meiotic spindle resulting in longer spindles (McNally *et al.*, 2006). In summary, katanin has a dual role in regulating spindle stability and structure in *M. polymorpha* combining functions identified in both plants and animal cells.

Cytokinesis in plant cells utilises a phragmoplast; a bipolar microtubule array which expands centrifugally to form a new cell plate between the two daughter nuclei. Katanin localises to

the distal phragmoplast arrays in *A. thaliana* to modulate microtubule length (Sasaki *et al.*, 2019). In Mp*ktn*, increased bending of the phragmoplast arrays reflects observations in At*ktn,* indicating a similar function in both plants (Panteris *et al.*, 2011; Panteris & Adamakis, 2012; Komis *et al.*, 2017). The phragmoplasts in Mp*ktn* cells often expanded in a curved or non-symmetrical plane and took double the time of wild type to divide the cell. Overall katanin is required for correct phragmoplast formation and expansion during cytokinesis

4.5.7 Katanin controls the plane of cell division by aligning the polar organiser and mitotic spindle axes and by stabilising the mitotic spindle

A variety of factors control cell division orientation: cell shape, the location of the pre-mitotic nucleus, the cortical division site, and the mitotic spindle orientation. In animals, the alignment of the mitotic spindle determines the division plane (Bringmann & Hyman, 2005). By contrast in plants, the division plane is accurately predicted prior to mitosis by the PPB (Rasmussen *et al.*, 2013). Although the PPB is dispensable, it improves the robustness of the division alignment (Schaefer *et al.*, 2017). In *M. polymorpha*, the polar organisers form prior to the PPB and are thought to orient the cell division (Brown & Lemmon, 2011a; Buschmann *et al.*, 2016). In timelapses of dividing wild type cells, the polar organiser axis aligns to the longitudinal cell axis, and the PPB aligns to the shortest cell axis. The mitotic spindle follows the polar organiser axis and the phragmoplast follows the PPB plane. This results in symmetrical periclinal divisions. By contrast, there were a series of defects in Mp*ktn* cells. First, there were supernumerary polar organisers which did not align with the longitude cell axis. Second, there was no true PPB. Third, the mitotic spindle axis differed from the polar organiser axis. Fourth, the mitotic spindle elongated and rotated overtime. These series of events were highly variable between cells resulting in a range of cell division planes, often asymmetrical and anticlinal. In summary, katanin controls the structure, orientation, stability, and transitions of the microtubule arrays during cell division.

Which of katanin's multiple roles during mitosis ultimately aligns the final division plane? In *A. thaliana* there are two conflicting models: the first proposes that katanin regulates spindle bipolarity to orient division (Panteris *et al.*, 2011), the second proposes that katanin regulates PPB narrowing and mitotic spindle stability to orient division (Komis *et al.*, 2017). My data indicates that katanin's role in alignment and stabilisation of the mitotic spindle axis is most determinative. I showed that the division plane follows the position of the mitotic spindle, and when the spindle reorientated in the Mp*ktn* mutant, the division plane aligned with the last spindle position. The mitotic spindle is partly positioned by the polar organisers, but my data shows that the spindle axis does not follow the polar organiser axis in the Mp*ktn* mutant. One limitation of my data is that the role of the PPB and mitotic spindle were hard to separate, as both were defective in the Mp*ktn* mutant. One possibility is that the PPB normally defines the division orientation, but the mitotic spindle can act as a backup mechanism in PPB absence. In summary, I propose that katanin orientates cell division in *M. polymorpha* predominantly through regulating mitotic spindle orientation and stability.

4.5.8 Conclusion

To summarise this chapter, I show that katanin is required for tissue morphogenesis, organ development and cortical microtubule organisation in *M. polymorpha.* Further, katanin is required for correct polar organiser formation, regulation of spindle length and stability, and orientation of the cell division plane. The most novel aspect of this work is the implication that katanin functions in the *de novo* formation of acentrosomal MTOCs in land plants, thereby providing new mechanistic insights to this relatively uncharacterised process.

4.6 Supplementary

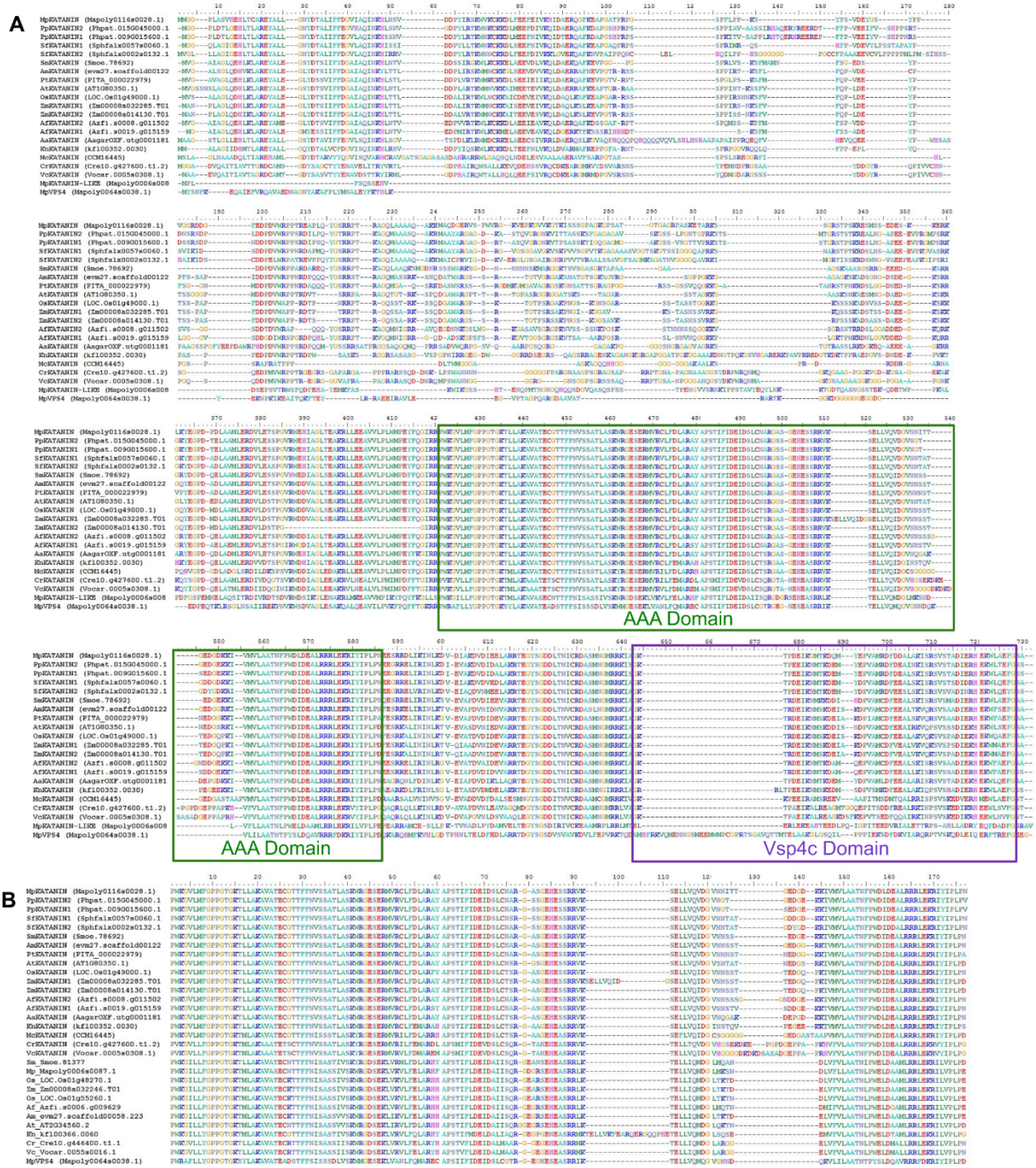

Supplementary Figure 4.1: Alignment of katanin and katanin like protein sequences from land plant and algal species

(A) Alignment of full KATANIN protein sequences from 15 plant and algal species. Includes MpKATANIN-LIKE (Mapoly006s0087) and MpVSP4 (Mapoly0064s0038) protein sequences. The AAA domain (green box) and Vsp4c domain (purple box) indicated.

(B) Alignment of the AAA ATPase domain of KATANIN and KATANIN-LIKE protein sequences from 15 plant and algal species. Includes the MpVSP4 (Mapoly0064s0038) protein sequence.

At, *Arabidopsis thaliana.* Am, *Amborella trichopoda.* Os, *Oryza sativa*. Zm, *Zea mays.* Pt, *Pinus taeda.* Af, *Azolla filiculoides.* Sm, *Selaginella moellendorffi.* Mp, *Marchantia polymorpha.* Pp, *Physcomitrium patens.* Sf, *Sphagnum fallax.* Aa, *Anthoceros agrestis.* Cr, *Chlamydomonas reinhardtii.* Mc, *Micromonas pusilla*. Vc, *Volvox carteri.* Kn, *Klebsormidium nitens*

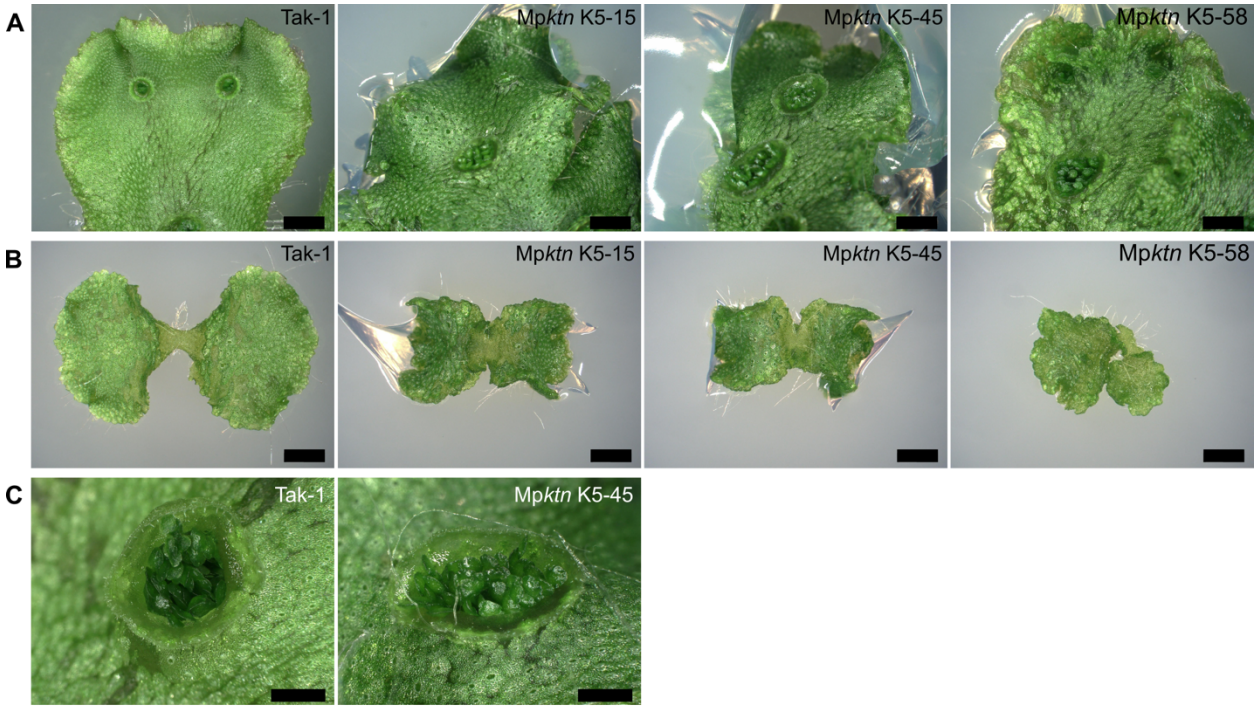

D

Plant line	Mutated gene sequence	Predicted protein sequence	Sex	Crossings
Wild type	ACGTTGGCCTCCAAATGGAGGGGTGAG	TLASKWRGE		
K3-7	ACGTTGGCCTCCAA - - - - - - - - GAGAGAG	TLASKRE...*	M	Failed
K3-8	ACGTTGGCCTCCAAACGTAGGAGGGGTG	TLASKRRRGE	F	Failed
K3-9	ACGTTGGCCTCCAAATGGGAGGGGTG	TLASKWEG*	F	Failed
K3-32	ACGTTGGCCTCCAAACAAACAAACCCAAGCCTCTCATGGAGGGGTGAG	TLASKQTNPSLSWRGE	M	Failed
K3-37	ACGTTGGCCTCCAACGAACGGAGGGGTGAG	TLASNERRGE	M	Success
K3-50	ACGTTGGCCTCCAA - GGGAGGGGCCAG	TLASKGG...*	F	Failed
K3-54	ACGTTGGCCTCCAAACGTAGCTGGACGTAGGTTGGAGGGGTGAGAG	TLASKRSWT*	M	Success
K3-66	ACGTTGGCCTCGTA - - GGAGGGGTGAG	TLAS*	M	Success
K3-85	ACGTTGGCCTCCAAATTGGAGGGGTGAG	TLASKLEG*	M	Success
Wild type	GAGGAGCTTGCCAGACGTACAGAGGGT	EELARRETG		
K5-15	GAGGAGCTTGCCAGACGTATAGCTTGCCAGAGGGT	EELARRIA...*	F	Failed
K5-45	GAGGAGCCCTTGCCA - - - - - - - - - - - -	EEPLPKFHA...	M	Success
K5-58	GAGGAGCTTGCCAGA - - - - - - - - GGGT	EELARGL*	M	Failed

Supplementary Figure 4.2: Mutations near the katanin Vsp4c domain induce similar defective plant phenotypes to mutations in the katanin AAA ATPase domain

(A) Dorsal thallus of wild type (Tak-1) and three Mp*ktn* K5 mutants. Scale bars, 2 mm.
(B) 10-day-old gemmalings of wild type (Tak-1) and three Mp*ktn* K5 mutants. Scale bars, 2 mm.
(C) Gemma cups on the dorsal thallus of wild type (Tak-1) and Mp*ktn* K5-45 plants. Scale bars, 1 mm.
(D) Full table of Mp*ktn* mutant alleles including their sex (F is female and M is male) and if they were successfully crossed to the microtubule reporter line, GFP-MpTUB1. Five further Mp*ktn* mutants were generated with a single T insertion in Exon 4 - the same mutation as K3-85 - but are not listed here and were not successfully crossed.

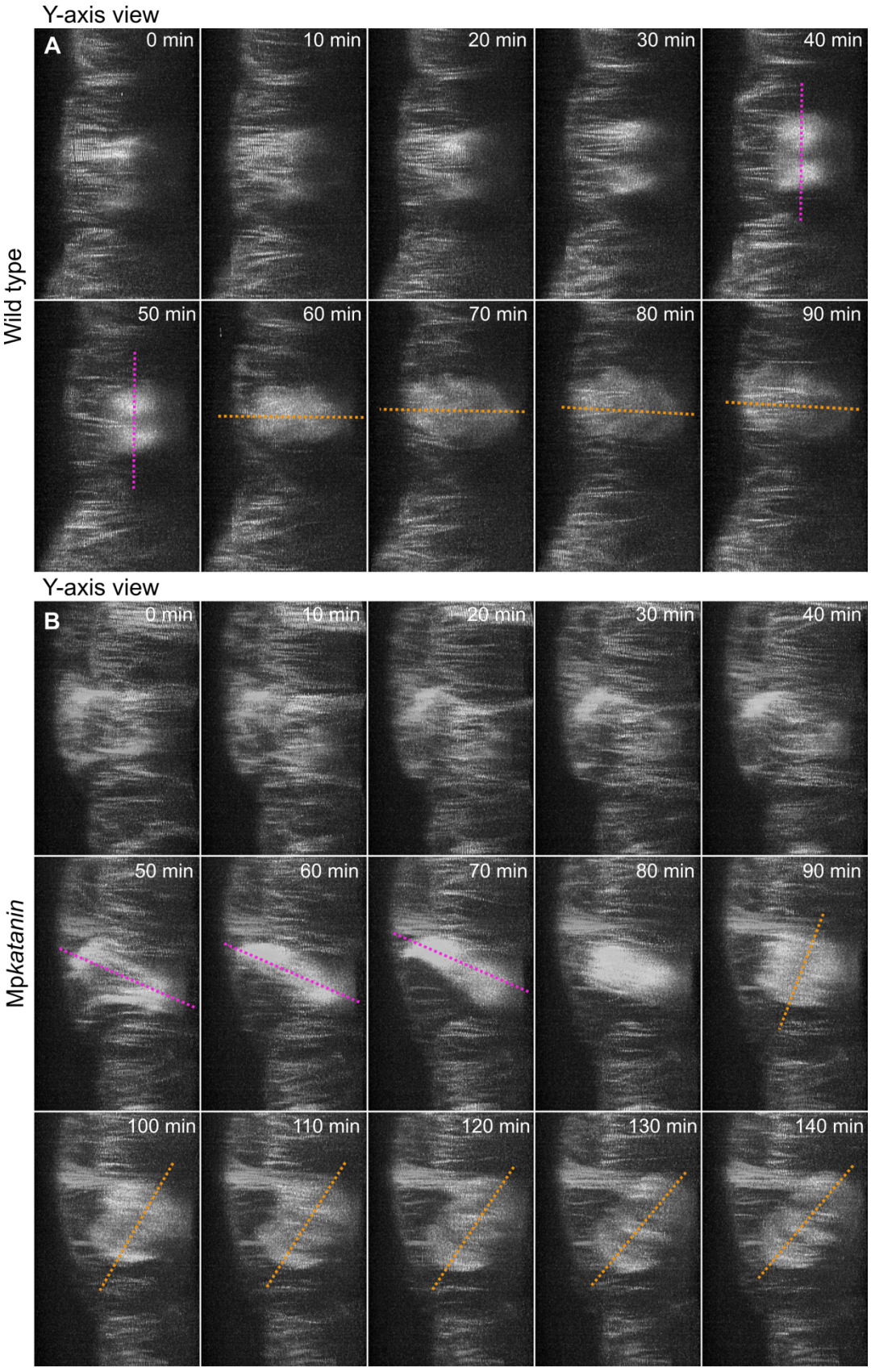
Y-axis view
A
0 min
10 min
20 min
30 min
40 min
50 min
60 min
70 min
80 min
90 min
Wild type
Y-axis view
B
0 min
10 min
20 min
30 min
40 min
50 min
60 min
70 min
80 min
90 min
100 min
110 min
120 min
130 min
140 min
Mpkatanin

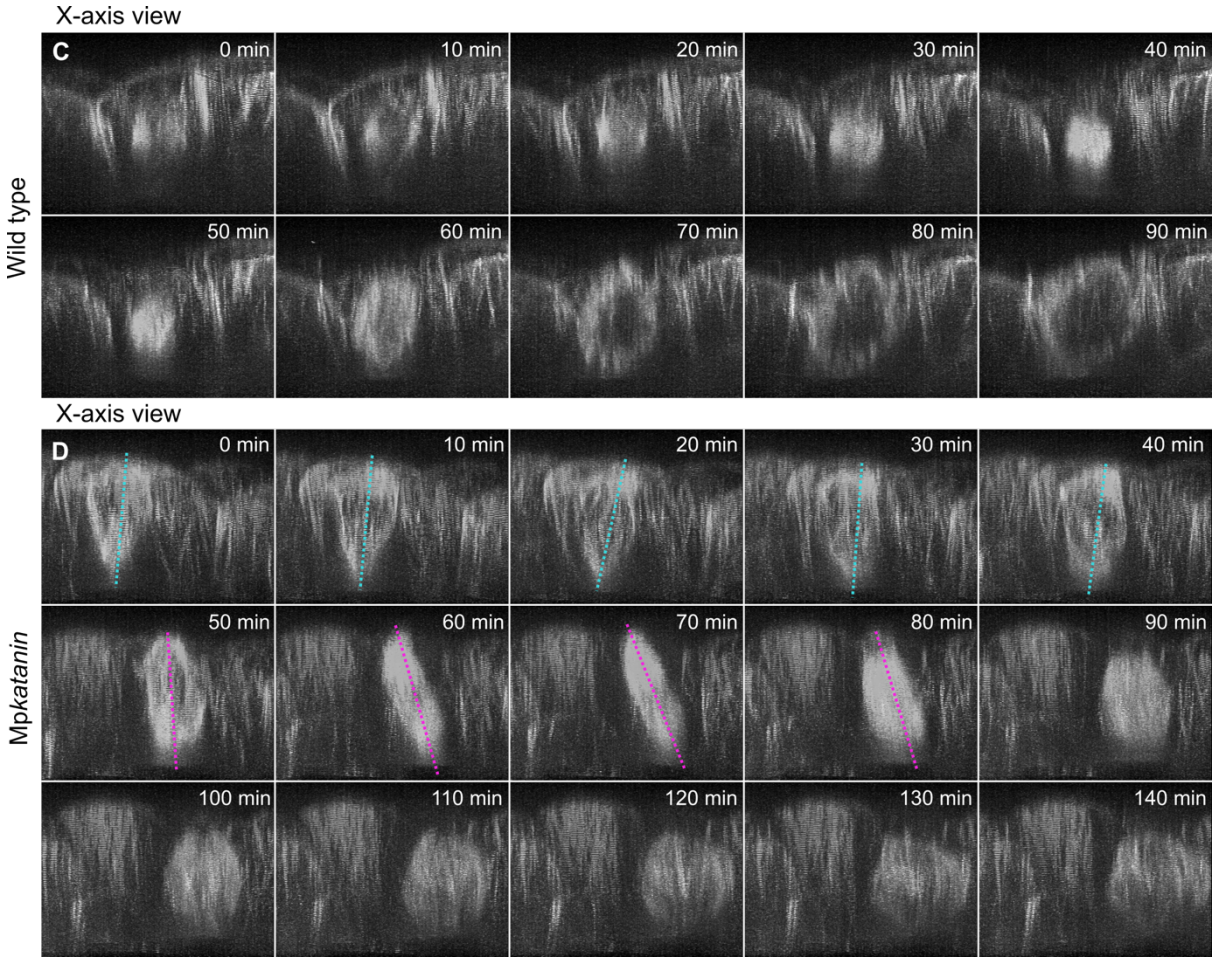

Supplementary Figure 4.3: Y- and X-axis views of dividing wild type and Mp*ktn* cells shows tilting of polar organisers, mitotic spindle and phragmoplast in the Mp*ktn* cell
Timelapses of dividing wild type (**A, C**) Mp*ktn* (K3-37) mutant (**B, D**) cells from **Figure 4.10.A, B** viewed through the Y axis (**A, B**) and the X axis (**C, D**). Cells are from 2-day-old gemmae expressing the microtubule reporter, *p*Mp*EF1α:GFP*-Mp*TUB1*. Presented are deconvolved Z-projections of slices through X and Y axis. Dotted cyan lines indicate the polar organiser axis, dotted magenta lines indicate the mitotic spindle axis and dotted orange lines indicate phragmoplast axis.

Chapter 5: General discussion

All multicellular land plants start life as a single cell. This cell – a spore or zygote - relies on polarisation followed by an asymmetric cell division to generate new cell lineages and establish the body plan. I aimed to investigate the subcellular and genetic mechanisms underpinning the polarisation of *M. polymorpha* spores, focusing my efforts on the cytoskeleton and its regulators. Here I will summarise my findings.

5.1 How does the organisation and dynamics of the nucleus and microtubules change during spore polarisation?

To understand the mechanisms driving polarisation of single plant cells, research has focused on the zygotes of angiosperms leaving a great diversity of plants untouched (Kimata *et al.*, 2016, 2019; Wang *et al.*, 2019). To expand this diversity and uncover novel polarity mechanisms, my research used the spore of *Marchantia polymorpha.* Spores are single haploid cells generated by meiosis, which undergo polarisation followed by an asymmetric division to establish the first apical-basal body axis. Up to now, spore polarity has been little described. In this thesis, I show that spores initially lack any observable asymmetry; spores are spherical with a central nucleus, disorganised cortical arrays, central MTOCs, symmetrical astral arrays, and evenly distributed chloroplasts. As the spore develops, a clear apical-basal asymmetry forms: the nucleus and MTOCs reposition to the basal pole; chloroplasts reorganise to the apical hemisphere; cortical and astral arrays deplete apically and gather basally; and an actin network forms between the nucleus and basal cortex (**Figure 5.1**). This apical-basal asymmetry is generated entirely internally as the spore remains spherical throughout this process with no morphological changes. In summary, the spore generates internal polarity starting from a non-polar state, thereby providing an exceptional and novel system for studying polarity establishment.

What are the mechanisms underpinning polarity establishment in the spore? Across the diversity of eukaryotic organisms, the cytoskeleton is universally involved in cell polarity and hence provided the entry point for my investigation. Through live timelapse imaging of spores expressing a microtubule reporter, I show that the two polar organisers – the MTOCs of *M. polymorpha* - form *de novo* on either side of the central nucleus at around 28 hours after germination. The nucleus and its associated microtubule arrays then move to the cell cortex led by one polar organiser, in agreement with Sakai *et al.*, 2022 (**Figure 5.1**). Uniquely, I discovered that this structure could reorient prior to migration and the basal polar organiser polymerised a dense, highly dynamic astral array. From this data I hypothesised a polarity mechanism in spores: astral arrays from one polar organiser anchor to a basal polar protein domain and pull or guide the polar organiser and nucleus to the basal cortex. MTOC relocation via dynamic astral arrays is a common mechanism used to generate polarity in cells containing centrosomes (Meiring *et al.*, 2020). However, *M. polymorpha* spores provide the first evidence of this mechanism being used in land plants.

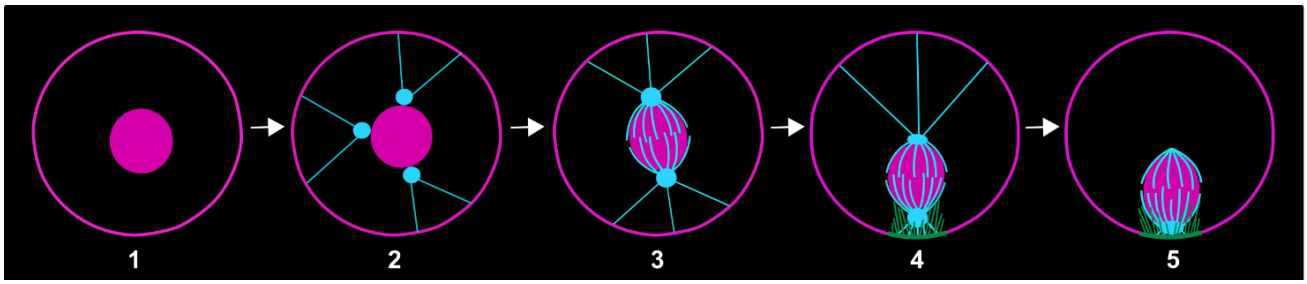

Figure 5.1: The organisation of the nucleus, microtubules, and actin filaments during the polarisation of *M. polymorpha* spores
Summary of the subcellular events during spore polarisation. Diagram depicts microtubules (cyan), actin filaments (green), the plasma membrane (magenta) and nucleus (magenta) in the central slice of a developing spore. **(1)** The nucleus is roughly central but there are no associated cytoskeleton filaments. **(2)** Microtubule foci form around the central nucleus. **(3)** The foci aggregate into two polar organisers with perinuclear arrays and astral arrays. **(4)** The nucleus migrates towards the cell cortex, led by the basal polar organiser and a dense astral array. Actin filaments accumulate at the basal cortex and extend around the nucleus base. **(5)** The basal polar organiser docks at the basal cortex where the actin network is positioned. The nucleus stays at the basal pole until mitosis.

5.2 The intersecting functions of the cytoskeleton in spore polarisation: could microtubules provide direction whilst actin filaments generate force?

With evidence of microtubule asymmetry in spores I next investigated the organisation of actin filaments. By imaging spores expressing an actin filament reporter, I discovered that an actin network forms at the basal cortex when the nucleus is basal-localised (**Figure 5.1**). Formation of a polarised actin network is a widespread mechanism across eukaryotes, often functioning to target vesicle trafficking, position organelles or direct cell outgrowth (Zhang *et al.*, 2023). In spores, the basal actin network appears to interact with the nucleus, which is consistent with the hypothesis that actin filaments function in nuclear migration or anchoring. Determining the exact timing of actin network formation e.g., before, during or after nucleus migration, could clarify the function of actin filaments during spore polarisation.

Actin filaments and microtubules often organise and function in distinct but interconnected ways to establish cell polarity (Li & Gundersen, 2008). In spores, microtubule arrays polymerise away from the polar organisers towards the cell cortex, whilst actin filaments appear to polymerise from the cortex towards the nucleus. Their overlapping localisations but opposing directionality suggests that microtubule and actin filaments interact with each other and the nucleus but have distinct functions. What are their respective roles in spores? As spores do not undergo directional growth, both elements must act to generate internal polarity. I speculate that microtubules orient the direction of nuclear migration, whilst actin filaments provide the force to pull the nucleus towards the basal pole. To determine their respective functions, spores expressing a nuclear reporter could be treated with actin or microtubule inhibitors and the nucleus position tracked over spore development.

5.3 Does katanin regulate acentrosomal MTOCs in plants?

Having established that microtubule and MTOC dynamics are essential in spore polarisation, I then took a genetic approach to discover proteins regulating this process. My efforts focused on katanin; a microtubule severing enzymes which controls microtubule dynamics

across eukaryotes (McNally & Vale, 1993; McNally & Roll-Mecak, 2018). I first set out to characterise the function of katanin in *M. polymorpha* development at the plant, tissue, cell, and subcellular level. By generating Mp*ktn* mutants, I discovered that katanin regulates thallus morphogenesis, plant growth, fertility, cell patterning, cortical array organisation and bundling. Katanin functions similarly in angiosperms (Luptovčiak *et al.*, 2017). Additionally, I show that katanin is required for correct polar organiser formation and organisation in *M. polymorpha*. Previous reports proposed that polar organisers are formed by bipolar aggregation of microtubule foci around the nucleus (Buschmann *et al.*, 2016). My research adds new details to this mechanism by proposing that dynamic astral arrays regulated by katanin are required to move and fuse these foci. Moreover, this is the first evidence of katanin severing aiding in the formation, organisation, and function of acentrosomal MTOCs.

5.4 Bringing it all together: is katanin-mediated regulation of microtubules essential for spore polarisation?

My data are consistent with the hypothesis that katanin controls polar organiser formation, microtubule organisation, spindle positioning and division plane orientation in *M. polymorpha*. This led me to speculate that katanin severing is necessary for nuclear migration and asymmetric division in *M. polymorpha* spores. Further, katanin is known to sever arrays in response to blue light in plants, and therefore I venture that katanin may form the link between blue light and the generation of subcellular polarity in spores (Lindeboom *et al.*, 2013). To test these hypothesises, one method is to generate Mp*ktn* spores and to characterise their microtubule dynamics, nuclear migrations, and division orientations. Differences compared to wild type spores would indicate a function for katanin.

In summary, by studying mutants in key cytoskeleton regulatory proteins, like katanin, we can now address broader questions regarding spore polarity: What proteins are induced by blue light to reorganise the spore cytoskeleton? Can spores still polarise if the cytoskeleton

dynamics are subtly disrupted? Further, what is the fate of the daughter cells if asymmetry is not established in the spore?

5.5 Conclusion

In this thesis I have discovered three fundamental events in the polarisation of *M. polymorpha* spores: nuclear migration, MTOC movement led by astral arrays, and formation of a basal actin network. Employing acentrosomal MTOCs in cell polarisation is a unique polarity mechanism undescribed in other plant cells. By characterising *M. polymorpha* spore development and producing genetic tools, this thesis provides a foundation for future research to discover how single cells generate polarity to give rise to multicellular plants.

References

Adams, A.E.M., Johnson, D.I., Longnecker, R.M., Sloat, B.F., & Pringle, J.R. (1990). CDC42 and CDC43, two additional genes involved in budding and the establishment of cell polarity in the yeast *Saccharomyces cerevisiae*. *Journal of Cell Biology*, 111(1), p. 131–142.

Alberts, B., Johnson, A., Lewis, J., Raff, M., Roberts, K., & Walter, P. (2007). Molecular Biology of the Cell 5th edition. *New York: Garland Science*.

Alessa, L. & Kropf, D.L. (1999). F-actin marks the rhizoid pole in living *Pelvetia compressa* zygotes. *Development*, 126(1), p. 201–209.

Baluška, F., Salaj, J., Mathur, J., Braun, M., Jasper, F., Šamaj, J., Chua, N.H., Barlow, P.W., & Volkmann, D. (2000). Root hair formation: F-actin-dependent tip growth is initiated by local assembly of profilin-supported F-actin meshworks accumulated within expansin-enriched bulges. *Developmental Biology*, 227(2), p. 618–632.

Behrens, R. & Nurse, P. (2002). Roles of fission yeast tea1p in the localization of polarity factors and in organizing the microtubular cytoskeleton. *Journal of Cell Biology*, 157(5), p. 783–793.

Bettencourt-Dias, M. & Glover, D.M. (2007). Centrosome biogenesis and function: Centrosomics brings new understanding. *Nature Reviews Molecular Cell Biology*, 8(6), p. 451–463.

Bichet, A., Desnos, T., Turner, S., Grandjean, O., & Höfte, H. (2001). BOTERO1 is required for normal orientation of cortical microtubules and anisotropic cell expansion in *Arabidopsis*. *Plant Journal*, 25(2), p. 137–148.

Bisgrove, S.R. & Kropf, D.L. (2001). Asymmetric cell division in Fucoid algae: A role for cortical adhesions in alignment of the mitotic apparatus. *Journal of Cell Science*, 114(23), p. 4319–4328.

Bloch, R. (1943). Polarity in plants. *Botanical Review*, 9(5), p. 261–310.

Bouquin, T., Mattsson, O., Næsted, H., Foster, R., & Mundy, J. (2003). The *Arabidopsis lue1* mutant defines a katanin p60 ortholog involved in hormonal control of microtubule orientation during cell growth. *Journal of Cell Science*, 116(5), p. 791–801.

Bowman, J.L. *et al.* (2017). Insights into land plant evolution garnered from the *Marchantia polymorpha* genome. *Cell*, 171(2), p. 287–304.

Bowman, J.L. *et al.* (2022). The renaissance and enlightenment of *Marchantia* as a model system. *The Plant Cell*, 17(00), p. 1–31.

Bringmann, H. & Hyman, A.A. (2005). A cytokinesis furrow is positioned by two consecutive signals. *Nature*, 436(7051), p. 731–734.

Brown, R.C. & Lemmon, B.E. (1990). Polar organizers mark division axis prior to preprophase band formation in mitosis of the hepatic *Reboulia hemisphaerica* (Bryophyta). *Protoplasma*, 156(1–2), p. 74–81.

Brown, R.C. & Lemmon, B.E. (2011a). Dividing without centrioles: Innovative plant microtubule organizing centres organize mitotic spindles in bryophytes, the earliest extant lineages of land plants. *AoB PLANTS*, 11(1), p. 1–9.

Brown, R.C. & Lemmon, B.E. (2011b). Spores before sporophytes: Hypothesizing the origin of sporogenesis at the algal-plant transition. *New Phytologist*, 190(4), p. 875–881.

Brown, R.C., Lemmon, B.E., & Horio, T. (2004). γ-Tubulin localization changes from discrete polar organizers to anastral spindles and phragmoplasts in mitosis of *Marchantia polymorpha L. Protoplasma*, 224(3–4), p. 187–193.

Burk, D.H., Liu, B., Zhong, R., Morrison, W.H., & Ye, Z.H. (2001). A katanin-like protein regulates normal cell wall biosynthesis and cell elongation. *Plant Cell*, 13(4), p. 807–827.

Burk, D.H. & Ye, Z.H. (2002). Alteration of oriented deposition of cellulose microfibrils by mutation of a katanin-like microtubule-severing protein. *Plant Cell*, 14(9), p. 2145–2160.

Buschmann, H., Holtmannspötter, M., Borchers, A., O'Donoghue, M.T., & Zachgo, S. (2016). Microtubule dynamics of the centrosome-like polar organizers from the basal land plant *Marchantia polymorpha*. *New Phytologist*, 209(3), p. 999–1013.

Buschmann, H. & Müller, S. (2019). Update on plant cytokinesis: Rule and divide. *Current Opinion in Plant Biology*, 52, p. 97–105.

Buschmann, H. & Zachgo, S. (2016). The evolution of cell division: From streptophyte algae to land plants. *Trends in Plant Science*, 21(10), p. 872–883.

Campanale, J.P., Sun, T.Y., & Montell, D.J. (2017). Development and dynamics of cell polarity at a glance. *Journal of Cell Science*, 130(7), p. 1201–1207.

Champion, C., Lamers, J., Shivas Jones, V.A., Morieri, G., Honkanen, S., & Dolan, L. (2021). Microtubule associated protein WAVE DAMPENED2-LIKE (WDL) controls microtubule bundling and the stability of the site of tip-growth in *Marchantia polymorpha* rhizoids. *PLoS Genetics*, 17(6), p. 1–20.

Chan, J., Calder, G.M., Doonan, J.H., & Lloyd, C.W. (2003). EB1 reveals mobile microtubule nucleation sites in *Arabidopsis*. *Nature Cell Biology*, 5(11), p. 967–971.

Chan, J., Calder, G., Fox, S., & Lloyd, C. (2005). Localization of the microtubule end binding protein EB1 reveals alternative pathways of spindle development in *Arabidopsis* suspension cells. *Plant Cell*, 17(6), p. 1737–1748.

Chugh, P. & Paluch, E.K. (2018). The actin cortex at a glance. *Journal of Cell Science*, 131(14), p. 1–9.

Corellou, F., Coelho, S.M.B., Bouget, F.Y., & Brownlee, C. (2005). Spatial re-organisation of cortical microtubules *in vivo* during polarisation and asymmetric division of *Fucus* zygotes. *Journal of Cell Science*, 118(12), p. 2723–2734.

Cowan, C.R. & Hyman, A.A. (2004). Centrosomes direct cell polarity independently of microtubule assembly in *C. elegans* embryos. *Nature*, 431(7004), p. 92–96.

Davidson, P.M. & Cadot, B. (2021). Actin on and around the nucleus. *Trends in Cell Biology*, 31(3), p. 211–223.

Deinum, E.E., Tindemans, S.H., Lindeboom, J.J., & Mulder, B.M. (2017). How selective severing by katanin promotes order in the plant cortical microtubule array. *Proceedings of the National Academy of Sciences*, 114(27), p. 6942–6947.

Dong, J., MacAlister, C.A., & Bergmann, D.C. (2009). BASL controls asymmetric cell division in *Arabidopsis*. *Cell*, 137(7), p. 1320–1330.

Dop, M. Van, Fiedler, M., Mutte, S., Keijzer, J. De, Olijslager, L., Albrecht, C., Liao, C.-Y., Janson, M.E., Bienz, M., & Weijers, D. (2020). DIX domain polymerization drives assembly of plant cell polarity complexes. *Cell*, 180, p. 1–13.

Duan, Z., Tanaka, M., Kanazawa, T., Haraguchi, T., Takyu, A., Era, A., Ueda, T., Ito, K., & Tominaga, M. (2020). Characterization of ancestral myosin XI from *Marchantia polymorpha* by heterologous expression in *Arabidopsis thaliana*. *Plant Journal*, 104(2), p. 460–473.

Edwards, E.S. & Roux, S.J. (1998). Influence of gravity and light on the developmental polarity of *Ceratopteris richardii* fern spores. *Planta*, 205(4), p. 553–560.

Era, A., Tominaga, M., Ebine, K., Awai, C., Saito, C., Ishizaki, K., Yamato, K.T., Kohchi, T., Nakano, A., & Ueda, T. (2009). Application of Lifeact reveals F-actin dynamics in *Arabidopsis thaliana* and the liverwort, *Marchantia polymorpha*. *Plant and Cell Physiology*, 50(6), p. 1041–1048.

Farache, D., Emorine, L., Haren, L., & Merdes, A. (2018). Assembly and regulation of γ-tubulin complexes. *Open Biology*, 8(3).

Flores-Sandoval, E., Romani, F., & Bowman, J.L. (2018). Co-expression and transcriptome analysis of *Marchantia polymorpha* transcription factors supports class C ARFs as independent actors of an ancient auxin regulatory module. *Frontiers in Plant Science*, 9(1345), p. 1–21.

Fowler, J.E. & Quatrano, R.S. (1995). Cell polarity, asymmetric division, and cell fate determination in brown algal zygotes. *Seminars in Developmental Biology*, 6(5), p. 347–358.

Frey, N., Klotz, J., & Nick, P. (2010). A kinesin with calponin-homology domain is involved in premitotic nuclear migration. *Journal of Experimental Botany*, 61(12), p. 3423–3437.

Gicking, A.M., Swentowsky, K.W., Dawe, R.K., & Qiu, W. (2018). Functional diversification of the kinesin-14 family in land plants. *FEBS Letters*, 592(12), p. 1918–1928.

Goodner, B. & Quatrano, R.S. (1993). *Fucus* embryogenesis: A model to study the establishment of polarity. *Plant Cell*, 5(10), p. 1471–1481.

Goshima, G. & Scholey, J.M. (2010). Control of mitotic spindle length. *Annual Review of Cell and Developmental Biology*, 26, p. 21–57.

Gundersen, G.G. & Worman, H.J. (2013). Nuclear positioning. *Cell*, 152(6), p. 1376–1389.

Hable, W.E. & Kropf, D.L. (1998). Roles of secretion and the cytoskeleton in cell adhesion and polarity establishment in *Pelvetia compressa* zygotes. *Developmental Biology*, 198(1), p. 45–56.

Hable, W.E. & Kropf, D.L. (2000). Sperm entry induces polarity in Fucoid zygotes. *Development*, 127(3), p. 493–501.

Hable, W.E. & Kropf, D.L. (2005). The Arp2/3 complex nucleates actin arrays during zygote polarity establishment and growth. *Cell Motility and the Cytoskeleton*, 61(1), p. 9–20.

Hadley, R., Hable, W.E., & Kropf, D.L. (2006). Polarization of the endomembrane system is an early event in Fucoid zygote development. *BMC Plant Biology*, 6, p. 1–10.

Hamada, T. (2014). Microtubule organization and microtubule-associated proteins in plant cells. *International Review of Cell and Molecular Biology*, 312, p. 1–52.

Hartman, J.J., Mahr, J., McNally, K., Okawa, K., Iwamatsu, A., Thomas, S., Cheesman, S., Heuser, J., Vale, R.D., & McNally, F.J. (1998). Katanin, a microtubule-severing protein, is a novel AAA ATPase that targets to the centrosome using a WD40-containing subunit. *Cell*, 93(2), p. 277–287.

Hartman, K.S. & Muroyama, A. (2023). Polarizing to the challenge: New insights into polarity-mediated division orientation in plant development. *Current Opinion in Plant Biology*, 74 (102383), p. 1–7.

Hartman, M.A. & Spudich, J.A. (2012). The myosin superfamily at a glance. *Journal of Cell Science*, 125(7), p. 1627–1632.

Henty-Ridilla, J.L., Li, J., Blanchoin, L., & Staiger, C.J. (2013). Actin dynamics in the cortical array of plant cells. *Current Opinion in Plant Biology*, 16(6), p. 678–687.

Hepler, P.K., Vidali, L., & Cheung, A.Y. (2001). Polarised cell growth in higher plants. *Annual Review of Cell and Developmental Biology*, (17), p. 159–187.

Higa, T., Suetsugu, N., Kong, S.G., & Wada, M. (2014). Actin-dependent plastid movement is required for motive force generation in directional nuclear movement in plants. *Proceedings of the National Academy of Sciences*, 111(11), p. 4327–4331.

Higaki, T., Kutsuna, N., Sano, T., Kondo, N., & Hasezawa, S. (2010). Quantification and cluster analysis of actin cytoskeletal structures in plant cells: Role of actin bundling in stomatal movement during diurnal cycles in *Arabidopsis* guard cells. *Plant Journal*, 61(1), p. 156–165.

Higaki, T. (2017). Quantitative evaluation of cytoskeletal organizations by microscopic image analysis. *Plant Morphology*, 29(1), p. 15–21.

Higaki, T., Kojo, K.H., & Hasezawa, S. (2010). Critical role of actin bundling in plant cell morphogenesis. *Plant Signaling and Behavior*, 5(5), p. 484–488.

Honkanen, S., Jones, V.A.S., Morieri, G., Champion, C., Hetherington, A.J., Kelly, S., Proust, H., Saint-Marcoux, D., Prescott, H., & Dolan, L. (2016). The mechanism forming the cell surface of tip-growing rooting cells is conserved among land plants. *Current Biology*, 26(23), p. 3238–3244.

Ishizaki, K., Chiyoda, S., Yamato, K.T., & Kohchi, T. (2008). *Agrobacterium*-mediated transformation of the haploid liverwort *Marchantia polymorpha L.*, an emerging model for plant biology. *Plant and Cell Physiology*, 49(7), p. 1084–1091.

Ishizaki, K., Nishihama, R., Yamato, K.T., & Kohchi, T. (2016). Molecular genetic tools and techniques for *Marchantia polymorpha* research. *Plant and Cell Physiology*, 57(2), p. 262–270.

Iwabuchi, K., Minamino, R., & Takagi, S. (2010). Actin reorganization underlies phototropin-dependent positioning of nuclei in *Arabidopsis* leaf cells. *Plant Physiology*, 152(3), p. 1309–1319.

Iwabuchi, K., Sakai, T., & Takagi, S. (2007). Blue light-dependent nuclear positioning in *Arabidopsis thaliana* leaf cells. *Plant and Cell Physiology*, 48(9), p. 1291–1298.

Katoh, K., Misawa, K., Kuma, K.I., & Miyata, T. (2002). MAFFT: A novel method for rapid multiple sequence alignment based on fast Fourier transform. *Nucleic Acids Research*, 30(14), p. 3059–3066.

Ketelaar, T., Faivre-Moskalenko, C., Esseling, J.J., De Ruijter, N.C.A., Grierson, C.S., Dogterom, M., & Emons, A.M.C. (2002). Positioning of nuclei in *Arabidopsis* root hairs: An actin-regulated process of tip growth. *Plant Cell*, 14(11), p. 2941–2955.

Kimata, Y., Higaki, T., Kawashima, T., Kurihara, D., Sato, Y., Yamada, T., Hasezawa, S., Berger, F., Higashiyama, T., & Ueda, M. (2016). Cytoskeleton dynamics control the first asymmetric cell division in *Arabidopsis* zygote. *Proceedings of the National Academy of Sciences,* 113(49), p. 14157–14162.

Kimata, Y., Kato, T., Higaki, T., Kurihara, D., Yamada, T., Segami, S., Morita, M.T., Maeshima, M., Hasezawa, S., Higashiyama, T., Tasaka, M., & Ueda, M. (2019). Polar vacuolar distribution is essential for accurate asymmetric division of *Arabidopsis* zygotes. *Proceedings of the National Academy of Sciences,* 116(6), p. 2338–2343.

Kirchhelle, C. & Moore, I. (2017). A simple chamber for long-term confocal imaging of root and hypocotyl development. *Journal of Visualized Experiments*, (123), p. 1–9.

Kohchi, T., Yamato, K.T., Ishizaki, K., Yamaoka, S., & Nishihama, R. (2021). Development and molecular genetics of *Marchantia polymorpha*. *Annual Review of Plant Biology*, 72, p. 677–702.

Kollmar, M. & Mühlhausen, S. (2017). Myosin repertoire expansion coincides with eukaryotic diversification in the Mesoproterozoic era. *BMC Evolutionary Biology*, 17(1), p. 1–18.

Komis, G., Luptovčiak, I., Ovečka, M., Samakovli, D., Šamajová, O., & Šamaj, J. (2017). Katanin effects on dynamics of cortical microtubules and mitotic arrays in *Arabidopsis thaliana* revealed by advanced live-cell imaging. *Frontiers in Plant Science*, 8, p. 1–19.

Kong, S.G. & Wada, M. (2011). New insights into dynamic actin-based chloroplast photorelocation movement. *Molecular Plant*, 4(5), p. 771–781.

Kosetsu, K., Murata, T., Yamada, M., Nishina, M., Boruc, J., Hasebe, M., Van Damme, D., & Goshima, G. (2017). Cytoplasmic MTOCs control spindle orientation for asymmetric cell division in plants. *Proceedings of the National Academy of Sciences*, 114(42), p. 8847–8854.

Krtková, J., Benáková, M., & Schwarzerová, K. (2016). Multifunctional microtubule-associated proteins in plants. *Frontiers in Plant Science*, 7, p. 1–13.

Kumar, S., Stecher, G., Li, M., Knyaz, C., & Tamura, K. (2018). MEGA X: Molecular evolutionary genetics analysis across computing platforms. *Molecular Biology and Evolution*, 35(6), p. 1547–1549.

Lampropoulos, A., Sutikovic, Z., Wenzl, C., Maegele, I., Lohmann, J.U., & Forner, J. (2013). GreenGate - A novel, versatile, and efficient cloning system for plant transgenesis. *PLoS ONE*, 8(12), p. 1–15.

Lau, S., Slane, D., Herud, O., Kong, J., & Jürgens, G. (2012). Early embryogenesis in flowering plants: Setting up the basic body pattern. *Annual Review of Plant Biology*, 63, p. 483–506.

Lee, Y.R.J. & Liu, B. (2019). Microtubule nucleation for the assembly of acentrosomal microtubule arrays in plant cells. *New Phytologist*, 222(4), p. 1705–1718.

Lei, Y., Lu, L., Liu, H.Y., Li, S., Xing, F., & Chen, L.L. (2014). CRISPR-P: A web tool for

synthetic single-guide RNA design of CRISPR-system in plants. *Molecular Plant*, 7(9), p. 1494–1496.

Letunic, I. & Bork, P. (2018). 20 years of the SMART protein domain annotation resource. *Nucleic Acids Research*, 46(D1), p. D493–D496.

Li, R. & Gundersen, G.G. (2008). Beyond polymer polarity: How the cytoskeleton builds a polarized cell. *Nature Reviews Molecular Cell Biology*, 9(11), p. 860–873.

Lin, D., Cao, L., Zhou, Z., Zhu, L., Ehrhardt, D., Yang, Z., & Fu, Y. (2013). Rho GTPase signaling activates microtubule severing to promote microtubule ordering in *Arabidopsis*. *Current Biology*, 23(4), p. 290–297.

Lindeboom, J.J., Nakamura, M., Hibbel, A., Shundyak, K., Gutierrez, R., Ketelaar, T., Emons, A.M.C., Mulder, B.M., Kirik, V., & Ehrhardt, D.W. (2013). A mechanism for reorientation of cortical microtubule arrays driven by microtubule severing. *Science*, 342, p. 1–11.

Liu, C., Zhang, Y., & Ren, H. (2018). Actin polymerization mediated by AtFH5 directs the polarity establishment and vesicle trafficking for pollen germination in *Arabidopsis*. *Molecular Plant*, 11(11), p. 1389–1399.

Loughlin, R., Wilbur, J.D., McNally, F.J., Nédélec, F.J., & Heald, R. (2011). Katanin contributes to interspecies spindle length scaling in *Xenopus*. *Cell*, 147(6), p. 1397–1407.

Love, J., Brownlee, C., & Trewavas, A.J. (1997). Ca2+ and calmodulin dynamics during photopolarization in *Fucus serratus* zygotes. *Plant Physiology*, 115(1), p. 249–261.

Luptovčiak, I., Komis, G., Takáč, T., Ovečka, M., & Šamaj, J. (2017). Katanin: A sword cutting microtubules for cellular, developmental, and physiological purposes. *Frontiers in Plant Science*, 8, p. 1–10.

Luptovčiak, I., Samakovli, D., Komis, G., & Šamaj, J. (2017). KATANIN 1 is essential for embryogenesis and seed formation in *Arabidopsis*. *Frontiers in Plant Science*, 8, p. 1–12.

Martin, S.G., McDonald, W.H., Yates, J.R., & Chang, F. (2005) Tea4p links microtubule plus ends with the formin for3p in the establishment of cell polarity. *Developmental Cell*, 8(4), p. 479–491.

McCurdy, D.W., Kovar, D.R., & Staiger, C.J. (2001). Actin and actin-binding proteins in higher plants. *Protoplasma*, 215(1–4), p. 89–104.

McNally, F.J. & Roll-Mecak, A. (2018). Microtubule-severing enzymes: From cellular functions to molecular mechanism. *Journal of Cell Biology*, 217(12), p. 4057–4069.

McNally, F.J. & Vale, R.D. (1993). Identification of katanin, an ATPase that severs and disassembles stable microtubules. *Cell*, 75(3), p. 419–429.

McNally, K., Audhya, A., Oegema, K., & McNally, F.J. (2006). Katanin controls mitotic and meiotic spindle length. *Journal of Cell Biology*, 175(6), p. 881–891.

Meiring, J.C.M., Shneyer, B.I., & Akhmanova, A. (2020). Generation and regulation of microtubule network asymmetry to drive cell polarity. *Current Opinion in Cell Biology*, 62, p. 86–95.

Miller, A.L. (2011). The contractile ring. *Current Biology*, 21(24), p. R976–R978.

Molendijk, A.J., Bischoff, F., Rajendrakumar, C.S.V., Friml, J., Braun, M., Gilroy, S., & Palme, K. (2001). *Arabidopsis thaliana* Rop GTPases are localized to tips of root hairs and control polar growth. *EMBO Journal*, 20(11), p. 2779–2788.

Moore, J., Stuchell-Brereton, M., & Cooper, J. (2009). Function of dynein in budding yeast: Mitotic spindle positioning in a polarized cell. *Cell Motility and the Cytoskeleton*, 66(8), p. 546–555.

Mulvey, H. & Dolan, L. (2023). RHO GTPase of plants regulates polarized cell growth and cell division orientation during morphogenesis. *Current Biology*, (33), p. 1–15.

Munro, E. & Bowerman, B. (2009). Cellular symmetry breaking during *Caenorhabditis elegans* development. *Cold Spring Harbor perspectives in biology*, p. 1–20.

Munro, E., Nance, J., & Priess, J.R. (2004). Cortical flows powered by asymmetrical contraction transport PAR proteins to establish and maintain anterior-posterior polarity in the early *C. elegans* embryo. *Developmental Cell*, 7(3), p. 413–424.

Muroyama, A., Gong, Y., Hartman, K.S., & Bergmann, D. (2023). Cortical polarity ensures its own asymmetric inheritance in the stomatal lineage to pattern the leaf surface. *Science*, 381, p. 54–59.

Muroyama, A., Gong, Y., & Bergmann, D.C. (2020). Opposing, polarity-driven nuclear migrations underpin asymmetric divisions to pattern *Arabidopsis* stomata. *Current Biology*, 30(22), p. 4467-4475.

Nakamura, M. (2015). Microtubule nucleating and severing enzymes for modifying microtubule array organization and cell morphogenesis in response to environmental cues. *New Phytologist*, 205(3), p. 1022–1027.

Nakamura, M., Ehrhardt, D.W., & Hashimoto, T. (2010). Microtubule and katanin-dependent dynamics of microtubule nucleation complexes in the acentrosomal *Arabidopsis* cortical array. *Nature Cell Biology*, 12(11), p. 1064–1070.

Nakazato, T., Kadota, A., & Wada, M. (1999). Photoinduction of spore germination in *Marchantia polymorpha L.* is mediated by photosynthesis. *Plant and Cell Physiology*, 40(10), p. 1014–1020.

Nebenführ, A. & Dixit, R. (2018). Kinesins and myosins: Molecular motors that coordinate cellular functions in plants. *Annual Review of Plant Biology*, 69(1), p. 329–364.

O'Hanlon, M.E. (1926). Germination of spores and early stages in development of gametophyte of *Marchantia polymorpha*. *Botanical Gazette*, 82(2), p. 215–222.

Ovečka, M., Luptovčiak, I., Komis, G., Šamajová, O., Samakovli, D., & Šamaj, J. (2020). Spatiotemporal pattern of ectopic cell divisions contribute to mis-shaped phenotype of primary and lateral roots of *katanin1* mutant. *Frontiers in Plant Science*, 11(734), p. 1–18.

Panteris, E., Adamakis, I.D.S., Voulgari, G., & Papadopoulou, G. (2011). A role for katanin in plant cell division: Microtubule organization in dividing root cells of *fra2* and *lue1 Arabidopsis thaliana* mutants. *Cytoskeleton*, 68(7), p. 401–413.

Panteris, E. & Adamakis, I.D.S. (2012). Aberrant microtubule organization in dividing root cells of p60-katanin mutants. *Plant Signaling and Behavior*, 7(1), p. 1–3.

Peremyslov, V. V., Mockler, T.C., Filichkin, S.A., Fox, S.E., Jaiswal, P., Makarova, K.S., Koonin, E. V., & Dolja, V. V. (2011). Expression, splicing, and evolution of the myosin gene family in plants. *Plant Physiology*, 155(3), p. 1191–1204.

Peters, N.T. & Kropf, D.L. (2010). Asymmetric microtubule arrays organize the endoplasmic reticulum during polarity establishment in the brown alga *Silvetia compressa*. *Cytoskeleton*, 67(2), p. 102–111.

Pollard, T.D. (2016). Actin and Actin-Binding Proteins. *Cold Spring Harbor perspectives in biology*, 8 (a018226), p. 1–17.

Ramalho, J.J., Jones, V.A.S., Mutte, S., & Weijers, D. (2022). Pole position: How plant cells polarize along the axes. *The Plant Cell*, 34(1), p. 174–192.

Raman, R., Pinto, C.S., & Sonawane, M. (2018). Polarized organization of the cytoskeleton: Regulation by cell polarity proteins. *Journal of Molecular Biology*, 430(19), p. 3565–3584.

Rasmussen, C.G., Wright, A.J., & Müller, S. (2013). The role of the cytoskeleton and associated proteins in determination of the plant cell division plane. *Plant Journal*, 75(2), p. 258–269.

Reddy, A.S. & Day, I.S. (2001). Analysis of the myosins encoded in the recently completed *Arabidopsis thaliana* genome sequence. *Genome biology*, 2(7), p. 1–19.

Richardson, D.N., Simmons, M.P., & Reddy, A.S.N. (2006). Comprehensive comparative analysis of kinesins in photosynthetic eukaryotes. *BMC Genomics*, 7(18), p. 1–37.

Riedl, J., Crevenna, A.H., Kessenbrock, K., Yu, J.H., Neukirchen, D., Bista, M., Bradke, F., Jenne, D., Holak, T.A., Werb, Z., Sixt, M., & Wedlich-Soldner, R. (2008). Lifeact: A versatile marker to visualize F-actin. *Nature Methods*, 5(7), p. 605–607.

Roeder, A.H.K., Otegui, M.S., Dixit, R., Anderson, C.T., Faulkner, C., Zhang, Y., Harrison, M.J., Kirchhelle, C., Goshima, G., Coate, J.E., Doyle, J.J., Hamant, O., Sugimoto, K., Dolan, L., Meyer, H., Ehrhardt, D.W., Boudaoud, A., & Messina, C. (2022). Fifteen compelling open questions in plant cell biology. *Plant Cell*, 34(1), p. 72–102.

Sahi, V.P. & Baluška, F. (2018). Concepts in cell biology - History and evolution. *Plant Cell Monograph*, vol 23.

Sakai, Y., Higaki, T., Ishizaki, K., Nishihama, R., Kohchi, T., & Hasezawa, S. (2022). Migration of prospindle before the first asymmetric division in germinating spore of *Marchantia polymorpha*. *Plant Biotechnology*, 12, p. 5–12.

Sakurai, N., Domoto, K., & Takagi, S. (2005). Blue-light-induced reorganization of the actin cytoskeleton and the avoidance response of chloroplasts in epidermal cells of *Vallisneria gigantea*. *Planta*, 221(1), p. 66–74.

Salbreux, G., Charras, G., & Paluch, E. (2012). Actin cortex mechanics and cellular morphogenesis. *Trends in Cell Biology*, 22(10), p. 536–545.

Sasaki, T., Tsutsumi, M., Otomo, K., Murata, T., Yagi, N., Nakamura, M., Nemoto, T., Hasebe, M., & Oda, Y. (2019). A novel katanin-tethering machinery accelerates cytokinesis. *Current Biology*, 29(23), p. 4060–4070.

Sauret-Güeto, S., Frangedakis, E., Silvestri, L., Rebmann, M., Tomaselli, M., Markel, K., Delmans, M., West, A., Patron, N.J., & Haseloff, J. (2020). Systematic tools for reprogramming plant gene expression in a simple model, *Marchantia polymorpha*. *ACS Synthetic Biology*, 9(4), p. 864–882.

Schaefer, E., Belcram, K., Uyttewaal, M., Duroc, Y., Goussot, M., Legland, D., Laruelle, E., De Tauzia-Moreau, M.L., Pastuglia, M., & Bouchez, D. (2017). The preprophase band of microtubules controls the robustness of division orientation in plants. *Science*, 356(6334), p. 186–189.

Schindelin, J., Arganda-Carreras, I., Frise, E., Kaynig, V., Longair, M., Pietzsch, T., Preibisch, S., Rueden, C., Saalfeld, S., Schmid, B., Tinevez, J.Y., White, D.J., Hartenstein, V., Eliceiri, K., Tomancak, P., & Cardona, A. (2012). Fiji: An open-source platform for biological-image analysis. *Nature Methods*, 9(7), p. 676–682.

Shaw, S.L. & Quatrano, R.S. (1996). The role of targeted secretion in the establishment of cell polarity and the orientation of the division plane in *Fucus* zygotes. *Development*, 122(9),

p. 2623–2630.

Shen, Z., Collatos, A.R., Bibeau, J.P., Furt, F., & Vidali, L. (2012). Phylogenetic analysis of the kinesin superfamily from *Physcomitrella*. *Frontiers in Plant Science*, 3, p. 1–19.

Shimamura, M. (2016). *Marchantia polymorpha*: Taxonomy, phylogeny and morphology of a model system. *Plant and Cell Physiology*, 57(2), p. 230–256.

Shimmen, T. & Yokota, E. (2004). Cytoplasmic streaming in plants. *Current Opinion in Cell Biology*, 16(1), p. 68–72.

Sieberer, B.J., Ketelaar, T., Esseling, J.J., & Emons, A.M.C. (2005). Microtubules guide root hair tip growth. *New Phytologist*, 167(3), p. 711–719.

Siller, K.H. & Doe, C.Q. (2009). Spindle orientation during asymmetric cell division. *Nature Cell Biology*, 11(4), p. 365–374.

Slaughter, B.D., Smith, S.E., & Li, R. (2009). Symmetry breaking in the life cycle of the budding yeast. *Cold Spring Harbor perspectives in biology*, 1(3), p. 1–18.

Smertenko, A. *et al.* (2017). Plant cytokinesis: Terminology for structures and processes. *Trends in Cell Biology*, 27(12), p. 885–894.

Smertenko, A., Hewitt, S.L., Jacques, C.N., Kacprzyk, R., Liu, Y., Marcec, M.J., Moyo, L., Ogden, A., Oung, H.M., Schmidt, S., & Serrano-Romero, E.A. (2018). Phragmoplast microtubule dynamics - A game of zones. *Journal of Cell Science*, 131(2), p. 1–11.

De Smet, I. & Beeckman, T. (2011). Asymmetric cell division in land plants and algae: The driving force for differentiation. *Nature Reviews Molecular Cell Biology*, 12(3), p. 177–188.

St Johnston, D. & Ahringer, J. (2010). Cell polarity in eggs and epithelia: Parallels and diversity. *Cell*, 141(5), p. 757–774.

Stoppin-Mellet, V., Gaillard, J., & Vantard, M. (2006). Katanin's severing activity favors bundling of cortical microtubules in plants. *Plant Journal*, 46(6), p. 1009–1017.

Sugano, S.S., Shirakawa, M., Takagi, J., Matsuda, Y., Shimada, T., Hara-Nishimura, I., & Kohchi, T. (2014). CRISPR/Cas9-mediated targeted mutagenesis in the liverwort *Marchantia polymorpha L*. *Plant and Cell Physiology*, 55(3), p. 475–481.

Sugano, S.S., Nishihama, R., Shirakawa, M., Takagi, J., Matsuda, Y., Ishida, S., Shimada, T., Hara-Nishimura, I., Osakabe, K., & Kohchi, T. (2018). Efficient CRISPR/Cas9-based genome editing and its application to conditional genetic analysis in *Marchantia polymorpha*. *PLoS ONE*, 13(10), p. 1–22.

Sun, H., Furt, F., & Vidali, L. (2018). Myosin XI localizes at the mitotic spindle and along the cell plate during plant cell division in *Physcomitrella patens*. *Biochemical and Biophysical Research Communications*, 506(2), p. 409–421.

Suo, J., Chen, S., Zhao, Q., Shi, L., & Dai, S. (2015). Fern spore germination in response to environmental factors. *Frontiers in Biology*, 10(4), p. 358–376.

Tanenbaum, M.E., Akhmanova, A., & Medema, R.H. (2011). Bi-directional transport of the nucleus by dynein and kinesin-1. *Communicative and Integrative Biology*, 4(1), p. 21–25.

Thamm, A., Saunders, T.E., & Dolan, L. (2020). MpFEW RHIZOIDS1 miRNA-mediated lateral inhibition controls rhizoid cell patterning in *Marchantia polymorpha*. *Current Biology*, 30(10), p. 1905-1915.

Thomas, C., Tholl, S., Moes, D., Dieterle, M., Papuga, J., Moreau, F., & Steinmetz, A. (2009). Actin bundling in plants. *Cell Motility and the Cytoskeleton*, 66(11), p. 940–957.

Vidali, L., Rounds, C.M., Hepler, P.K., & Bezanilla, M. (2009). Lifeact-mEGFP reveals a dynamic apical F-actin network in tip growing plant cells. *PLoS ONE*, 4(5), p. 1–15.

Vidali, L., Burkart, G.M., Augustine, R.C., Kerdavid, E., Tüzel, E., & Bezanilla, M. (2010). Myosin XI is essential for tip growth in *Physcomitrella patens*. *Plant Cell*, 22(6), p. 1868–1882.

Vidali, L. & Hepler, P.K. (2001). Actin and pollen tube growth. *Protoplasma*, 215(1–4), p. 64–76.

Vogelmann, T.C., Brassel, A.R., & Miller, J.H. (1981). Effects of microtubule-inhibitors on nuclear migration and rhizoid differentiation in germinating fern spores (*Onoclea sensibilis*). *Protoplasma*, 109, p. 295–316.

Wallner, E., Dolan, L., & Bergmann, D.C. (2023). *Arabidopsis* stomatal lineage cells establish bipolarity and segregate differential signaling capacity to regulate stem cell potential. *Developmental Cell*, p. 1–14.

Wallner, E.S. (2020). The value of asymmetry: How polarity proteins determine plant growth and morphology. *Journal of Experimental Botany*, 71(19), p. 5733–5739.

Wang, K., Chen, H., Miao, Y., & Bayer, M. (2019). Square one: Zygote polarity and early embryogenesis in flowering plants. *Current Opinion in Plant Biology*, 53, p. 128–133.

Webb, M., Jouannic, S., Foreman, J., Linstead, P., & Dolan, L. (2002). Cell specification in the *Arabidopsis* root epidermis requires the activity of ECTOPIC ROOT HAIR 3 - a katanin-p60 protein. *Development*, 129(1), p. 123–131.

Wickham, H. (2009). ggplot2: Elegant graphics for data analysis. *Springer New York*.

Wickstead, B. & Gull, K. (2007). Dyneins across eukaryotes: A comparative genomic analysis. *Traffic*, 8(12), p. 1708–1721.

Wightman, R., Chomicki, G., Kumar, M., Carr, P., & Turner, S.R. (2013). SPIRAL2 determines plant microtubule organization by modulating microtubule severing. *Current Biology*, 23(19), p. 1902–1907.

Wu, S.Z., Ritchie, J.A., Pan, A.H., Quatrano, R.S., & Bezanilla, M. (2011). Myosin VIII regulates protonemal patterning and developmental timing in the moss *Physcomitrella patens*. *Molecular Plant*, 4(5), p. 909–921.

Wu, S.Z. & Bezanilla, M. (2014). Myosin VIII associates with microtubule ends and together with actin plays a role in guiding plant cell division. *eLife*, 3, p. 1–20.

Yamada, M. & Goshima, G. (2018). The KCH kinesin drives nuclear transport and cytoskeletal coalescence to promote tip cell growth in *Physcomitrella patens*. *Plant Cell*, 30(7), p. 1496–1510.

Yoshida, S., van der Schuren, A., van Dop, M., van Galen, L., Saiga, S., Adibi, M., Möller, B., ten Hove, C.A., Marhavy, P., Smith, R., Friml, J., & Weijers, D. (2019). A SOSEKI-based coordinate system interprets global polarity cues in *Arabidopsis*. *Nature Plants*, 5(2), p. 160–166.

Zhang, Q., Fishel, E., Bertroche, T., & Dixit, R. (2013). Microtubule severing at crossover sites by katanin generates ordered cortical microtubule arrays in *Arabidopsis*. *Current biology*, 23(21), p. 2191–2195.

Zhang, R., Xu, Y., Yi, R., & Shen, J. (2023). Actin cytoskeleton in the control of vesicle transport, cytoplasmic organization, and pollen tube tip growth. *Plant Physiology*, p. 1–17.